ARRESTINS REGULATE CELL SPREADING AND MOTILITY VIA FOCAL ADHESION DYNAMICS

By

Whitney Marie Cleghorn

Dissertation submitted to the

Faculty of the Graduate School of Vanderbilt University

in partial fulfillment of the requirements for the degree of

DOCTOR OF PHILOSOPHY

in

Pharmacology

August 2012

Nashville, Tennessee

Approved:

Professor Vsevolod V. Gurevich

Professor Brian E. Wadzinski

Professor Heidi E. Hamm

Professor Roy Zent

Professor Alissa M. Weaver

I dedicate the work in this thesis to my mom. Even if she wasn't my mother, I would choose her as a friend.

ACKNOWLEDGEMENTS

I came to grad school as a timid fresh-out-of-college Ohio girl with no real idea what it meant to be a scientist. I have to say that joining the Department of Pharmacology is one of the best decisions I have made in this regard. In the beginning it seemed like there were endless "hoops" to jump through to get to graduation. But with every hoop I gained more of a voice, more confidence, more patience, and more persistence. Facing the last and most fulfilling hoop, the defense, I would like to thank the department for all of these gifts. Pharm is notorious for being difficult, but it was the push backed by this department that helped me to think like a scientist.

For all of the times in between my arrival, and the completion of these projects, I want to thank my committee members Drs. Roy Zent, Alissa Weaver, Heidi Hamm, and Brian Wadzinski for their countless hours both inside and outside of our scheduled meetings. I left every meeting with a revived sense of direction, often times this was much needed. I also want to give extra thanks to Dr. Roy Zent, and Dr. Alissa Weaver, who not only were committee members, but also became collaborators along the way. This work would have not been accomplished if it weren't for you and your lab members Nada Bulus, Dong Chen, and Kevin Branch.

The Gurevich lab has essentially become my home, its members my family. They've grown to know me well in the lab environment, and ultimately embraced my work style. The papers, reagents, and equipment on my bench started flowing into theirs long ago and still is to this day. They never complained once, although, I am sure when I leave they will feel less claustrophobic. For all of their patience and guidance, I am

deeply thankful. I specifically want to acknowledge Sue Hanson, Xiufeng Song, Luis Gimenez and Seunghyi Kook for all of their help scientifically and personally, and Sergey Vishnivetskiy for all of the times he realized I needed to relax and told me as much: "Ma'am. Relaaaaaaax." It may not have helped in the moment, but I look back on all those times with total gratitude (he was right). I could not have asked for a better bay mate.

Most of my thanks in lab however, goes to my mentor Seva. After all is said and done, it was Seva who gave me the greatest scientific gift of all: a "fighting spirit". I may not have realized what he was doing at the time, but through his mentoring style he encouraged me to fight for my ideas and helped me find the confidence to question them. This is what is at the heart of every good scientist, and I owe this to him.

And lastly I want to thank my friends and family for all of their support. There were a lot of moments of frustration and wondering if I would ever make it out alive on the other end. I owe my mom and dad, my partner in crime, Aaron, and my good friend, Fyza, dinner in the least, and gratitude forever. My mom especially, she and I are very similar people. Without being a scientist, she understood everything I was going through and that simple understanding made a world of difference.

To everyone else who shared beers of condolence, beers of congratulations, or beers that were simply just beers, thank you for making my outside Nashville life awesome. I am lucky to know so many amazing people.

TABLE OF CONTENTS

Appendix

LIST OF FIGURES

LIST OF TABLES

LIST OF ABBREVIATIONS

GPCRs	G protein coupled receptors
G proteins	heterotrimeric GTP-binding proteins
Gα	G protein alpha subunit
Gβγ	G protein beta gamma subunits
PKA	Protein kinase A
PKC	Protein kinase C
GRKs	G protein receptor kinase
JNK3	c-Jun NH_2-terminal kinase
ERK1/2	Extracellular signal-related kinases
MAPK	Mitogen-activated protein kinase
AT1AR	Angiotensin type 1A receptor
NES	Nuclear exclusion site
xArr3	*Xenopus* arrestin-3
CE	Convergent extension
FH	Formin homology
GEF	Guanine nucleotide exchange factor
GAP	GTPase activating protein
GDI	Guanine nucleotide dissociation inhibitor
fMLP	fMet-Leu-Phe receptor
CIN	Chronofin
LIMK	LIM kinase

PAR2	Protease activated receptor 2
ARNO	Arf nucleotide binding site opener
ARF6	ADP ribosylating factor 6
ELMO	Engulfment and cell motility protein
Rh	Inactive receptor
Rh*	Active receptor
P-Rh*	Phosphorylated activated receptor
OS	Outer segment
IS	Inner segment
RPE	Retina pigment epithelium
MTs	microtubules
SDSL	site-directed spin labeling
EPR	Electron paramagnetic resonance
DKO	Arrestin2/3 double knock-out
WT	Wild-type
MEFs	Mouse embryonic fibroblasts
FN	Fibronectin
PDL	Poly-D-lysine
FAs	Focal adhesions
FAK	Focal adhesion kinase
GFP	Green fluorescent protein
FACs	Fluorescence-activated cell sorting
ROCK	Rho-associated protein kinase

cGMP	Cyclic guanosine monophosphate
ERG	Electroretinography
DEER	Double electron electron resonance
VSV-CL	cysteine-less base mutant of arrestin-1
NMR	Nuclear magnetic resonance spectroscopy
MLCK	Myosin light chain kinase
IGF-IR	Insulin-like growth factor I receptor
TIRF	Total internal reflection fluorescence

CHAPTER 1

INTRODUCTION

Arrestins and G protein-coupled receptors

G protein-coupled receptors (GPCRs) are the largest superfamily of proteins with approximately 1000 known members in the human genome (1). They are activated by a variety of different ligands such as light, calcium ions, odorants, small molecules, protein hormones, extra-cellular proteases, etc. With such a wide array of stimulants, it is unsurprising GPCRs mediate many processes including neurotransmission, olfactory, immune, and hormone responses, chemotaxis, and vision. Despite extensive diversity amongst family members, GPCRs share many of the same structural and functional characteristics. First, they are composed of 7-transmembrane helical structures, with an external N-terminal region, and an intracellular C-terminus (2). Their principal function is to transmit information from the extracellular environment to the inside of the cell to promote a signaling response. Upon ligand binding, GPCRs undergo a conformational change that promotes binding to heterotrimeric GTP-binding proteins (G proteins). Engagement with the receptor leads to an exchange of GDP for GTP on the α subunit of the G protein, causing it to disengage from the receptor and dissociate into Gα and Gβγ subunits (3). These G protein subunits amplify GPCR signals by activating a wide variety of effector proteins such as adenylate cyclase, phosphodiesterases, Ca^{2+} or K^{+} channels, and phosopholipases.

After G protein activation and subsequent signal amplification it becomes imperative that signal transduction cascades be shut down. Cells have developed an adaptive response through receptor desensitization, which prevents harmful effects caused by constant receptor stimulation. There are two types of receptor desensitization. Second-messenger-regulated kinases, PKA (protein kinase A) and PKC (protein kinase C), can phosphorylate both active and inactive GPCRs leading to "heterologous" desensitization (4). G protein-coupled receptor kinases (GRKs) on the other hand are serine/threonine kinases that only phosphorylate agonist-stimulated receptors, resulting in "homologous" desensitization. Seven mammalian GRK genes have been identified (GRK1-GRK7) (3). Receptor desensitization by GRKs occurs by a two-step process. First, GRKs phosphorylate the serines and threonines on the C-terminus or other cytoplasmic elements of the receptor. Second, when the number of receptor-attached phosphates reaches a threshold (usually 2 or 3), arrestin recognizes the active phosphorylated receptor and binds with high affinity, ultimately precluding further G protein activation (5).

The stable binding of arrestin is the terminal step in G protein-mediated receptor signaling: the receptor is unable to respond to additional ligand unless it has been re-sensitized. The receptor must be desensitized, internalized, dephosphorylated, and recycled back to the plasma membrane to become responsive again. Arrestins' role in this process became clear when studies showed that arrestins interact with clathrin, and the expression of mutant arrestins that do not bind β2-adrenergic receptor or clathrin reduced receptor endocytosis. It was later shown that arrestins bind with high affinity to clathrin (6) and adaptor protein AP2 (7) and that receptor-bound arrestin serves as an link

between receptors and clathrin coated pit formation (Figure 1-1) (8). The receptor is then internalized to endosomes, dephosphorylated, and recycled back to the plasma membrane for further activation (9, 10). In some cases, receptors are targeted for lysosomes where they are degraded.

The Arrestin family of proteins

There are 4 known arrestin subtypes, two visual arrestins, arrestin-1 and arrestin-4 which are expressed exclusively in rod and cone photoreceptors, and two non-visual arrestins, arrestin-2 and arrestin-3, which are ubiquitously expressed. The first arrestin discovered, arrestin-1, was shown to bind GPCR rhodopsin and influence light dependent signaling in rod photoreceptors (11-14). Because arrestins first known function was to terminate rhodopsin signaling, its name is derived from its ability to "arrest" further G-protein activation. One other retinal-specific arrestin was cloned, arrestin-4, which shows ~50% homology to arrestin-1 and is found predominantly in cone photoreceptors (whereas arrestin-1 is found in both rod and cone photoreceptors) (15).

Like the visual arrestins, the non-visual arrestins were discovered in the early 90's to bind the β-adrenergic G protein coupled receptor. Their original names, β-arrestin-1 and β-arrestin-2, were chosen because of their preference for β-adrenergic receptors over rhodopsin (16). It was later discovered that unlike their visual counterparts, that have preference for only rhodopsin (arrestin-1) or cone opsins (arrestin-4), the non-visual arrestins have broad receptor specificity and are capable of binding to hundreds of different GPCRs. Therefore, they were later renamed arrestin-2 and arrestin-3. Arrestin-2 is the predominant arrestin expressed in most tissue types (17), with arrestin-3 the

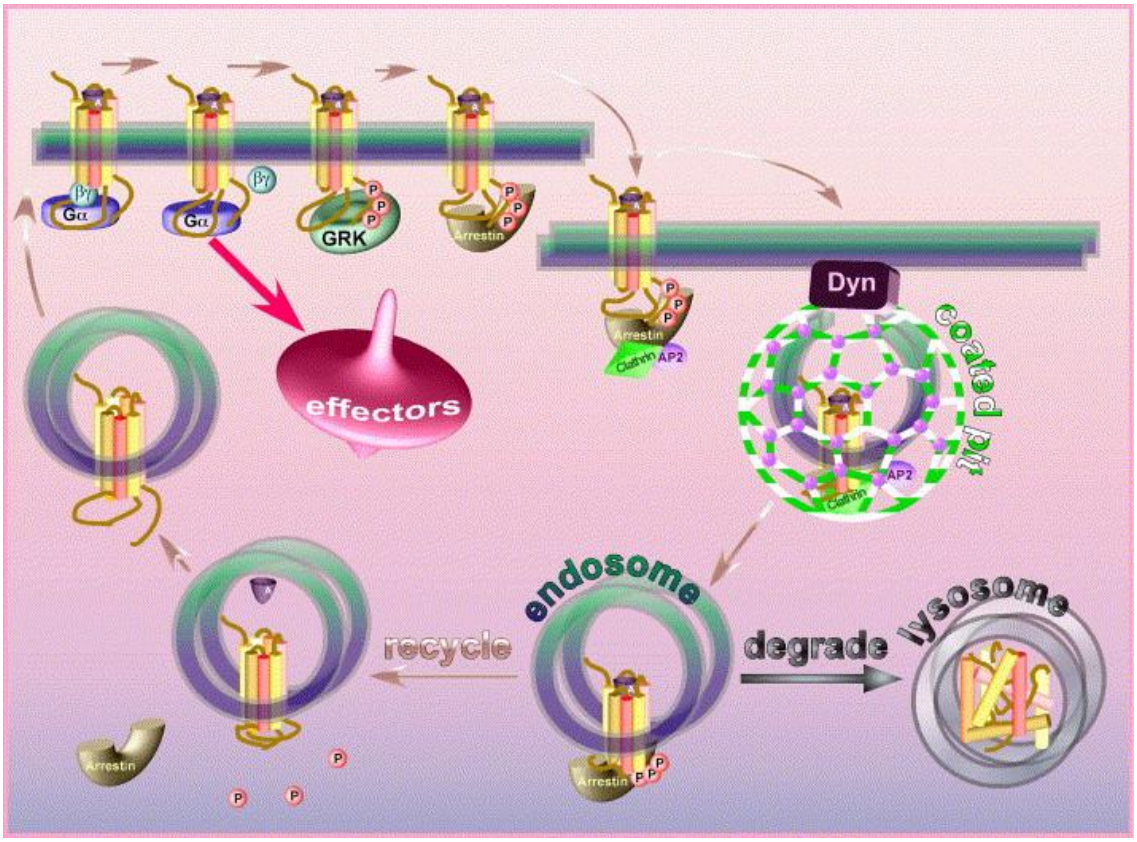

Fig. 1-1. The ‘‘classical’’ model of arrestin-mediated GPCR desensitization. The agonist-activated receptor activates cognate heterotrimeric G proteins that subsequently stimulate various signaling cascades increasing the activity of protein kinases PKA, PKC, etc. Active receptor is specifically phosphorylated by GRKs. Arrestin binds the active phosphoreceptor with high affinity, precluding further G protein activation. Arrestin serves as an adaptor linking the receptor to the internalization machinery of the coated pit (clathrin, adaptor complex AP-2), facilitating receptor internalization. Low pH in the endosome promotes agonist dissociation, which facilitates the release of arrestin, whereupon the receptor can be dephosphorylated and recycled back to the plasma membrane (resensitization). Alternatively, the receptor can be transported to lysosomes and destroyed (down-regulation). (Adapted from (18))

predominant form in olfactory epithelium (19). In addition to differences in expression level, they demonstrate certain receptor specificity, have different affinities for clathrin, and differentially activate MAP kinase cascades. For example, both arrestin-2 and arrestin-3 are able to bind the kinases of JNK3 activation cascade, but only when bound to arrestin-3 is JNK3 activated (20). However, despite functional differences, they are able to compensate if one or the other arrestin is knocked down. Mice lacking either arrestin-2 or arrestin-3 show no overt abnormalities and very small differences in phenotype, however, knock-out of both proteins is embryonic lethal (21). This finding is not surprising, the non-visual arrestins share 78% identical amino acid sequence and remarkable structural homology (22).

Arrestin structure and binding

Structurally arrestins are elongated two-domain (the N- and the C-domain) molecules with a tertiary structure that is conserved between all four subtypes (23). Arrestin is maintained in its cytosolic free state by two intra-molecular interactions. The first is a series of charged residues called the 'polar core' that bridge the domains of the protein. The second involves interaction between β-strand-1 and α-helix-1 of the N-domain, and the C-tail of the protein (three element interaction). Receptor binding disrupts both these interactions, causing a distinct conformational change in arrestin (Figure 1-2a). The 'polar core' acts as a phosphate sensor, and interaction with phosphorylated receptor breaks the bridge between the two domains, allowing arrestin to bind with high affinity (24, 25). Disruption of the three element interaction results in the release of the C-tail from the body of the protein. Upon release of these two critical

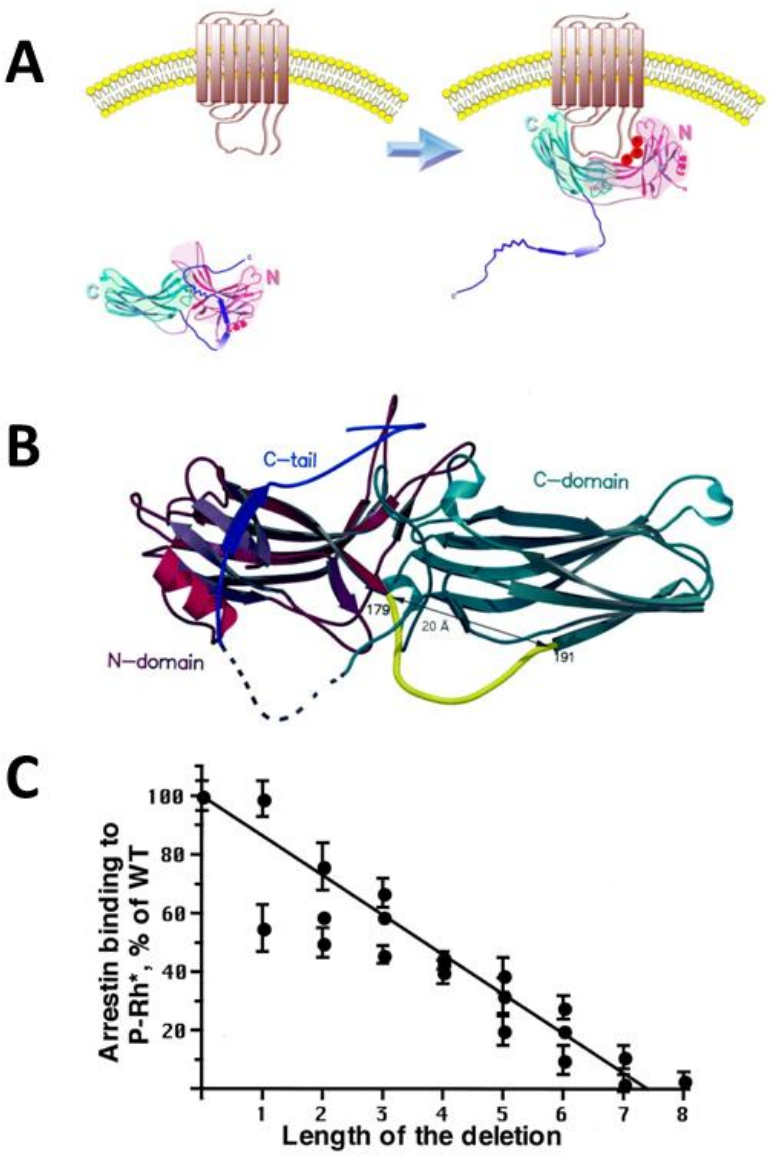

Figure 1-2. The conformation of receptor bound arrestin
(A) Arrestin undergoes a major conformational change upon binding to GPCRs. **(B)** The hinge region is colored in yellow. Residues 179 and 191 denote the borders of the hinge. The distance indicated by the line is measured from the Cα of residue 179 to the Cα of residue 190. The hashed blue section represents a crystallographically disordered part of the polypeptide. **(C)** The P-Rh* binding of 24 mutants with various deletions in the hinge region was analyzed as a function of the total number of deleted residues. The correlation was found to be statistically significant ($r = 0.91$, $F(1,23) = 107$; $p < 0.0001$). (Adapted from (26))

"clasps" that hold the protein in its free cytosolic state, the two domains of the protein are free to move relative to each other (27).

To ensure proper domain movement, a large amount of flexibility between the two domains must be present. Indeed arrestin has a 12 amino acid inter-domain connector, or hinge region, that makes this movement possible (28) (Figure 1-2b). Interestingly, the number of amino acids required to span the two domains is only five, suggesting that the additional amino acids provide flexibility through substantial 'slack' (29-31) . Additionally the hinge region has several conserved residues, all of which are prolines, glycines, and alanines further implicating the importance of flexibility. Successive deletions of this hinge region show that receptor binding is completely abolished when seven amino acids are removed, i.e., when the hinge is just long enough to cover the distance between the two domains (Figure 1-2c).

Arrestins as signaling scaffolds

Shortly after the discovery that arrestins bind to GPCRs and terminate their signaling, a variety of additional binding partners were discovered. AP2 and clathrin were among the first, and their binding sites were localized to arrestins C-tail. Furthermore, the release of the C-tail from the body of arrestin upon interaction with the receptor promotes AP2 and clathrin binding. Another interaction partner, c-Src, was also shown to be recruited to receptor-rich membranes in an arrestin dependent manner, resulting in the spatially controlled activation of extracellular signal-regulated kinases (ERK1/2) (32). The fact that several proteins, including clathrin, AP2, c-Src, and ERK preferentially bind activated arrestin (i.e. interact with the arrestin-receptor complex) (33)

suggests that the conformations of free and receptor-bound arrestin are dramatically different. Additionally it implicates arrestin as an adaptor to redirect GPCR signaling by linking signaling proteins to the receptor. Consistent with this, receptor binding elements were found to be limited to the concave sides of both arrestin domains, leaving the backside of the molecule exposed for interactions with other proteins (Figure 1-3).

Over the years the number of additional binding partners has rapidly increased. These include ARF6, ARNO, PDE4, NSF, Mdm2, IκBα, calmodulin, and a variety of protein kinases, such as Yes, cRaf1, JNK3, and ASK1 (reviewed in (34)). A majority of these proteins were also originally shown to have preference for receptor-bound arrestin, with a few exceptions. Calmodulin, was shown to bind the C-domain and a loop in the center of the arrestin molecule (35). These binding sites significantly overlap with receptor binding elements, suggesting arrestin interactions with GPCRs and calmodulin are mutually exclusive (Figure 1-3).

However, several recent studies have shown that the interactions of arrestin with its non-receptor binding partners are not so black and white. For example, the binding sites for PDE4 (36) and ARF6 (37) are exposed on either receptor-bound or free arrestin, allowing these proteins to bind either state. Additionally, ubiquitin ligase Mdm2 has higher affinity for arrestin in its free conformation. However, the receptor-arrestin complex is likely a better substrate for Mdm2, the level of arrestin ubiqutination by Mdm2 is proportional to the stability of the receptor-arrestin complex (38). This suggests that free arrestin in the basal conformation binds Mdm2, brings it to the receptor, and releases it upon receptor binding (39).

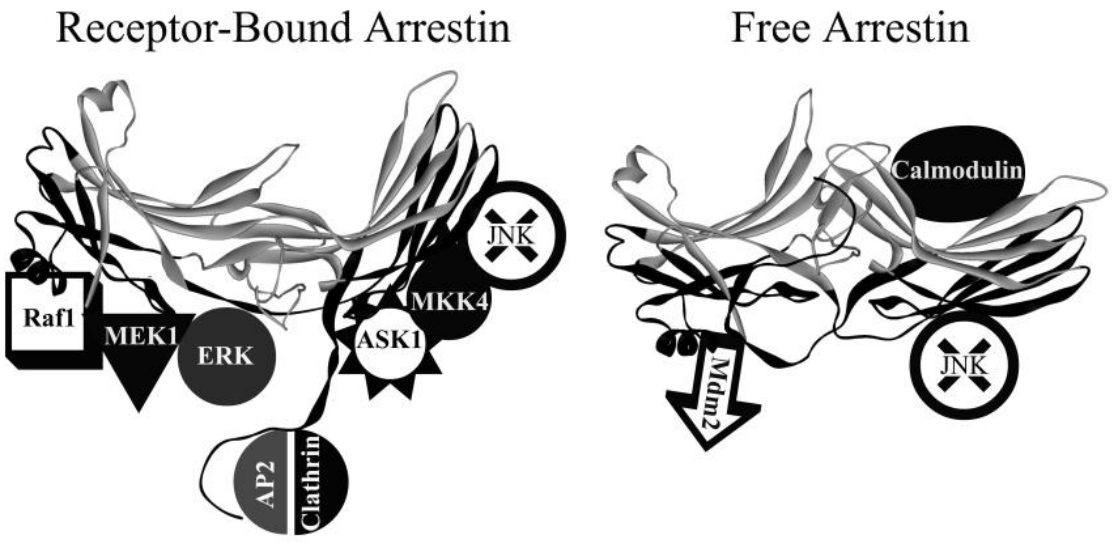

Figure 1-3. Conformational dependence of arrestin interactions with signaling proteins. Although the effect of arrestin conformation on the binding of the majority of arrestin partners remains to be elucidated, differential interactions of several proteins with free and receptor-bound arrestin have been demonstrated. Clathrin and AP2 preferentially bind receptor-associated arrestin via its released C-tail; it is not known whether microtubule binding-induced C-tail release has similar effect. Calmodulin binding site includes the elements involved in receptor and microtubule interaction, so that it can only bind free arrestin. Ubiquitin ligase Mdm2 binds all forms of arrestin, but apparently has lower affinity for the receptor-bound state. JNK3 binds free and receptor-bound arrestin. Note that in real life receptor-bound arrestin cannot simultaneously interact with all the partners shown here. (Adapted from (40))

One of the most well studied arrestin scaffolds underscores the complexity of arrestin signaling. Arrestin-2 and arrestin-3 were first reported to scaffold c-Jun NH_2-terminal kinase3 (JNK3) (41), ERK1/2 (42, 43), and p38 (44) MAP kinase activation cascades in a complex with different receptors. These cascades consist of three different kinases MAPKKK (such as Raf1), MAPKK (such as MEK), and MAPK (such as ERK1/2). Each kinase is activated by phosphorylation by the kinase that precedes it in the cascade (45). How these proteins are able to come into close quarters to each other for activation with any specificity is determined by scaffolding proteins that link the proteins together into a signaling module. Arrestin serves as a link for the proteins in these cascades, and the complexity of these interactions is only growing.

Initial data showed that JNK3 binds arrestin-3, but not arrestin-2, in a receptor-dependent manner. Activation of angiotensin 1A receptor ($AT_{1A}R$) leads to arrestin-3-dependent recruitment to the plasma membrane and subsequent activation of JNK3. Additionally, only arrestin-3 was shown to be responsive to receptor activation in this system, with arrestin-2 showing a dominant negative role in regulating JNK3 activity (46). However, later studies showed that JNK3 binding is not limited to arrestin-3. All four arrestin subtypes bind all members of the JNK3 cascade (ASK1, MKK4, JNK3) with comparable affinity (20). Only arrestin-3 was able to activate JNK3, proving that JNK3 binding to arrestin does not necessarily translate into activation. This finding partially explains the dominant-negative role of arrestin-2, where arrestin-2 is capable of binding JNK3 and keeps it in its inactive form. Moreover, an arrestin-3 hinge deletion mutant that is deficient in receptor binding was also capable of activating JNK3, proving that receptor interaction is not required (20). The fact that only arrestin-3 is capable of

activating JNK3, and that receptor interaction is not required, suggests that arrestin-3 is capable of holding ASK1, MKK4, and JNK3 in a particular configuration that promotes signal transduction (20). If this is the case, JNK3 activation likely involves only a few key residues on arrestin-3 due to the significant homology between the arrestin proteins. Indeed, multiple residues on the non-receptor binding surface of arrestin were found to be crucial in JNK3 activation (47). These studies showed that arrestin-3 can bind and activate JNK3 in both a receptor-dependent, and a receptor-independent manner.

One function of JNK3 is to translocate to the nucleus to phosphorylate various transcription factors such as ATF2 and members of the Jun family (45). To further complicate how and when arrestins bind to JNK3, the non-visual arrestins were shown to shuttle between the nucleus and the cytoplasm (48). Arrestin-3 has a functional nuclear export signal (NES) in its C-terminus and is capable of removing JNK3 from the nucleus to the cytoplasm (48, 49). Additionally, all free arrestins are able to bind JNK3 with high enough affinity to bring it out of the nucleus and dramatically change its subcellular localization (39), most likely to regulate transcription in the nucleus. Thus arrestins regulate JNK3 activity at the receptor, in the cytoplasm, and in the nucleus.

These data taken together show that arrestin-3 can activate JNK3 regardless of its conformation under different conditions (receptor-specific, and receptor-independent activation) and for different functions (Figure 1-3). However, how arrestins decide when and how to scaffold certain MAP kinase cascades largely remains a mystery.

The ability of arrestins to scaffold a variety of different proteins under a broad range of conditions underscores the wide diversity of its function, and the momentum of new discoveries is only gaining. New functions are being discovered for “old” signaling

partners such as ERK1/2 and many new interaction partners are still being discovered. One area of research where arrestins are significantly gaining territory is in the regulation of cytoskeletal-mediated events (50-53).

Arrestins regulate proteins involved in cytoskeletal rearrangement

With the growing interest in the ways cells sense chemical gradients in the environment around them, investigators hypothesized that arrestins play a role in directed migration. First, as the cell migrates the signaling must be quenched at the trailing edge of the cell. The role of arrestin in receptor desensitization and signal termination made them perfect candidates to facilitate this process. Secondly, migration requires the coordinated activation of hundreds of proteins in distinct spatial regions of the cell (54). Because arrestins are well known scaffolding proteins capable of generating their own signals and localizing proteins to distinct regions of the cell, they are also heavily suspected to regulate various signaling proteins involved in generating the forces that promote movement.

Arrestins regulate chemokine-mediated migration

Chemotaxis is the phenomenon in which cells direct their movements according to certain chemicals in their environment. This process requires an external chemical ligand interacting with a cell-surface receptor, a coordinated signaling response that leads to cytoskeletal rearrangement, cell polarization, and subsequent motility in the direction of the chemoattractant (55, 56). Two defining processes make chemotaxis possible. The formation of the leading edge, which provides the force to drive directed migration, and de-adhesion of the trailing edge, which allows the cell to move forward. These processes

are largely mediated by chemokine receptors, GPCRs that respond to chemokines released by sites of injury or inflammation (57). There are several families of chemokine receptors, each having several members. Two major families are the CXC family of chemokine receptors (CXCR1-7), activated by different CXC ligands, and CC chemokine receptors (CCR1-10), each responding to a variety of different CC ligands. These receptors are found in a variety of cell types (some have wide distribution, some are cell type specific, e.g., found only on B or T lymphocytes) (57). The first demonstration that arrestins were required for chemotaxis showed that CXCR4-mediated lymphocyte chemotaxis was defective in cells lacking either arrestin-3 or GRK6 (58). Shortly after, arrestins were implicated in a variety of other chemotactic events involving CXCR1, CXCR2, CXCR3, and CCR5, although the exact mechanisms are not known (59-61).

The role of arrestins as mediators of receptor endocytosis led investigators to hypothesize that arrestin-dependent desensitization of chemokine receptors is key to chemotaxis. Indeed, arrestin co-localization studies showed arrestins associate with chemokine receptors, but the relationship between these two proteins is complex. All of the experiments conducted to examine arrestin-dependent receptor desensitization were done in different cell types with different ligands, most of which resulted in different outcomes. For example, one study clearly showed that a chimera of CXCR1 and CXCR2 was unable to bind arrestin-3 and failed to internalize. However, chemotaxis was unaffected, suggesting that internalization is not essential for this process (62). Conversely, other studies showed that arrestin-dependent internalization is required; both CXCR1 and CXCR2 when treated with either a dominant-negative arrestin (which is unable to target receptors for clathrin coated pit formation), or when the C-terminal

phosphate sites required for arrestin binding were removed, showed defects in both internalization and chemotaxis (63). Other reports showed that when a single amino acid of the second intracellular loop of CCR5 required for arrestin-dependent chemotaxis was mutated, the receptor still underwent ligand-induced endocytosis but chemotaxis was inhibited (60, 64). These data suggest that the chemokine response systems are quite complex.

One study in particular highlights the complexity of chemokine receptor signaling. CXCR3, which is activated by three ligands (CXCL9, -10, -11), can produce dramatically different outcomes based on the ligand and the conditions. For example, activation by CXCL11 results in higher level of internalization than CXCL9 or -10. Additionally, chemotaxis as a result of treatment of cells with high levels of CXCL9 and CXCL11 but not CXCL10 requires residues in the third intracellular loop of the receptor. Conversely, the C-terminus of the receptor is required for chemotaxis when cells are treated with CXCL10 and CXCL9, but not CXCL11. These data show that different components of the receptor are used in ligand-biased ways, where CXCL10 and CXCL9 predominantly induce a pathway dependent on the receptor C-terminus, and CXCL11 predominantly promotes signaling initiated by other elements of the receptor. Additionally, the concentrations of these ligands also play a role in determining the outcome of chemokine receptor signaling as evidenced by the different pathways activated by treatment with either high or low levels of CXCL9 (65).

Data showing that internalization is not required for chemotaxis for some receptors, or that arrestin-dependent chemotaxis was inhibited even when some receptors were internalized suggests that arrestins play a role beyond mediating endocytosis.

Arrestins also act as signaling scaffolds for a variety of cytoskeletal regulatory proteins, and are capable of localizing them to particular compartments of the cell, or scaffolding them for activation.

Arrestins as regulators of the small GTPases

There is growing evidence for a role of the non-visual arrestins in facilitating small GTPase-mediated events. Rho family GTPases are small G proteins that act as bimolecular switches that regulate the signal transduction pathways that connect the plasma membrane receptors to the cytoskeleton of the cell (66). The three most characterized Rho GTPases are RhoA which promotes stress fiber formation, Rac1, important for membrane ruffling and lamellipodia, and Cdc42 a well-known inducer of filopodia formation (67, 68). They regulate many important cellular processes that range from cytoskeletal rearrangement, gene expression, membrane trafficking, and are essential for motility in most systems (69). The first study to link arrestins to RhoA activity showed that RhoA is coordinately activated by arrestin-2 and Gαq/G11 upon activation of the Angiotensin II type 1A receptor ($ATII_{1A}R$). This leads to stress fiber formation mediated through Rho-associated protein kinase. Knock-down of either Gαq/G11 or arrestin-2 (but not arrestin-3) significantly reduces RhoA activity (70). However, the precise mechanism through which arrestin-2 and Gαq/G11 activate RhoA in a concerted manner was not addressed. However, both direct and indirect mechanisms by which arrestins regulate RhoA activity were later described.

First, arrestin-3 was shown to directly bind RhoA in Xenopus embryos. The movement of cells in gastrulation and axis formation are critical for vertebrate development. Depletion of Xenopus arrestin-3 (xArr3) in embryos resulted in major

developmental defects in convergent extension (CE), a process that involves cell migration to define and extend the antieror/posterior axis. In particular, loss of xArr3 results in delay of blastopore closure, failure of neural tube closure and anterior/posterior axis formation. These defects resemble those caused by altered signaling of Wnt pathway components, including downstream protein RhoA (71). Experiments to determine whether RhoA is involved in the xArr3 specific defects demonstrated that xArr3 binds directly to RhoA, resulting in its recruitment and accumulation at the plasma membrane. In addition, xArr3 also bound to Daam1, a formin homology (FH) protein involved in scaffolding and activating RhoA. Daam1-RhoA-xArr3 interaction resulted in the activation of RhoA and regulation of CE movements at the plasma membrane (72).

The key feature of the small GTPases is the ability to switch between inactive and active forms. To achieve this balance, they interact with three types of regulatory proteins: guanine nucleotide exchange factors (GEFs), which exchange GDP for GTP to render small G proteins active, guanine nucleotide dissociation inhibitors (GDIs), a regulatory protein that prevents GDP/GTP exchange and inhibits membrane localization, and GTPase-activating proteins (GAPs), which accelerate the GTPase activity and promote hydrolysis of GTP to inactivate the small G protein (73). Arrestin-2 but not arrestin-3 was shown to indirectly regulate RhoA activity by direct interaction with ARHGAP21, a GAP protein known to localize to the Golgi apparatus were it can act as a GAP for RhoA, Rac1, and Cdc42. Importantly, arrestin-2 binds directly with GAP domain of the protein: the interface that interacts with RhoA to accelerate hydrolysis of GTP. Arrestin-2 binding essentially inhibits the interaction of ARHGAP21 with RhoA, resulting in prolonged RhoA activity. Direct disruption of the ARHGAP-Arrestin-2 complex results in more active ARHGAP21, and less

RhoA activity. Interestingly, this complex is not dependent on receptor activation, however, the concentration of the ARHGAP21-Arrestin-2 complex increases upon activation of the AT1AR receptor (74). The mechanism is not well known, however it is proposed that the conformation of receptor-bound arrestin may bind ARHGAP21 with higher affinity.

Arrestin was also shown to interact with another, less studied, GTPase. Under basal conditions, inactive Ral-GDS is localized within the cytosol of the cell as a result of interaction with cytosolic arrestin-2. Upon fMet-Leu-Phe receptor (fMLP) stimulation, arrestin translocates to the plasma membrane, bringing Ral-GDS within the proximity of RalA. Disruption of the Ral-GDS-arrestin interaction results in Ral-GDS activation of the Ral effector pathway and subsequent membrane ruffling (75). Depletion of arrestin-2 in these cells inhibits Ral-mediated membrane ruffling. While arrestin interaction does not result in activation of these proteins, this study underscores the importance of arrestin as a shuttle for proper localization of signaling proteins.

The role of arrestins in actin assembly

Recent investigations show that arrestins act as a scaffold for proteins involved in actin assembly. Cofilin is an actin filament-severing protein that causes depolymerization at the minus ends of actin filaments by creating positive ends, a process that is tightly regulated spatially and temporally. Cofilin is regulated by a recently identified cofilin-specific phosphatase, chronophin (CIN), that dephosphorylates residue Ser3 resulting in its activation. Conversely, phosphorylation at this site by LIM kinase (LIMK) renders cofilin inactive (76, 77). Because cell migration involves rapid turnover and formation of protrusions at the leading edge of the cell, the non-visual arrestins were prime candidates to localize cofilin to its site of action at the plasma membrane. Indeed,

it was shown that arrestin-2 and arrestin-3 bind all three proteins: cofilin, chronophin, and its inhibitor LIMK, and recruit them to the leading edge of the cell upon PAR-2 receptor stimulation. The result of this scaffold leads to arrestin-dependent activation of cofilin (78). Conversely, knock-down of arrestin through siRNA showed that PAR-2 stimulation led to an increase in LIMK activity, suggesting that arrestin may bind LIMK to "keep it away" from the phosphorylation site on cofilin to prevent its deactivation. Therefore, the scaffold has three essential functions: 1) To localize cofilin to compartments of the cell where it can modify the actin cytoskeleton to create membrane protrusions, 2) bring cofilin in proximity to its activating protein, cronophin, leading to its activation, and 3) recruits LIMK to possibly "dock" it away from cofilin to prevent its deactivation. Interestingly, while PAR-2 induced cofilin dephosphorylation and filament severing can be mediated by either arrestin, arrestin-3 was found to colocalize with cofilin predominantly in the back of F-actin-rich protrusions, and arrestin-2 was predominantly found at the tips. Additionally, arrestin-2 associated with CIN within 5 minutes of PAR-2 stimulation but arrestin-3 could not be co-immunoprecipitated with CIN. This suggests a role for arrestins in regulating the spatial restriction of cofilin activity, and that the role of arrestin-2 and arrestin-3 in mediating actin filament severing is different.

Receptor desensitization meets cytoskeletal organization

ARNO (Arf nucleotide binding site opener) has been reported to interact with the non-visual arrestins to regulate receptor desensitization (79). ARNO is also a GEF for ARF6 (ADP-ribosylating factor 6) which couples to the cytoskeleton via ELMO (engulfment and cell motility protein) to regulate lamellipoda formation and cell

migration (80). Arrestin acts as a scaffolding protein for the ARNO-Arf6-ELMO signaling network, which is activated upon stimulation of the calcium-sensing receptor (CaSR) in an arrestin-dependent manner (81). This suggests that arrestins localize these proteins to the receptor for activation, while also promoting endocytosis through an ARNO dependent mechanism. With this model it is easy to imagine a scenario where arrestins bring regulatory proteins to the leading edge to promote cytoskeleton rearrangement, while also desensitizing receptors to facilitate gradient sensing.

Arrestins and cancer

Recently it has been reported that arrestin-3 acts as a scaffold protein in mitogen-activated protein kinase (MAPK) cascades that positively regulate chemotaxis. Arrestin-3 depletion promotes CXCR2-mediated cellular signaling, including excisional wound closure and angiogenesis. To further investigate the role of arrestin-3 in tumorigenesis, a murine model of lung cancer was used to compare arrestin-3-deficient mice (Arr3-/-), and control littermates (Arr3+/+). In mice deficient in arrestin-3, tumor growth occurred 3.2-fold faster as compared with littermate controls. Additionally, the number of metastatic lung nodules in Arr3-/- mice was significantly greater; with ~5.66-fold higher colonization in the lungs relative to wild-type animals. In addition, tumor infiltrates form Arr3-/- deficient mice showed a significant decrease in NK+ cells, CD3+, CD4+, and CD8+ lymphocytes relative to Arr3+/+ mice (61). Whether or not this decrease in T cell infiltration contributes to the significant increase in tumor development and metastasis is unclear.

It is clear that arrestins regulate the cytoskeletal proteins on many levels. They desensitize and internalize chemokine receptors so they can be recycled back to the

plasma membrane to promote continual gradient sensing. Arrestins also act as shuttling proteins that localize cytoskeleton associated proteins to the plasma membrane such Ral-GDS or the ARNO/Arf6 complex. They assemble regulatory proteins with their activation proteins, such as RhoA and Daam1, or cofilin with chronophin, leading to their activation. All of these studies implicate arrestins as indirect regulators of the cytoskeleton, however, recent studies show that arrestins may play a more direct role. The first indication of this was the discovery that visual arrestin-1 binds directly to the cytoskeleton in the visual system. Because arrestins bind to and recruit a vast array of signaling proteins, this interaction could potentially result in many functional outcomes.

Arrestins bind directly to the cytoskeleton

Arrestin-1 function and translocation in rod photoreceptors

The best characterized signaling proteins for any GPCR-mediated signaling pathway are involved in vertebrate phototransduction. They include rhodopsin, the GPCR responsible for light detection, transducin, the visual G protein, and rhodopsin kinase (GRK1). All players in this cascade have served as structural and functional models for their non-visual counterparts. Upon activation by light, 11-cis-retinal covalently linked to rhodopsin is photoisomerized to all-trans-retinal, rendering rhodopsin active (R*). R* causes the rapid exchange of GDP for GTP on the G protein transducin, thus propagating the phototransduction cascade. Because rods demonstrate single photon sensitivity, the shut-off mechanism for rhodopsin must maintain high temporal resolution and sub-second kinetics (82-84). To this end, rhodopsin is desensitized in a two-step mechanism. The first step occurs when a specific kinase,

GRK1, recognizes the activated receptor and phosphorylates its C-tail. When the number of phosphates reaches three (P-Rh*) (85, 86), arrestin-1 binds the receptor with high affinity, thereby sterically precluding transducin from further interaction with rhodopsin (87, 88). P-Rh* subsequently decays to phosphoopsin, loses all-trans-retinal, is reconstituted with 11-*cis*-retinal produced by the retinal pigment epithelium, and is dephosphorylated. Ultimately, these processes regenerate the inactive state of Rh that does not bind transducin or arrestin with appreciable affinity.

Even though rhodopsin activation and termination serves as a model for nearly all GPCRs, photoreceptor signaling is unique in many ways. Rod photoreceptors are polarized elongated neurons that are comprised of an outer segment (OS) where rhodopsin, transducin, and GRK1 are located, an inner segment (IS) where visual arrestin-1 is retained in the dark, a cell body for cell maintenance, and the synapse. There are approximately 1 billion rhodopsins per photoreceptor cell in the OS, implicating the massive potential each photoreceptor has to amplify light into electrical signal. Arrestin-1 binds rhodopsin at ~1:1 ratio (89, 90), suggesting that nearly all of the arrestin in the photoreceptor (expressed at a similar concentration to rhodopsin) would be required to shut down signaling in situations of prolonged illumination. Since arrestin is kept in the IS of the cell in the dark, this would require mass translocation to the OS. In the dark, arrestin is almost completely excluded from the outer segment, whereas it concentrates in this compartment in the light (Figure 1-4). Although this massive translocation of arrestin from the IS to the OS was described long ago, how it is transported to the OS during illumination and how it is retained in the IS in the dark were only recently demonstrated.

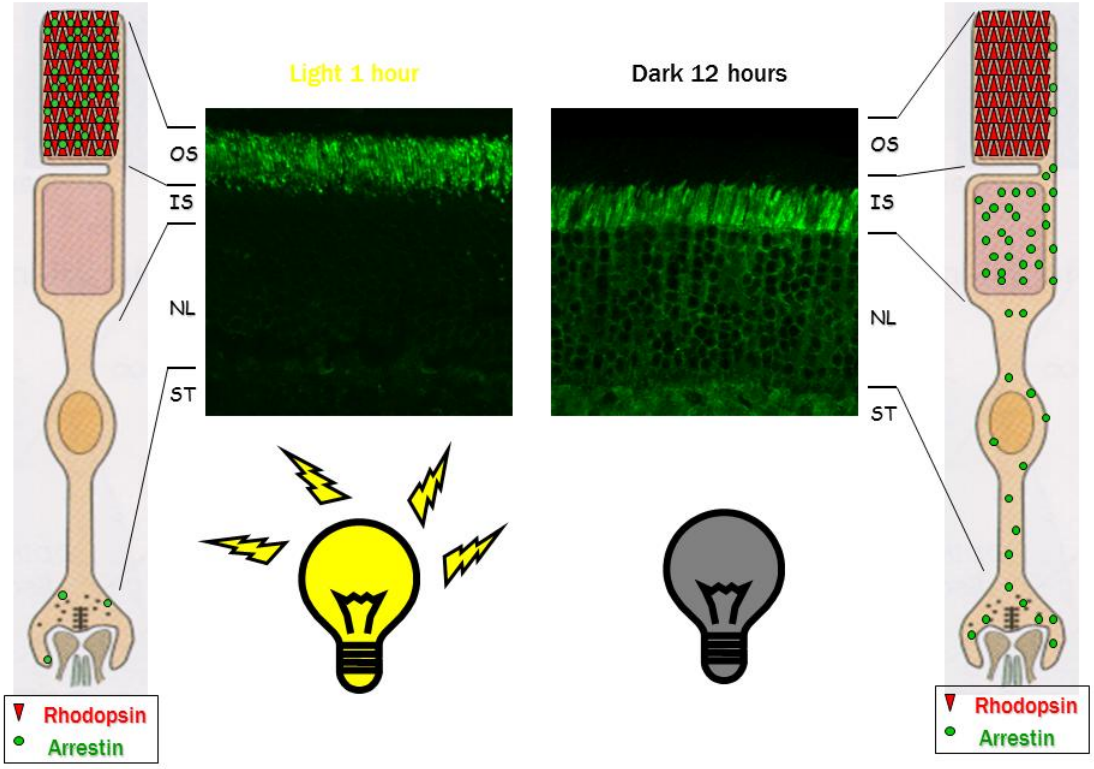

Figure 1-4. Light-dependent movement of arrestin in rod photoreceptors. Arrestin-1 undergoes robust light-dependent translocation, localizing to the OS in the light, whereas in dark-adapted rods it is predominantly detected in the IS, perinuclear area, and synaptic terminals. Arrestin-1 binding to P-Rh* necessary for the effective photoresponse shutoff occurs within 150ms after the flash or even faster, whereas arrestin-1 translocation to the OS happens on the time scale of many minutes. Thus, arrestin-1 already present in the OS is responsible for the termiantion of photoresponse of dark-adapted rods. The estimates of the fraction of arrestin-1 in the OS of WT mice vary widely, from 2-9% of the total.

Data clearly show that arrestin translocation occurs by diffusion and is energy independent; even when ATP has been depleted from the photoreceptors translocation is not affected. Furthermore, in mice with impaired synthesis of 11-*cis*-retinal ($RPE65^{-/-}$), light does not induce arrestin movement to the OS, indicating that active rhodopsin is required for this process (91). Interestingly, the amount of arrestin-1 that can translocate to the OS in the light is limited by the amount of rhodopsin present in this compartment (92) indicating that rhodopsin is the binding partner that holds arrestin-1 in the OS in the light.

Arrestin interaction with microtubules

However, simple diffusion cannot explain why arrestin accumulates in the IS in the dark. With diffusion alone, the concentration of arrestin would only equalize in the OS and the inner compartments. However, its precise localization in different light-dark states suggests arrestin-1 needs an anchoring mechanism. Because arrestin does not have lipid modifications that restrict it in different compartments, the most likely mechanism would involve direct interaction with binding partners. This interaction partner must be sufficiently abundant in the IS, considering the high expression of arrestin in rods (93). Importantly, the inner segments of photoreceptor cells are incredibly abundant in microtubules, with most polymerized microtubules (MTs) in the axoneme of the cell with a much smaller proportion extending into the OS. Additionally, in an attempt to identify arrestin docking proteins by affinity chromatography, tubulin was shown to directly bind to arrestins, making it a strong candidate for arrestin localization in the IS (94). Additional studies showed that a fraction of arrestin is retained in the dark-adapted OS in

amphibian rods, where it colocalizes with the axoneme (95), and arrestin-1 in mouse rods was detected near microtubules by electron microscopy (96).

To investigate whether arrestin binding to microtubules plays a role in its light-dependent translocation, association of arrestins with cytoskeletal fractions in light- and dark-adapted mouse retinas were examined. Virtually all arrestin in the OS was soluble in the light, whereas within 15 min in the dark, a significant proportion of arrestin became associated with the cytoskeleton. This fraction of arrestin remained bound to the cytoskeleton for up to 12 hours until light exposure of the dark-adapted mice triggered its return to the soluble fraction (97). Additional experiments with purified proteins show that microtubules and rhodopsin compete for arrestin binding, suggesting that the interactions of arrestin with rhodopsin and microtubules are mutually exclusive (94).

Given that arrestin is retained in a microtubule rich compartment, that light facilitates the release of arrestin from microtubules, and that receptors and microtubules compete for receptor binding, microtubules most likely serve as a "default" arrestin binding partner, where it is sequestered in the dark and from which it is quickly released.

Arrestin does not affect tubulin polymerization and microtubule bundling

To determine whether arrestins affect microtubule function, the rate of tubulin polymerization was measured in the presence of arrestin. Interestingly, arrestin had no effect on tubulin polymerization. Additionally, microtubule bundling detected by fluorescence microscopy showed no differences in the presence or absence of arrestin-1. These data suggest that the primary function of arrestin-1 binding with pre-existing microtubules is to localize arrestin in the IS of the cell, and not to regulate microtubules (98).

All four arrestin subtypes bind microtubules in living cells

The massive movement of visual arrestin from rod inner segments to the outer segments of photoreceptor cells upon rhodopsin activation reveals the importance of its proper distribution throughout the cell. Remarkable structural homology between arrestin family members (99) suggests that other arrestin subtypes may also interact with MTs. Cytoskeletal fraction experiments showed that indeed, all arrestin subtypes interact with microtubules. In fact, other arrestins bind microtubules better than arrestin-1, with arrestin-3 showing the highest binding. The quantification of soluble and cytoskeleton-associated arrestins showed that about 2-3 % of wild type arrestin-1, arrestin-4, and arrestin-2 are associated with MTs, and this proportion increases to ~8% for arrestin-3 (Figure 1-5a). Moreover, both arrestin-2 and arrestin-3 were shown to colocalize to microtubules in living cells. Additionally, truncated arrestin-2, which binds MTs better than WT, co-localizes with microtubules to a much greater extent in cells (Fig.1-5b). Thus, the association with microtubules in cells is a common characteristic of all arrestin subtypes (100).

The conformation and binding sites of microtubule-bound arrestin-2

Numerous lines of evidence demonstrate that the conformations of free and receptor-bound arrestin are substantially different (101-103). The N- and C-domains of arrestin are connected by a 12-residue loop termed the “hinge region” (Figure 1-2b) (104). Interestingly, progressive deletions in the inter-domain hinge that severely impede receptor binding, actually enhance MT binding of all arrestins, suggesting that the conformation of MT-bound arrestin differs from that of the receptor-bound form.

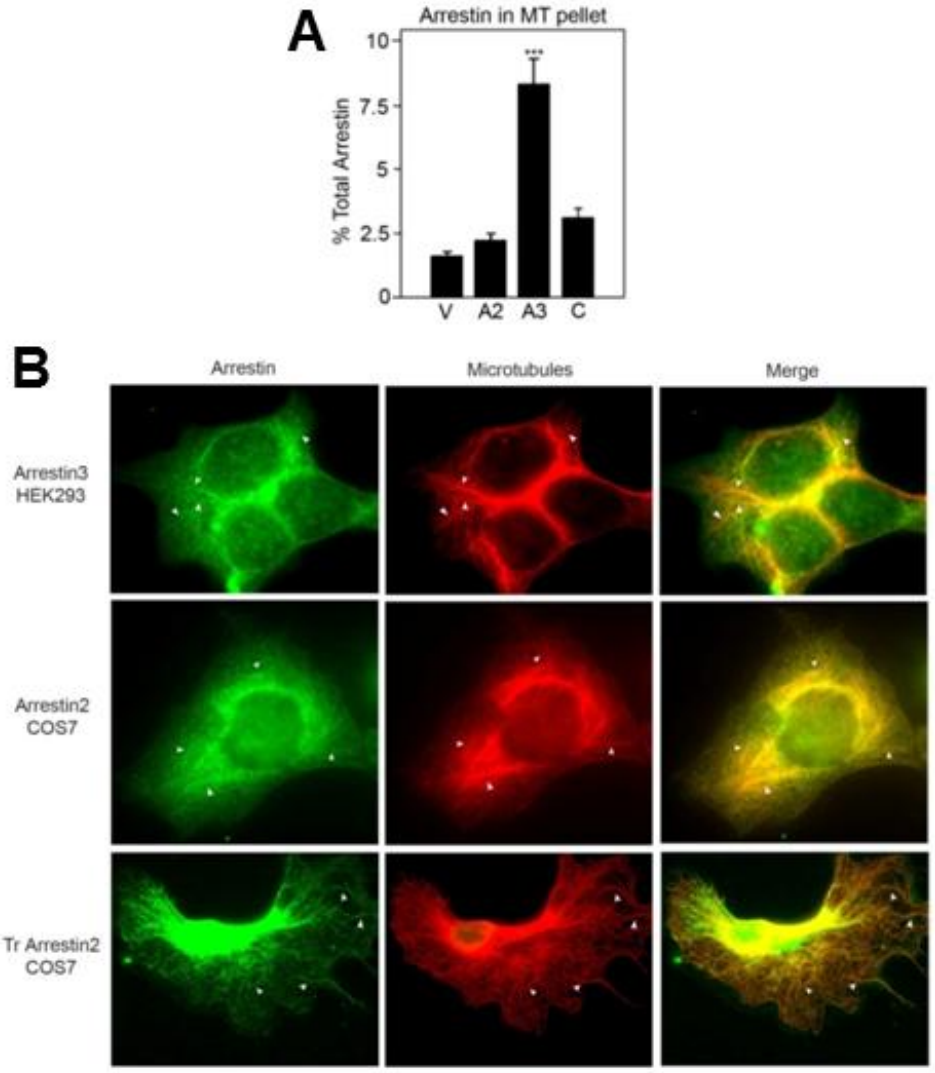

Figure 1-5. Arrestins bind microtubules in cells.
(A) The percentage of arrestin in the cytoskeletal pellet fraction was quantified and analyzed by one-way ANOVA with arrestin type as the main factor. The percentage of arrestin3 in the pellet fraction is significantly greater than that of the other arrestins (*** $p<0.001$). **(B)** HEK293 cells expressing Flag-tagged arrestin3 or COS7 cells expressing untagged WT or Tr arrestin2 were fixed and stained as described in the Methods. White arrowheads indicate places where arrestin colocalization with microtubule bundles is most pronounced. Abbreviations: V, wild type visual rod arrestin; VD7, rod arrestin hinge deletion mutant; A2, wild type arrestin2; A2D7, arrestin2 hinge deletion mutant; A2Tr, truncated arrestin2(1-382); A3, wild type arrestin3; C, wild type cone arrestin. (Adapted from (100))

Importantly, the MT association of arrestin hinge deletion mutants was similarly enhanced in cells.

To investigate binding elements of arrestin important for microtubule binding, site-directed spin labeling (SDSL) electron paramagnetic resonance (EPR) spectroscopy was used. This method requires the elimination of reactive native cysteines from the protein, the introduction of a unique cysteine at the position of interest, and subsequent modification of the cysteine with a sulfhydryl-specific spin label to generate the side chain R1. Cysteine residues at 16 different positions spanning the entire molecule on the background of fully functional cysteine-less arrestin-2 were introduced. These spin-labeled proteins were examined by EPR to determine microtubule-induced changes in R1 mobility.

Changes in mobility were detected for several positions on the β-strands of the concave sides of both arrestin-2 domains. Some of the most dramatic changes occurred at four positions in the flexible "finger loop" between β-strands V and VI. Interestingly, both the concave sides of the N- and C-domain and the "finger loop" were recently shown to play a key role in receptor binding (Figure 1-6a) (105). Other residues located on the concave surface showed little to know movement in the presence of microtubules. Overall, the positions with the strongest changes in the spin label mobility define an extensive microtubule "footprint" on the arrestin-2 molecule (100) localized on the same surface that was previously implicated in receptor binding (102, 105, 106) (Figure 1-6b)

Because the MT-binding site covers the concave surfaces of both domains and significantly overlaps with the receptor-binding site indicating that arrestin cannot interact with the receptor and microtubules simultaneously. Conceivably, arrestin

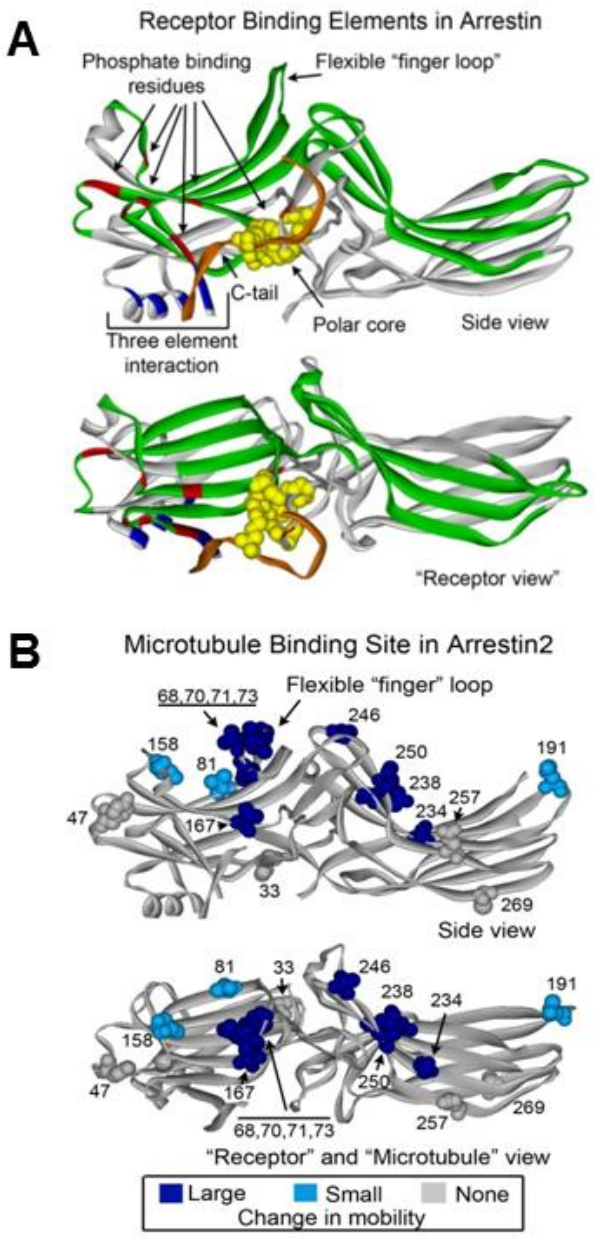

Figure 1-6. Arrestins bind microtubules with the same interface as the receptor. **(A)** Visual arrestin crystal structure highlighting functional elements important for receptor binding as follows: the "phosphate sensing" polar core, yellow; other phosphate binding residues, red; C-tail, orange; bulky hydrophobic residues participating in the three element interaction between b-strand I, a-helix I, and C-tail, blue; b-strands and loops shown to participate in receptor binding, green. **(B)** Summary of the changes in spin label mobility induced by arrestin interaction with MTs. Large changes in mobility indicate residues important in microtubule binding. The magnitude of the detected changes are highlighted on the arrestin2 crystal structure as follows: positions with large decreases in mobility, dark blue; small decreases, light blue; no change, gray. (Adapted from (18) and (100))

association with MTs may serve three functions (which are not mutually exclusive): 1) to keep arrestins away from receptors, similar to its apparent role in rod photoreceptors (107); 2) to sequester arrestin binding partners to regulate their activation; 3) to mobilize signaling proteins to the cytoskeleton and direct their activity toward MT-associated substrates. The full range of biological implications of the functional link between arrestins and the cytoskeleton is unknown.

CHAPTER II

ARRESTIN MOBILIZES SIGNALING PROTEINS TO THE CYTOSKELETON AND REDIRECTS THEIR ACTIVITY

Much of the work in this chapter was published in the Journal of Molecular Biology in February 2007 (100)

The paper was a collaborative effort between the laboratories of Vsevolod V. Gurevich, Vladlen Z. Slepak, and Candice S. Klug.

Introduction

As their name implies, arrestins were originally described as proteins that terminate G protein-mediated signaling by binding the activated phosphorylated forms of their cognate G protein-coupled receptors (GPCRs) (reviewed in (5, 103, 108)). Recent discoveries of their interactions with numerous other binding partners revealed the role of arrestins as multi-functional regulators of cell signaling (reviewed in (109, 110)). Arrestins redirect GPCR signaling to G protein-independent pathways and determine the intracellular localization of key regulatory proteins. In particular, arrestin retains ERK2 and JNK3 in complex with the receptor in the cytoplasm and removes Mdm2 and JNK3 from the nucleus (reviewed in (109, 111, 112)).

Most non-receptor partners bind the arrestin-receptor complex, engaging arrestin elements that are not involved in receptor binding (109, 112). Recently, we identified microtubules (MTs) as an interaction partner of visual arrestin-1. The MT-binding site

on arrestins significantly overlaps with the receptor-binding site, but the conformations of MT-bound and receptor-bound arrestin are different. We found that arrestins recruit ERK1/2 and ubiquitin ligase Mdm2 to microtubules, differentially affecting their activity. Arrestin-dependent mobilization of signaling molecules to the cytoskeleton is an earlier unappreciated link in the network of cellular regulatory pathways.

Materials and Methods

Arrestin binding to microtubules in cells

HEK-293A cells were transfected with expression plasmids encoding untagged arrestins and/or HA-Mdm2 and/or HA-ubiquitin using Lipofectamine 2000. 48 hours post-transfection cells were incubated with 5 μM taxol for 1.5 hours at 37^{o}C and washed with 80 mM PIPES pH 6.8, 70 mM NaCl, 1 mM $MgCl_2$ (PB). Cells were cross-linked by incubation in PB, 5 μM taxol, and 2 mM DSP (Pierce) for 30 min and quenched by 50mM Tris pH 7.4 for 15 min at RT before lysis in PB supplemented with 0.2% NP-40 and 1mM PMSF. Lysates were centrifuged at 400x*g* for 5min to remove cell debris. The supernatant was loaded onto a 60% glycerol cushion made in PB and microtubules were pelleted by centrifugation for 20 min at 25 °C at 90,000 rpm in a TLA 120.1 rotor in a Beckman TL100 ultracentrifuge. The pellet was dissolved in Laemmli's sample buffer and aliquots of the lysate, supernatant, and pellet were analyzed by Western blot using arrestin (F4C1), α-tubulin, Mdm2, HA (Sigma), ERK1/2, PP-ERK, JNK3, PP-JNK3 (Cell Signaling) or PP2A (BD Biosciences) antibodies. The cross-linking step was omitted in experiments designed to measure protein ubiquitination.

Results

Functional consequences of the arrestin-microtubule interaction.

Receptor-bound arrestins function as adaptors mobilizing the components of the trafficking machinery (6, 7) and recruiting a variety of signaling proteins to agonist-activated GPCRs (109, 112). Non-visual arrestins serve as scaffolds for the ASK1-MKK4-JNK3 and Raf-MEK-ERK1/2 MAP kinase cascades and target active ERK1/2 and JNK3 to specific subcellular locations (109, 113-115). Ubiquitin ligase Mdm2 interacts with receptor-bound (116) and free (117, 118) arrestins and plays a role in receptor ubiquitination (116, 119). The MT-binding site mapped by two different methods covers a large portion of the concave surface of both arrestin domains and overlaps with the receptor-binding site (102, 105, 106). Thus, arrestin cannot interact with the receptor and microtubules simultaneously. Most importantly, in MT- and receptor-bound arrestin the docking sites for non-receptor partners may be equally accessible, enabling arrestin-dependent mobilization of signaling proteins to the cytoskeleton. To test this idea, we examined the localization of two known arrestin partners, ERK1/2 and Mdm2, in cells expressing different arrestins.

We found that the proportion of endogenous ERK1/2 present in the cytoskeletal fraction is significantly increased in cells expressing visual arrestin (arrestin-1), arrestin-2 or arrestin-3 (Figure 2-1a,c), indicating that these three subtypes bring ERK to the microtubules. Arrestin-dependent mobilization of ERK to the receptor results in ERK activation by upstream kinases, c-Raf-1 and MEK1 (114). We tested whether this is also the case for ERK mobilized to MTs. The amount of active PP-ERK detected in the MT pellet fraction was negligible. However, the level of PP-ERK in the soluble fraction was

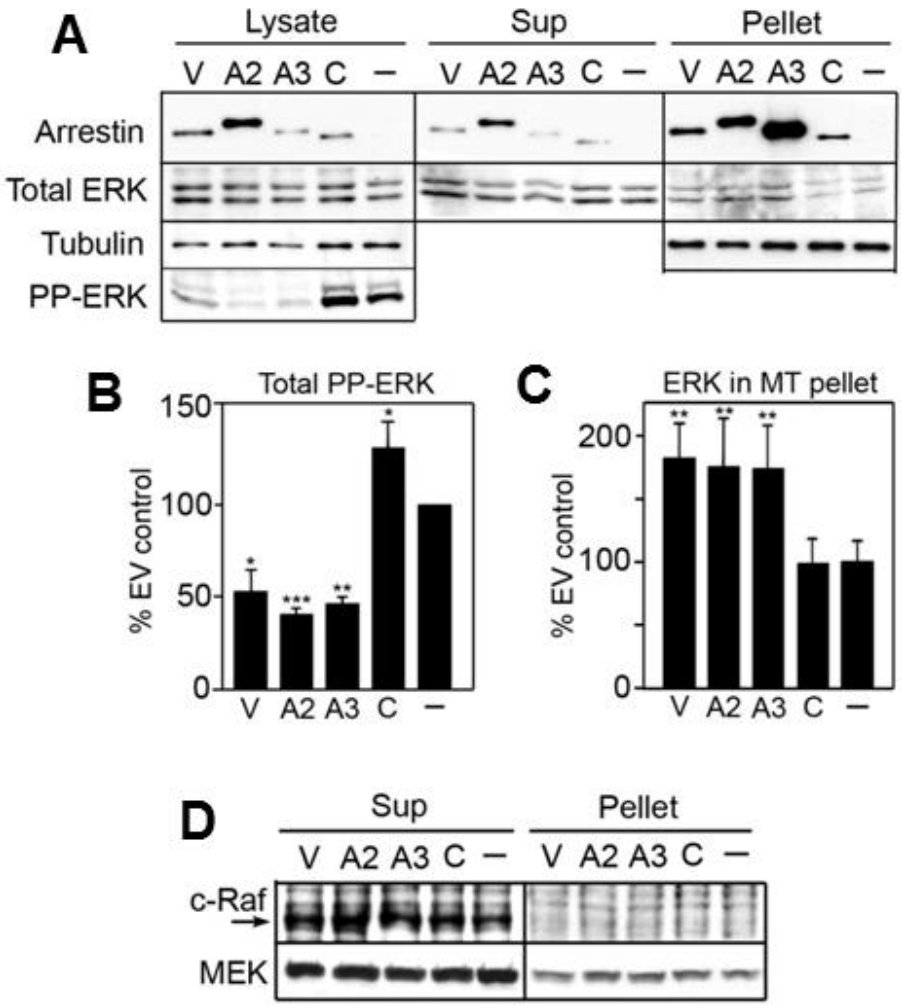

Figure 2-1. Arrestin-mediated sequestration of ERK to microtubules.
(A,D) HEK-293 cells transfected with the indicated arrestins or empty vector (-) were fractionated as described in the Methods and analyzed by Western blot. Representative blots from 5 experiments demonstrating the relative amount of each protein in the lysate, soluble (sup), and cytoskeletal (pellet) fractions are shown. PP-ERK1/2 in the lysate **(B)** and total ERK1/2 in the cytoskeletal fraction **(C)** was quantified. The data were analyzed by one-way ANOVA with arrestin type as the main factor. *$p<0.05$, **$p<0.01$, *** $p<0.001$, compared to control. The percentage of ERK1/2 in the cytoskeletal fraction of control cells was 1.24 $\pm$ 0.41 % of the total ERK in the cell. Abbreviations: V, WT visual arrestin-1; A2, WT arrestin-2; A3, WT arrestin-3; C, WT arrestin-4; PP-ERK, phosphorylated active ERK.

significantly affected by arrestin expression (Figure 2-1a,b). Rod and non-visual arrestins dramatically reduced active ERK (by ~50%). Importantly, cone arrestin, which does not mobilize ERK to MTs, did not have this effect, suggesting that arrestin-dependent mobilization of ERK to MTs decreases the total level of active ERK in the cell by removing ERK from cellular compartments where it can be activated. Indeed we found that arrestins do not increase the proportion of upstream kinases MEK1 and c-Raf-1 in the cytoskeletal fraction (Figure 2-1d), suggesting that the sequestration of an individual member of the MAP kinase cascade to MTs dampens signaling.

The amount of endogenous Mdm2 present in the cytoskeletal fraction is also significantly increased in cells expressing rod and non-visual arrestins, but not cone arrestin (Figure 2-2a,b). Overexpressed HA-Mdm2 follows the same pattern (Figure 2-2b). Because Mdm2 is an E3 ubiquitin ligase, we tested whether its arrestin-dependent mobilization to microtubules affects the ubiquitination status of associated proteins. As shown in Figure 2-2, rod arrestin dramatically increases the ubiquitination of numerous proteins in the cytoskeletal fraction. Rod arrestin also increases the overall level of protein ubiquitination, whereas arrestin-3 and cone arrestin reduce the total ubiquitination of most substrates, as compared to control cells (Figure 2-2a, total=sup+pellet; Figure 2-2c, left panel). Interestingly, even though arrestin-3 significantly reduces total ubiquitination (more than any other arrestin), the percentage of the ubiquitinated proteins in the MT fraction of arrestin-3-expressing cells is elevated to the same extent as in cells expressing rod arrestin (Figure 2-2a, pellet; Figure 2-2c, right panel). Thus, the four arrestin subtypes differentially affect the mobilization of Mdm2 to microtubules and the ubiquitination of soluble and cytoskeletal proteins.

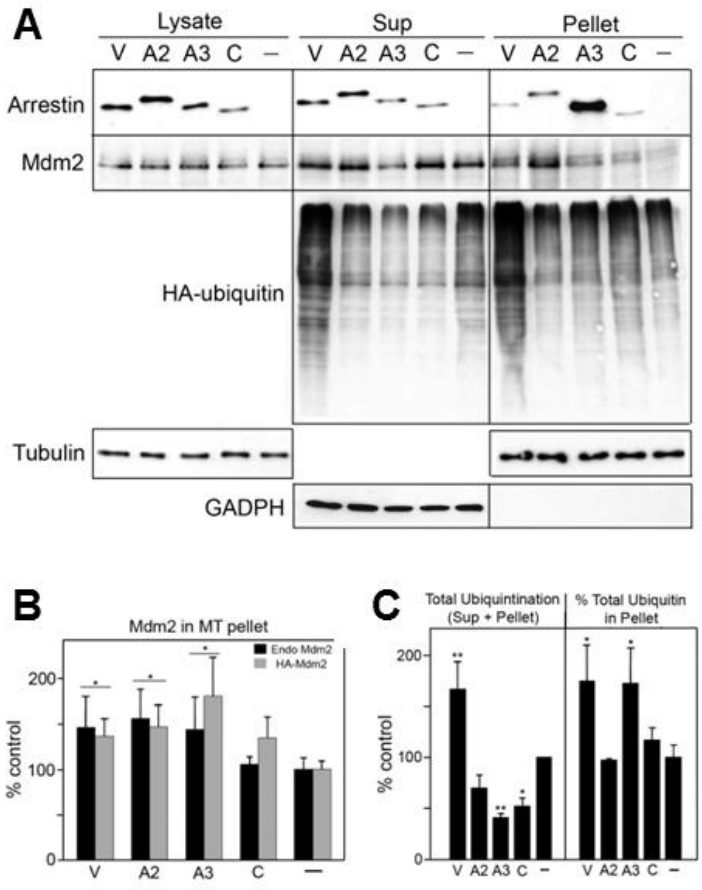

Figure 2-2. Arrestin recruits Mdm2 to microtubules.
(A) HEK-293 cells transfected with the indicated arrestins or empty vector (-) were fractionated and analyzed by Western blot. A strong GADPH signal was detected in the supernatant, with no appreciable signal in the pellet. To measure ubiquitination of soluble and cytoskeletal substrates, cells were co-transfected with HA-tagged ubiquitin and ubiquitinated proteins were visualized with anti-HA antibody. Representative blots from 3 experiments demonstrating the relative amount of each protein in the lysate, soluble (sup), and cytoskeletal (pellet) fractions are shown. Total ubiquitination was determined to be the amount of ubiquitinated substrate in the sup + pellet samples combined. **(B)** Endogenous Mdm2 in the cytoskeletal fraction in cells expressing different arrestins (black bars) (as shown in **(A)**) or endogenous plus overexpressed HA-Mdm2 (gray bars) was quantified and analyzed by one-way ANOVA with arrestin type as the main factor. *$p<0.05$, as compared to control. The amount of Mdm2 in the cytoskeletal fraction of control cells was 5.2 ± 0.7 % and 8.7 ± 0.8 % of the total Mdm2 for cells that did or did not express HA-Mdm2, respectively. **(C)** The total amount of ubiquitination (sup+pellet) (left graph) and percentage of protein-incorporated ubiquitin in the cytoskeletal fraction (pellet/(sup+pellet)) (right graph) was quantified by Western blot and analyzed by one-way ANOVA with arrestin type as the main factor. *$p<0.05$, **$p<0.01$, compared to control. Abbreviations: V, WT visual rod arrestin; A2, WT arrestin2; A3, WT arrestin3; C, WT cone arrestin.

Additional experiments showed that arrestins recruit signaling proteins to MTs more selectively than to the receptor. In particular, we observed no arrestin-dependent mobilization of a different MAP kinase JNK3, phospho-JNK3 (113), or protein phosphatase 2A (120) (Figure 2-3). In summary, among the six binding partners tested, arrestins only bring two (ERK1/2 and Mdm2) to the microtubules. Apparently, the distinct conformation of MT-bound arrestin can only interact with a subset of proteins that have been shown to bind the arrestin-receptor complex.

Discussion

The localization of the interaction sites for the non-receptor partners on the other side of the molecule allows arrestin to mobilize various signaling proteins to the receptor (109, 112). Our data show that microtubules bind to the same arrestin surface as the receptor (121), suggesting that the elements involved in the interactions with the non-receptor partners should be accessible in the MT-bound form. Indeed, our finding that arrestin mobilizes ERK1/2 to the cytoskeleton clearly shows that this is the case (Figure 2-1a,c). However, the functional capabilities of MT- and receptor-bound arrestin are different: arrestin mobilizes ERK, Mdm2, but not c-Raf-1, MEK1, or JNK3, whereas all of these partners are recruited to the arrestin-receptor complex.

Receptor binding induces a global conformational change in arrestin (103) that is widely believed to facilitate the binding of clathrin, AP2, Src, MAP kinases, and other proteins to the complex (109, 112). Deletions in the inter-domain hinge impede arrestin transition into this active conformation, thereby dramatically reducing arrestin binding to the receptor (104). In contrast, hinge deletions actually enhance arrestin binding to MTs,

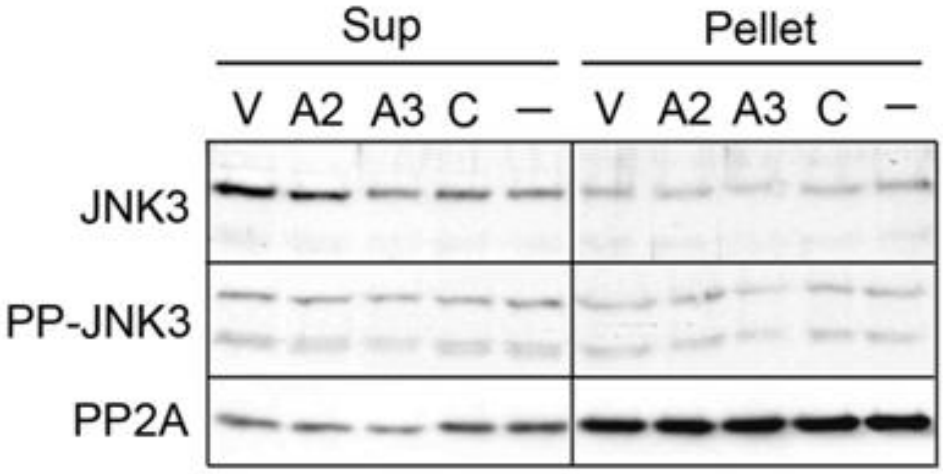

Figure 2-3. Arrestins do not affect the subcellular distribution of JNK3 and PP2A. HEK-293 cells transfected with the indicated arrestins or empty vector (-) were fractionated as described in the Methods and analyzed by Western blot. Representative blots from 2-3 experiments demonstrating the relative amount of JNK3, phosphorylated JNK3 (PP-JNK3), and protein phosphatase 2A (PP2A) in the soluble (sup), and cytoskeletal (pellet) fractions are shown. For JNK3 experiments, cells were irradiated with UV for 30min at RT prior to crosslinking to increase the overall level of PP-JNK3.

suggesting that the conformations of MT-bound and receptor-bound arrestins are different. Not surprisingly, the functional consequences of arrestin-dependent ERK mobilization to the MTs is opposite to its recruitment to GPCRs. Receptor-bound arrestin facilitates ERK activation (114), whereas cytoskeletal localization of ERK by arrestin keeps it inactive, likely because arrestins do not mobilize the upstream kinases c-Raf-1 and MEK1 to microtubules (Figure 2-4).

The binding of arrestin proteins to microtubules with affinities that ensure their partial co-localization with the cytoskeleton in intact cells is a novel link in the network of cellular signaling pathways. Accumulating evidence shows that a number of signaling proteins that were believed to selectively interact with receptor-bound arrestin actually bind free arrestin in the cytoplasm (117, 122, 123) and the microtubule-bound form. Notably, two out of the six arrestin partners tested in our study are recruited to microtubules in arrestin-dependent fashion. It is tempting to speculate that a number of other known binding partners may also be mobilized to the cytoskeleton via an arrestin-dependent mechanism with significant functional consequences. The recruitment of signaling molecules may affect their activation state and/or microtubule dynamics, which is known to be regulated by post-translational modifications of tubulin and associated proteins (124). The full range of biological implications of the functional link between arrestins and the cytoskeleton remains to be elucidated.

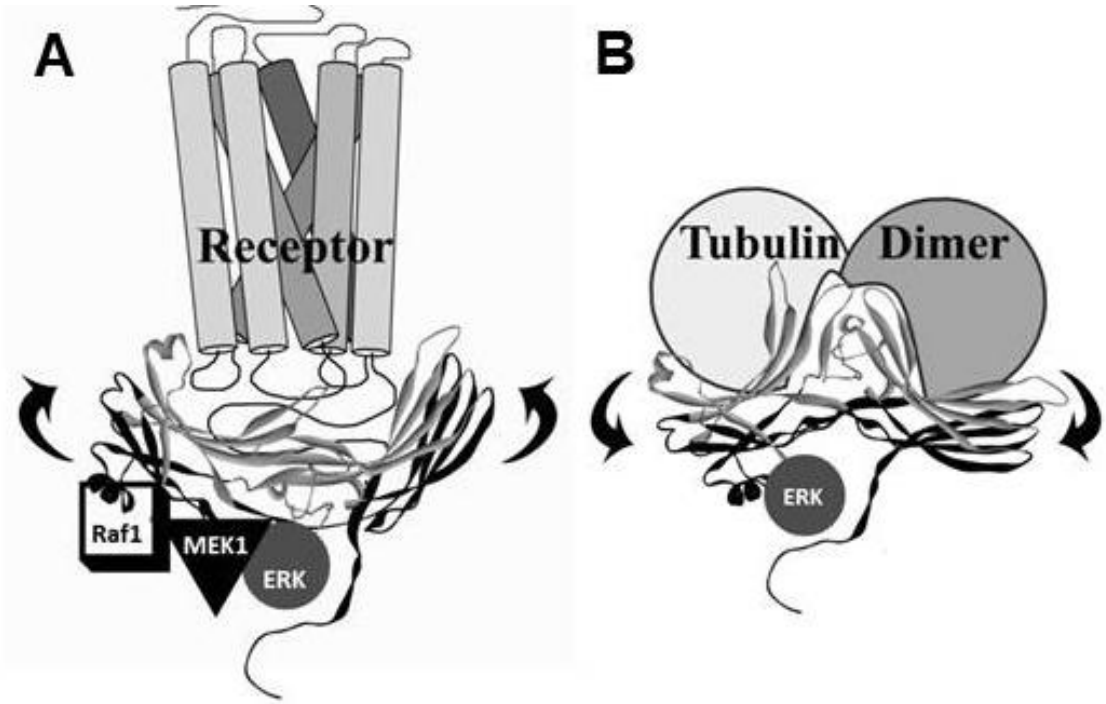

Figure 2-4. Arrestin differentially recruits signaling proteins to the receptor and microtubules. Arrestins recruit ERK opposite to its recruitment to GPCRs. Receptor-bound arrestin facilitates ERK activation by also recruiting its upstream kinases Raf1 and MEK1. However, localization of ERK to the microtubules keeps in its inactive form, most likely because arrestins do not recruit its upstream kinases. As a result, arrestin dependent ERK1/2 mobilization to microtubules reduces ERK1/2 phophorylation level in the cell. The difference in recruitment is most likely the result of the different conformations of receptor-bound and microtubule-bound arrestin.

CHAPTER III

ARRESTINS REGULATE CELL SPREADING AND MOTILITY VIA FOCAL ADHESION DYNAMICS

Introduction

Arrestins regulate G protein-coupled receptor (GPCR) signaling (1) and bind >100 non-receptor partners (125). The interactions of many proteins with GPCR-bound arrestin localizes them to receptor-rich membranes (126). Recent studies implicated non-visual arrestins in regulation of actin cytoskeleton and cell migration (50-53), but how arrestins contribute to these processes is unclear. Arrestin-2 activates small GTPase RhoA coordinately with Gαq following the activation of angitotensin II 1A receptor ($ATII_{1A}R$) (70). Arrestin-2 also regulates RhoA activity by binding and inhibiting ARHGAP21, a RhoA GTPase activating protein, in response to $ATII_{1A}R$ stimulation (74). Arrestin-3 interacts with actin treadmilling protein cofilin upon activation of another GPCR, PAR2 (78). Both arrestin-2 and -3 regulate small GTPase ralGDS upon activation of fMLP receptor (75), and ELMO-ARF cascade upon calcium-sensing receptor stimulation (81). All these studies suggest that arrestins regulate the cytoskeleton upon stimulation of specific GPCRs. Our finding that arrestins bind microtubules and recruit signaling proteins to them (100) suggests that arrestins may regulate the cytoskeleton independently of GPCRs. While this interaction has been characterized structurally (100, 127), its functional significance was not fully elucidated. Therefore, we investigated the role of arrestins in cell migration and regulation of cell shape.

Here we show for the first time that both arrestin-2 and arrestin-3 regulate signaling machinery involved in cell migration and spreading on two different levels. Arrestins affect the activity of small GTPases RhoA and Rac1, and also regulate focal adhesion dynamics independently of GPCRs and small GTPases.

Material and Methods

Antibodies

Rhodamine-phalloidin (for actin staining) was from Invitrogen (Invitrogen Carlsbad, CA); anti-glyceraldehyde-3-phosphate dehydrogenase (GAPDH), anti-HA, phospho-paxillin (Y118), and monoclonal anti-Cdc42 antibodies were from Cell Signaling (Beverly, MA); anti-GFP monoclonal antibody, active 9EG7 and total Hmβ1-1 CD29 β1-integrin, and monoclonal paxillin were from BD Biosciences (Palo Alto, CA); rat IgGa,κ and hamster IgG isotype controls were from Biolegend (San Diego, CA). Monoclonal rat anti-HA antibody for cell staining was from Roche Molecular Biochemicals (Indianapolis, IN); antibodies against mouse FAK, phospho-FAK (Y397), vinculin, and rabbit polyclonal α-tubulin were from Abcam (Cambridge, MA). Anti-Rac1 and Anti-RhoA antibodies were from Millipore (Temecula, CA). Mouse monoclonal pan-arrestin F4C1 antibody recognizing epitope DGVVLVD (residues 43-47) in the N-domain was a generous gift of Dr. L.A. Donoso (Wills Eye Institute). Arrestins were detected with arrestin-2- (128) (1:6000) or arrestin-3-specific (129) (1:700) affinity-purified rabbit polyclonal antibodies. Total integrin antibody M-106 for Western blot and focal adhesion kinase (FAK) antibody for pull-down assay was from Santa Cruz Biotechnology (Santa Cruz, CA).

Cell culture, transfection, and retroviral infection of cells

Arrestin DKO and WT MEF cell lines (21) (a gift from Dr. R.J. Lefkowitz, Duke University) were cultured in DMEM with 10% FBS and 1% penicillin-streptomycin (P/S) at 37 °C and 5% CO_2. Cells were retrovirally infected using genes inserted into pFB murine retrovirus vector (Stratagene) transfected using Lipofectamine 2000 (Sigma, St. Louis, MO) into Phoenix cell line. Fugene HD (Promega, *Fitchburg, WI*) (1:3 DNA:lipid) was used to transfect cells in some cases.

Protein Preparation and Western-blotting

Cells were lysed in Lysis solution (Ambion) or 1% SDS lysis buffer and boiled for 5 min at 95°C. Protein concentration was measured with Bradford reagent (Bio-Rad). The protein was precipitated with nine volumes of methanol, pelleted by centrifugation (10,000xg, 10 min at RT), washed with 90% methanol, dried and dissolved in SDS sample buffer at 0.5 mg/ml. Equal amounts of protein were analyzed by reducing SDS-PAGE and Western blotting onto Immobilon-P (Millipore, Bedford, MA). The membrane was blocked with 5% non-fat dry milk in TBS with 0.1% Triton X-100 (TBST) and incubated with appropriate primary and then secondary antibodies coupled with horseradish peroxidase (Jackson Immunoresearch Laboratories, West Grove, PA) in TBST with 1% BSA. Bands were visualized with SuperSignal enhanced chemiluminescence reagent (Pierce, Rockford, IL) and detected by exposure to X-ray film (Fujifilm). Where appropriate, the bands were quantified using VersaDoc and QuantityOne software (BioRad).

Cell spreading and focal adhesion analysis

All staining experiments were done as follows unless otherwise noted. Serum-starved cells were plated on 8-well slides coated with 1.25 ug/mL fibronectin or 0.1 mg/mL poly-D-lysine. Cells were fixed with 4% paraformaldehyde, permeabilized with 0.4% Triton X-100, and blocked with 2% BSA in PBS. Most cells were stained with rhodamine-phalloidin. Rescue experiments where DKO cells were infected to express HA-RhoA, HA-Rac mutants or HA-tagged arrestins were also stained with anti-HA antibody to detect expression. Most images were taken on Nikon wide field microscope. Focal adhesion numbers and size were quantified from confocal images taken on LSM 510 Meta Confocal with 40X oil objective and analyzed with Image J.

Migration Assay

Cell migration analysis was performed as described in Transwell tissue culture inserts containing membranes with 0.8 μM pores that were coated with 0.32 ug/mL fibronectin in PBS on the underside and kept overnight at 4^{o}C. Membranes were blocked in 1.5% bovine serum albumin (BSA) for 1 h at 37^{o}C. The 24-well inserts were placed in serum free medium and 10^{6} cells were seeded on the upper surface of the chamber and allowed to migrate for 4 h at 37^{o}C. Cells that migrated were stained with 1% crystal violet and 6 randomly chosen fields were counted at 200x magnification. Migration rescue experiments were performed using cells infected with bicistronic vector co-expressing arrestin and GFP, or GFP alone. Cells were sorted for GFP expression on a BD FACSAria III cell sorter.

Adhesion Assay

Adhesion assays were performed as described (130). 96-well plates were coated with increasing concentrations of fibronectin, 0.01 µg/mL to 1.25 µg/mL, and blocked with 5% milk in PBS at room temp for 2 hrs. Serum-starved cells ($6x10^5$) were plated and allowed to adhere for 15 or 30 min. Unattached cells were removed using Percoll flotation medium (73mL Percoll (Sigma, density, 1.13g/mL), 27mL of distilled water, and 900mg NaCl) and the remaining cells were fixed for 15 min with 25% gluteraldehyde (Sigma), washed with PBS, and stained with 0.5% crystal violet (Sigma) in 20% methanol for 10 min. Plates were washed with PBS and eluted with 20% acetic acid. Absorbance was read at 595nm. Bars represent mean absorbance ± SEM of each condition tested in triplicate.

Replating Assay

Replating assays were performed by trypsinizing cells, incubating them in suspension in serum-free DMEM and then plating serum-starved DKO and WT cells on 1.25µg/mL fibronectin for 0, 30, 60, and 120 min. Cells were lysed with 1% SDS lysis buffer. Levels of phosphorylated and total paxillin and FAK, and total vinculin were determined in cell lysates (5 µg/lane) by Western blot.

Flow Cytometry

To measure activity and surface expression of β1-integrin levels, cells incubated in Hanks balance salt solution (HBSS) (Cellgro, Manassas, VA) overnight were washed with Tris-buffered saline (TBS) (24 mM Tris-HCl, pH 7.4, 137 mM NaCl, 2.7 mM KCl) and

resuspended in 5% bovine serum albumin (BSA). Cells were incubated with 5mM $MnCl_2$ or 2mM EDTA for 30 min at 37°C, then for 1 h with rat 9EG7 (active integrin) or hamster HMβ1-1 (total integrin) antibodies, or rat and hamster isotype controls. Cells were washed three times with 1% BSA in TBS and incubated for 45 min on ice with either Alexa Fluor 488 rabbit anti-rat (Invitrogen, Carlsbad, CA) or DyLight 488 conjugated goat anti-hamster (Jackson Immunoresearch Laboratories, West Grove, PA) secondary antibodies. At least 10,000 cells were analyzed using a 3 Laser LSRII machine to obtain mean fluorescence intensity values. To investigate total β1-integrin levels, equal numbers of DKO or WT cells were cultured for 2 days. Cell lysates were prepared in SDS lysis buffer after washing with PBS. Equal amounts of proteins were analysed by Western on 10% SDS-PAGE.

GTPase Pulldown Assays

The levels of GTP-liganded Rho were analyzed using the Rho activation pulldown kit according to manufacturer's instructions (Millipore, Temecula, CA). Equal volumes of cell lysates were used to measure total Rho. PAK1-PBD-conjugated glutathione-Sepharose beads were prepared as described (131). Cells were serum-starved for 24 hrs and lysed. Equal volumes of lysates were added to 30 μl of PAK1-PBD–conjugated glutathione-Sepharose beads and incubated at 4°C for 1 h with gentle rocking. After four washes with 125 mM HEPES, pH 7.5, 750 mM NaCl, 5% Igepal CA-630, 50 mM MgCl2, 5 mM EDTA and 10% glycerol, the beads were resuspended in 15 μl of 2× Laemmli SDS sample buffer, boiled for 5 min, and resolved on 15% SDS-PAGE. Equal volumes of total lysates were run for comparison. The proteins were transferred to a

nitrocellulose membrane and incubated with anti-Rac1 or anti-Cdc42 antibodies in 2% BSA at 4°C overnight.

RhoA Inhibition

WT cells were infected with retrovirus to express either dominant-negative RhoN19-HA or GFP and plated on fibronectin or poly-D for 2 hrs. Cell size was measured in all conditions, focal adhesions were analyzed on fibronectin only. Cells were stained with Rhodamine-phalloidin and anti-HA or paxillin and anti-HA. Alternatively, cells were allowed to spread for 2 h, and then incubated with 0.5µg/mL C3 Transferase (Cytokeleton, Denver, CO), a permeable Rho inhibitor, or with 1µM Y-27632, a selective inhibitor for Rho-associated kinases (ROCK) (EMD Chemicals, Inc., Darmstadt, Germany) for 4 hrs. Cells were fixed and stained with rhodamine-phalloidin and anti-paxillin antibody.

Live Cell Imaging

Imaging was performed using an Applied Precision DeltaVision Core microscope with a Plan Apo 60X oil immersion objective lens. DKO and WT cells expressing GFP-paxillin were placed in a heated microscope chamber at 37°C for 2 h prior to imaging. Images were then obtained every min and processed with 10 iterations of constrained iterative deconvolution using Softworx 5.0 (Applied Precision, Issaquah, WA). Images were binned 2x2. Rescue experiments were performed with cells expressing either arrestin-2-HA or arrestin-3-HA, mcherry-arrestin, and GFP.

Co-IP

Rat-1 cells (60 mm plates) were lysed in 0.75 ml lysis buffer (10mM Tris-HCl(pH7.4), 5mM EDTA, 150mM NaCl, 1% TritonX-100, 10% Glycerol, 1mM PMSF and 1mM NA_3VO_4) for 30-60 min at 4^oC. After centrifugation, supernatants were pre-cleared by 35 μl of protein G agarose. Supernatants (500 μg of total protein) were incubated with 2ul of Arrestin2 antibody (178) for 4 h, then with 20 μl of protein G agarose beads (50% slurry) for 2 h. The beads were washed three times with 1 ml of lysis buffer, and the proteins were eluted with 50 μl SDS sample buffer, boiled for 5 min, and analyzed by Western blot**.**

Nocodazole Washout

Serum-starved DKO and WT MEFs were grown overnight and treated with 10 μM nocodazole for 2 h to depolymerize microtubules. The drug was washed out 10x with serum-free medium and microtubules were allowed to repolymerize for 30, 60, 120 min. To stain for microtubules, cells were fixed with 1% gluteraldehyde in 1xBRB80 followed by permeabilization with 0.5% TritonX-100 in 1xBRB80, or fixed with 4% PFA in PBS followed by treatment with 0.4% TritonX-100 in PBS before processing for immunofluorescence. Cells were stained with paxillin or α-tubulin antibodies. Focal adhesion numbers were quantified in confocal images acquired with 40x oil objective using Image J.

Image and Statistical Analysis

Most data were analyzed by one-way ANOVA with genotype as the main factor and subject to Bonferroni /Dunn *post hoc* test with correction for multiple comparisons unless noted otherwise. Cell size analysis was from 10-15 randomly selected fields per experiment, and measured for area using Image J. Cells with moderate expression of either HA-arrestins or HA-small GTPases were selected for cell size and focal adhesion number rescue measurements. Focal adhesion size and number were measured from confocal images using Image J with qualifications for focal adhesion area: 0.5-100μm^2. Focal adhesion lifetimes were calculated using focal adhesions containing GFP-paxillin that assembled and disassembled from the leading edge of the cell. Focal adhesion size and lifetime distributions were measured using nonparametric analysis Kolmogorov Smirnov. In all experiments a p value <0.05 is considered significant.

Results

Arrestins regulate cell morphology by altering the cytoskeleton.

Arrestin-2/3 double knock-out (DKO) mouse embryonic fibroblasts (MEFs) were introduced more than a decade ago (21), but their peculiar shape, dramatically different from that of wild type (WT) MEFs, was routinely ignored. The actin cytoskeleton (visualized by Rhodamine-phalloidin staining) of arrestin DKO cells plated on fibronectin (FN) is drastically different from arresin-2 single knock-out (A2KO), arrestin-3 single knock-out (A3KO) and WT cells (Figure 3-1a). In addition, DKO cells are twice as large as A3KO and WT cells (Figure 3-1b), with the size of A2KO cells intermediate between cell types. To determine whether the increase in cell spreading of DKO cells was

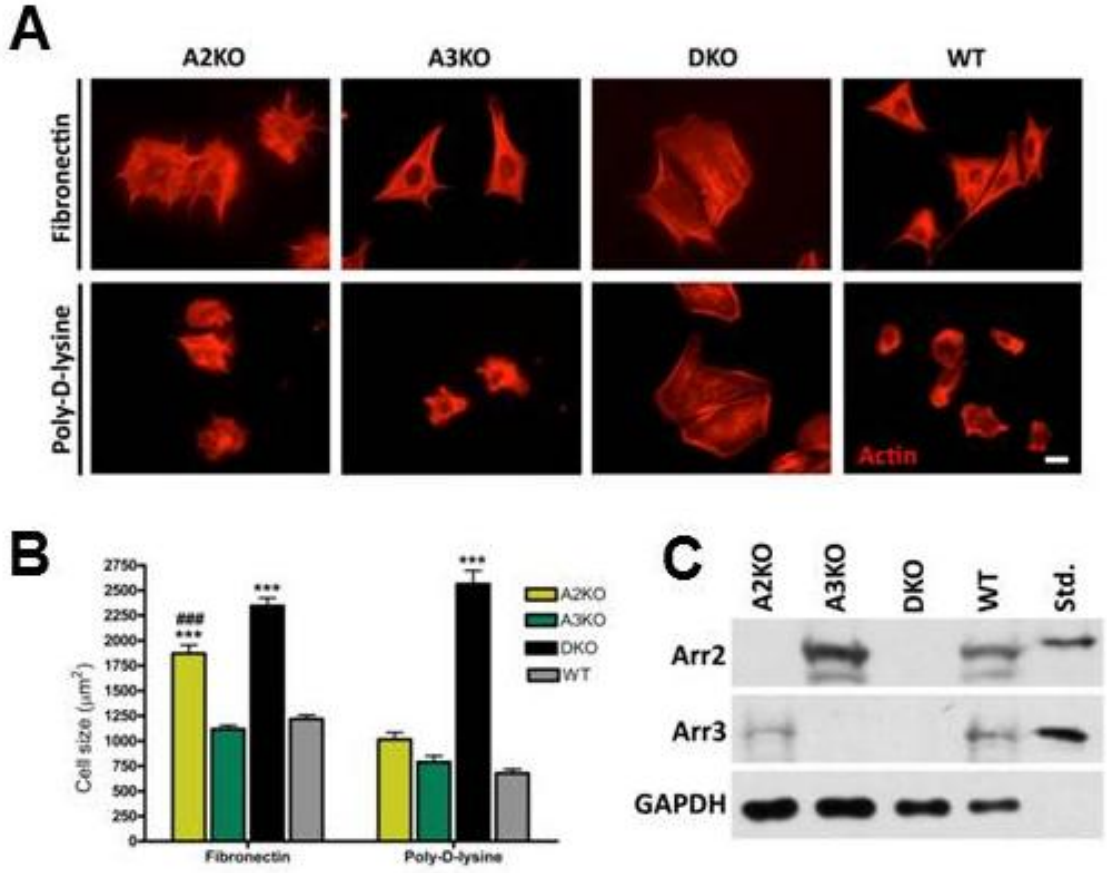

Figure 3-1. Knock-out of both arrestins results in dramatically altered cytoskeleton. **(A)** A2KO, A3KO, DKO and WT cells were stained with Rhodamine Phalloidin after spreading 2 h on FN or PDL. Scale bar = 10μm. **(B)** The size of 50 cells in three experiments was quantified at each time point on either FN or poly-D-lysine ***p<0.001 compared to WT, ###<p0.001 compared to A2KO. **(C)** Expression of arrestins in A2KO, A3KO, DKO and WT cells were detected by western blot, with arrestin2 and arrestin3 bovine standards for comparison. Abbreviations: A2KO, arrestin-2 single knock-out MEFs; A3KO, arrestin-3 single knock-out MEFs; DKO, Arrestin2/3 double knock-out MEFs; WT, wild-type MEFs; FN, fibronectin; PDL, Poly-D-lysine.

matrix dependent, we also plated cells on poly-D-lysine (PDL), which binds integrins but does not promote their clustering and activation. Interestingly, DKO cells spread as well on PDL as on FN (Figure 3-1a). In contrast, all other cell types do not spread as well on PDL: the average cell area was reduced nearly by half from 1219 um^2 on FN to 678 um^2 (Figure 3-1b).

To ascertain that the absence of arrestin-2/3 is responsible for the morphological phenotype of DKO cells, we tested whether expression of arrestin-2 or arrestin-3 rescues them, using cells expressing GFP as controls (Figure 3-2a). Cells plated on FN or PDL were stained for HA-tagged arrestins and actin cytoskeleton (Figure 3-2b). The expression of either non-visual arrestin (Figure 3-2e) reduces DKO cell size nearly back to WT on FN and PDL. Cells expressing arrestin-3 are closer to WT, whereas the rescue by arrestin-2 is partial Figure 3-2c,d). Thus, each non-visual arrestin significantly affects cell spreading.

The best characterized function of arrestins is their high-affinity binding to active phosphorylated GPCRs (18). To test whether arresin interactions with GPCRs play a role in cell spreading, we used receptor binding-deficient arrestin mutants with 7-residue deletion in the inter-domain hinge (Δ7) (100, 132). Similar to WT arrestin-2 and -3, both Δ7 mutants effectively reduced the size of DKO cells to WT level on FN and PDL (Figure 3-2b,c,d,e). Thus, GPCR binding is not involved in arrestin-dependent regulation of cell spreading.

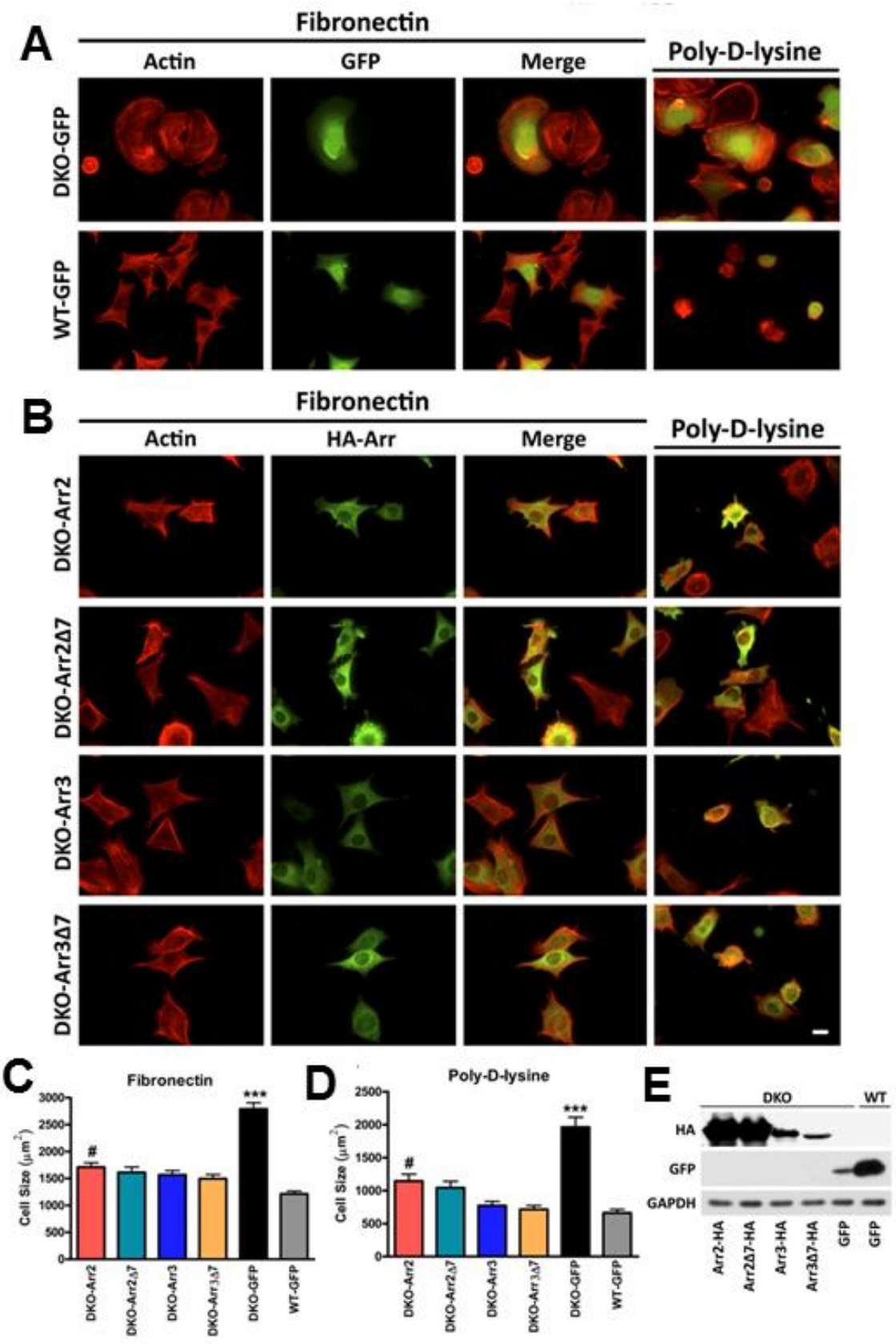
A
Fibronectin
Actin
GFP
Merge
Poly-D-lysine
DKO-GFP
WT-GFP
B
Fibronectin
Actin
HA-Arr
Merge
Poly-D-lysine
DKO-Arr2
DKO-Arr2Δ7
DKO-Arr3
DKO-Arr3Δ7
C
Fibronectin
Cell Size (μm²)
3000
2500
2000
1500
1000
500
0
#
***
DKO-Arr2
DKO-Arr2Δ7
DKO-Arr3
DKO-Arr3Δ7
DKO-GFP
WT-GFP
D
Poly-D-lysine
Cell Size (μm²)
2500
2000
1500
1000
500
0
#
***
DKO-Arr2
DKO-Arr2Δ7
DKO-Arr3
DKO-Arr3Δ7
DKO-GFP
WT-GFP
E
DKO
WT
HA
GFP
GAPDH
Arr2-HA
Arr2Δ7-HA
Arr3-HA
Arr3Δ7-HA
GFP
GFP

Figure 3-2. Arrestin expression rescues DKO phenotype.
DKO cells were retrovirally infected with HA-tagged arrestin-2, arrestin-2-Δ7, arrestin-3, arrestin-3-Δ7, or GFP as a control (DKO and WT). Cells were plated on FN and PDL. Arrestin expressing cells were stained for actin and HA **(B)** and control cells were stained for actin and GFP **(A)**. Scale bar = 10μm. Arrestin expression is shown in **(E)**. Cell size was measured on FN **(C)** and analyzed by one-way ANOVA with genotype as the main factor, ***p<0.001 DKO from all other conditions, DKO cells expressing arrestin-2 were statistically different from WT, ###p<0.01 according to Bonferroni /Dunn *post hoc* test with correction for multiple comparisons. Data are from 37-82 cells per condition from 3-4 experiments. Cell size was also measured on PDL from 29-54 cells in 3 experiments **(D)** ***p=<0.001 DKO from all other conditions, DKO cells expressing arrestin2 were statistically different from WT, #p<0.05.

The activity of Rho family GTPases plays a role in DKO phenotype.

Rho family GTPases (RhoA, Rac1, and Cdc42) regulate cytoskeleton via multiple effectors, controlling actin dynamics and cell shape (66). Altered cytoskeleton and abnormal spreading of DKO cells are reminiscent of disregulated activity of small GTPases. Therefore, we measured the activity of RhoA, Rac1, and Cdc42 (133-135). The activity of RhoA and Rac1, but not Cdc42, was significantly decreased in DKO cells relative to WT (Figure 3-3a,b,c,d). MEFs where only arrestin-2 or arrestin-3 was missing had similarly decreased Rac1 activity (Figure 3-3f), suggesting that arrestin-2 and arrestin-3 regulate Rac1 via the same pathway. Conversely, cells lacking individual arrestins had near-normal RhoA activity (Figure 3-3e), suggesting that either arrestin can enhance RhoA activity and compensate for the loss of the other subtype. Indeed, overexpression of arrestin-2 or arrestin-3 in HEK293a cells dramatically increased RhoA activity (Figure 3-3g,h,i). Thus, both non-visual arrestins independently facilitate RhoA activation in different cell types. Therefore, the absence of both non-visual arrestins accounts for the decreased activity of RhoA and Rac1 in DKO cells.

To test whether reduced RhoA and/or Rac1 activity fully explains DKO phenotype, in DKO cells we expressed HA-tagged constitutively-active and dominant-negative RhoA and Rac1 mutants (136). The cells were stained for HA and actin (Figure 3-4b) and measured the expression of GTPases (Figure 3-4e). DKO and WT cells expressing GFP alone served as controls (Figure 3-4a). The expression of constitutively active RacV12 did not reduce DKO cell size on FN, and even significantly increased it on PDL (Figure 3-4c,d,e). Since Rac1 activation promotes cells spreading and membrane ruffling (68, 137), this is not surprising. Further suppression of Rho or Rac activity by

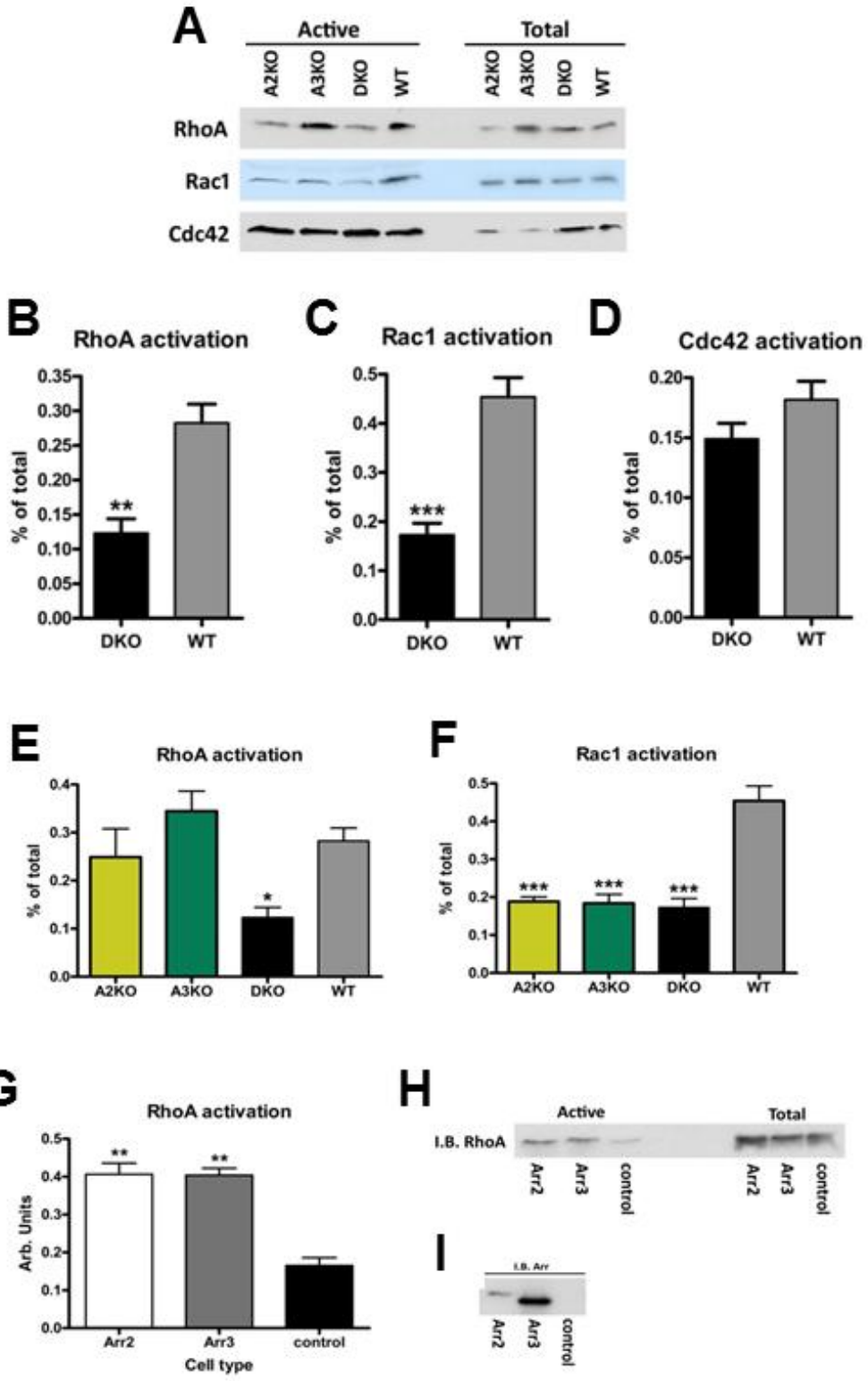
A
Active
Total
A2KO
A3KO
DKO
WT
RhoA
Rac1
Cdc42
B
RhoA activation
% of total
C
Rac1 activation
D
Cdc42 activation
E
RhoA activation
F
Rac1 activation
G
RhoA activation
Arb. Units
Arr2
Arr3
control
Cell type
H
Active
Total
I.B. RhoA
I
I.B. Arr

Figure 3-3. Arrestins regulate the activity of RhoA and Rac1.
(A) The levels of active RhoA, Rac1, and Cdc42 were detected by Western blot and active protein was quantified as a percent of total **(B,C,D)**. Data were analyzed by one-way ANOVA with cell type as the main factor **p<0.01, ***p<0.001 according to Bonferroni /Dunn *post hoc* test with correction for multiple comparisons. Data taken from 3-4 experiments. **(E,F)** The levels of active RhoA and Rac1 in arrestin-2 and arrestin-3 single knock-outs were also were also compared to DKO and WT cells. The data were analyzed by one-way ANOVA with cell type as the main factor. *p<0.05 compared to A3KO, ***p<0.001 compared to WT, #<0.05 compared to DKO according to Bonferroni /Dunn *post hoc* test with correction for multiple comparisons. Data taken from 3 experiments. **(G)** RhoA activity was measured using a GST-pulldown assay for active Rho in Hek293a cells overexpressing arrestin-2 or arrestin-3. **(H)** Representative blot showing increase in activity. Expression levels of arrestin were measured by Western blot with pan-arrestin (F4C1) antibody **(I)**. Data from two different experiments were analyzed by one-way ANOVA, followed by post hoc Scheffe test with correction for multiple comparisons. **p=0.045 arrestin-2 compared to control, **p=0.0046 arrestin-3 compared to control.

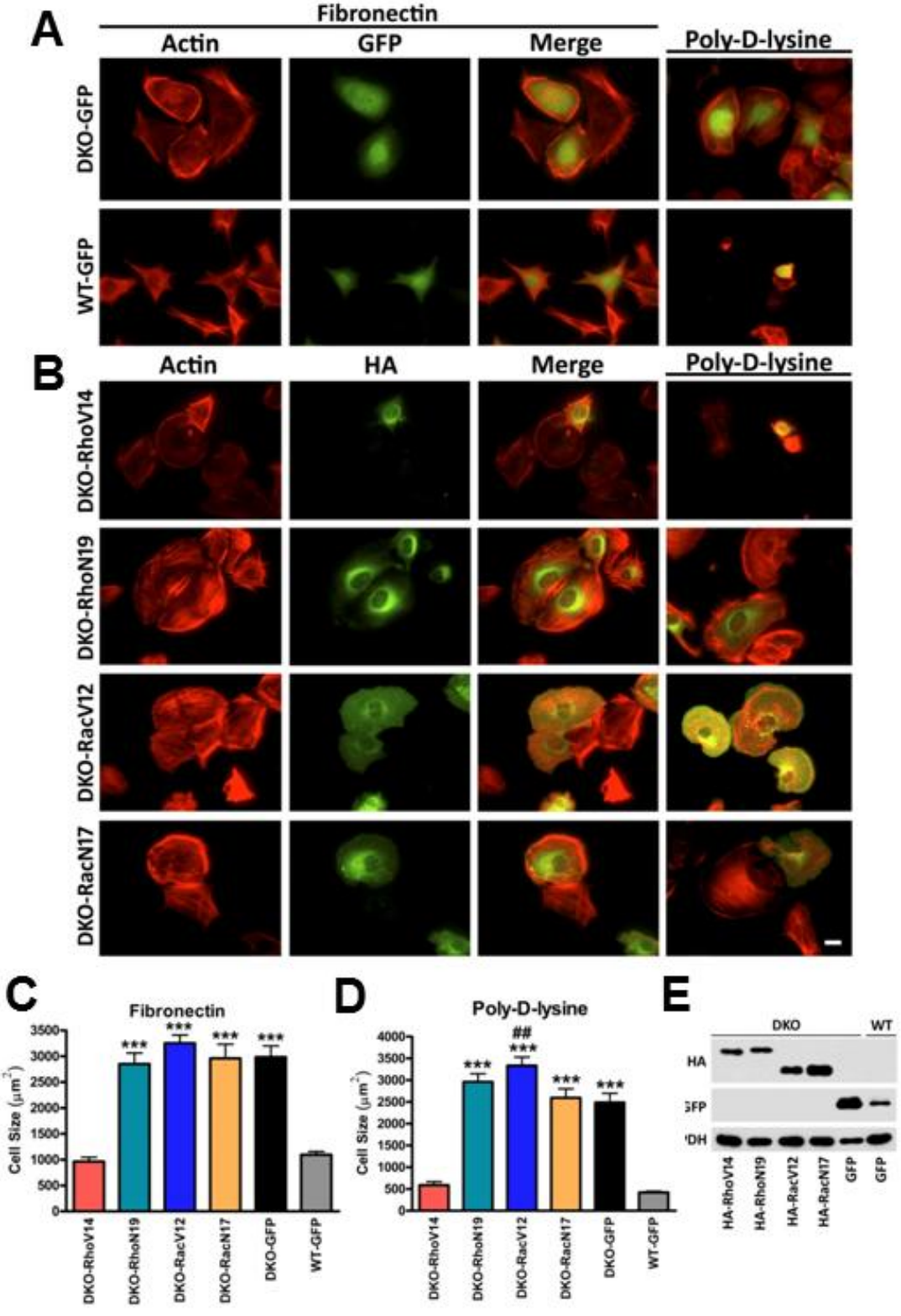
A
Fibronectin
Actin
GFP
Merge
Poly-D-lysine
DKO-GFP
WT-GFP
B
Actin
HA
Merge
Poly-D-lysine
DKO-RhoV14
DKO-RhoN19
DKO-RacV12
DKO-RacN17
C
Fibronectin
Cell Size (μm²)
D
Poly-D-lysine
E
DKO
WT
HA
GFP
GAPDH
HA-RhoV14
HA-RhoN19
HA-RacV12
HA-RacN17
GFP
GFP

Figure 3-4. Small GTPase RhoA affects cell spreading.
(A) DKO and WT cells were retrovirally infected with GFP as control and DKO cells were infected with HA-RhoV14, HA-RhoN19, HA-RacV12, HA-RacN17 **(B)**. **(E)** Expression of HA-tagged small GTPase mutants or GFP was determined by Western blot. Cells were plated on FN or PDL. Scale bar = 10μM. Cell size was measured on FN (27-50 cells from 3 experiments) **(C)** and analyzed by one-way ANOVA, ***$p<0.001$. Cell size was also measured on PDL (26-40 cells from 3 experiments) **(D)** ***$p<0.001$ from WT-GFP and DKO-RhoV14 cells. DKO cells expressing HA-RacV12 were significantly larger than control (GFP expressing) DKO cells, ##$p<0.01$.

dominant-negative RhoN19 or RacN17 did not change the morphology of DKO cells (Figure 3-4c,d,e). However, the expression of constitutively active RhoV14 significantly reduced DKO cell size to WT levels on both FN and PDL (Figure 3-4c,d). Thus, arrestin-dependent RhoA, but not Rac1, activation contributes to the spreading phenotype of DKO cells.

To further explore the effect of decreased RhoA on spreading we expressed dominant-negative RhoN19 in WT cells and plated them on FN or PDL (Figure 3-5a,b). As expected, WT cells expressing RhoN19 had fewer stress fibers than surrounding cells, but their size remained similar to GFP-expressing controls. Importantly, on PDL WT cells expressing RhoN19 spread significantly better than WT-GFP cells (Figure 3-5c). Similar effects were observed when RhoA signaling was suppressed in WT cells by a direct Rho inhibitor C3-transferase, or indirectly through ROCK inhibitor Y-27632. Under both conditions, treated WT cells spread significantly better than controls on PDL, but not FN (Figure 3-5d,e). Thus, constitutively active RhoA reduces DKO cell size to WT level, whereas suppression of RhoA activity in WT cells increases their size on PDL, suggesting that decreased RhoA activity significantly contributes to abnormal spreading of DKO MEFs.

Arrestins regulate migration and adhesion.

Cytoskeletal rearrangements drive cell movement and adhesion. Therefore, we tested whether the lack of arrestins affects adhesion and migration. DKO cells demonstrated 3.8-fold reduced migration towards FN substrate in transwell assay (Figure 3-6a). The adhesion of DKO cells was similar to WT after initial attachment (15 min)

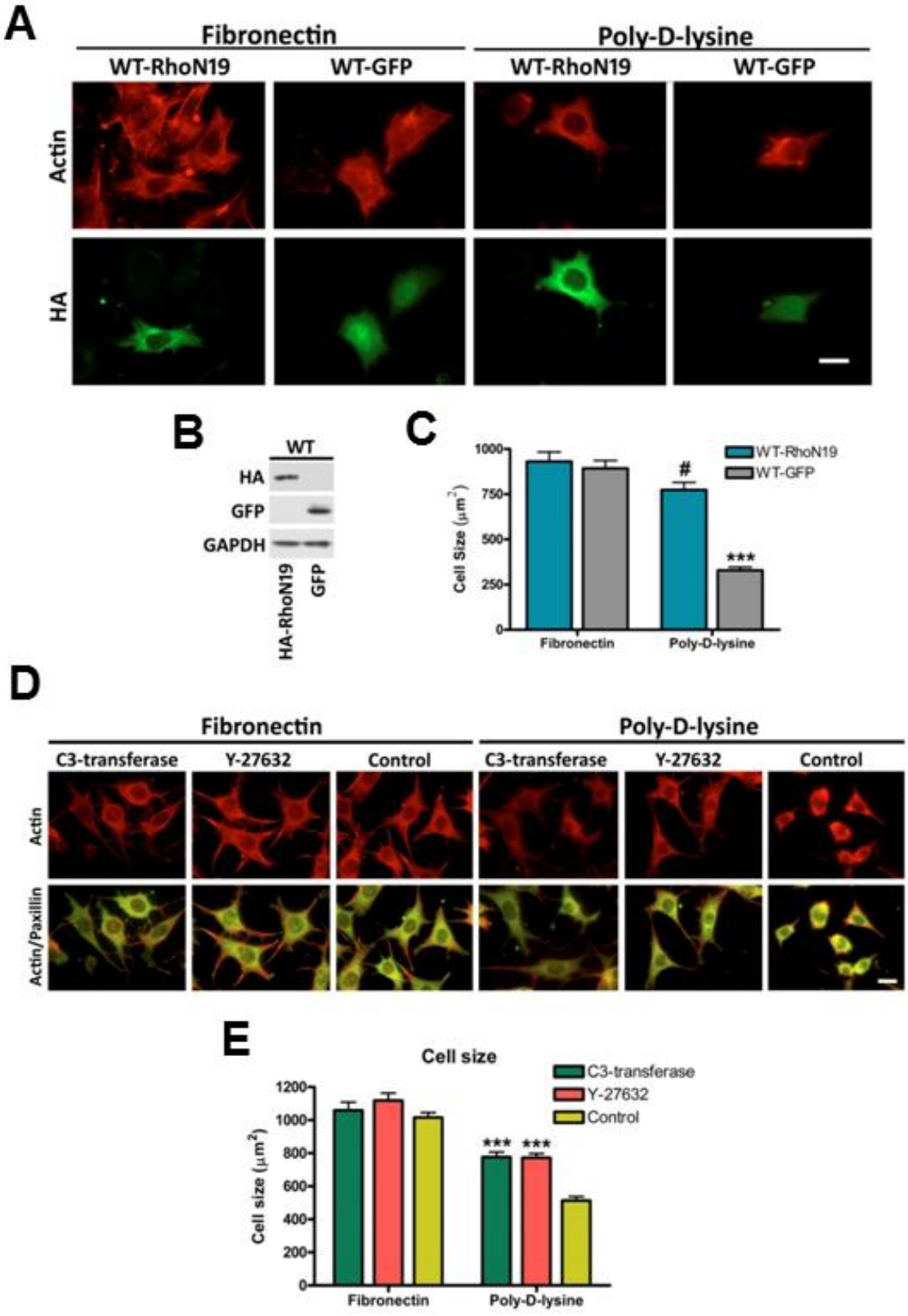
A
Fibronectin
Poly-D-lysine
WT-RhoN19
WT-GFP
WT-RhoN19
WT-GFP
Actin
HA
B
WT
HA
GFP
GAPDH
HA-RhoN19
GFP
C
WT-RhoN19
WT-GFP
Cell Size (μm²)
1000
750
500
250
0
#
***
Fibronectin
Poly-D-lysine
D
Fibronectin
Poly-D-lysine
C3-transferase
Y-27632
Control
C3-transferase
Y-27632
Control
Actin
Actin/Paxillin
E
Cell size
C3-transferase
Y-27632
Control
Cell size (μm²)
1200
1000
800
600
400
200
0
***
***
Fibronectin
Poly-D-lysine

Figure 3-5. Reduced RhoA activity in WT cells increases cell spreading.
(A) WT cells were infected with dominant-negative HA-RhoN19 or GFP; the expression levels are shown in **(B)**. Cells were plated on FN or PDL and stained for HA or Rhodamine-phalloidin. Cell size measurements are shown in **(C)** ***$p<0.001$ compared to all other conditions, #$p<0.05$ WT-RhoN19 on poly-D compared to WT-RhoN19 on FN. Data from 55-69 cells in 4 experiments (means $\pm$ SD) are shown. **(D)** WT cells plated for two hours on FN or PDL and treated with C3-transferase (RhoA specific inhibitor), Y-27632 (ROCK inhibitor) or DMSO (control) for 4 hours. Cells were then stained with rhodamine-phalloidin and paxillin. The size was measured in 73-101 cells in 3 experiments **(E)**. ***$p<0.001$ compared to control cells plated on PDL. Scale bar = 10μM.

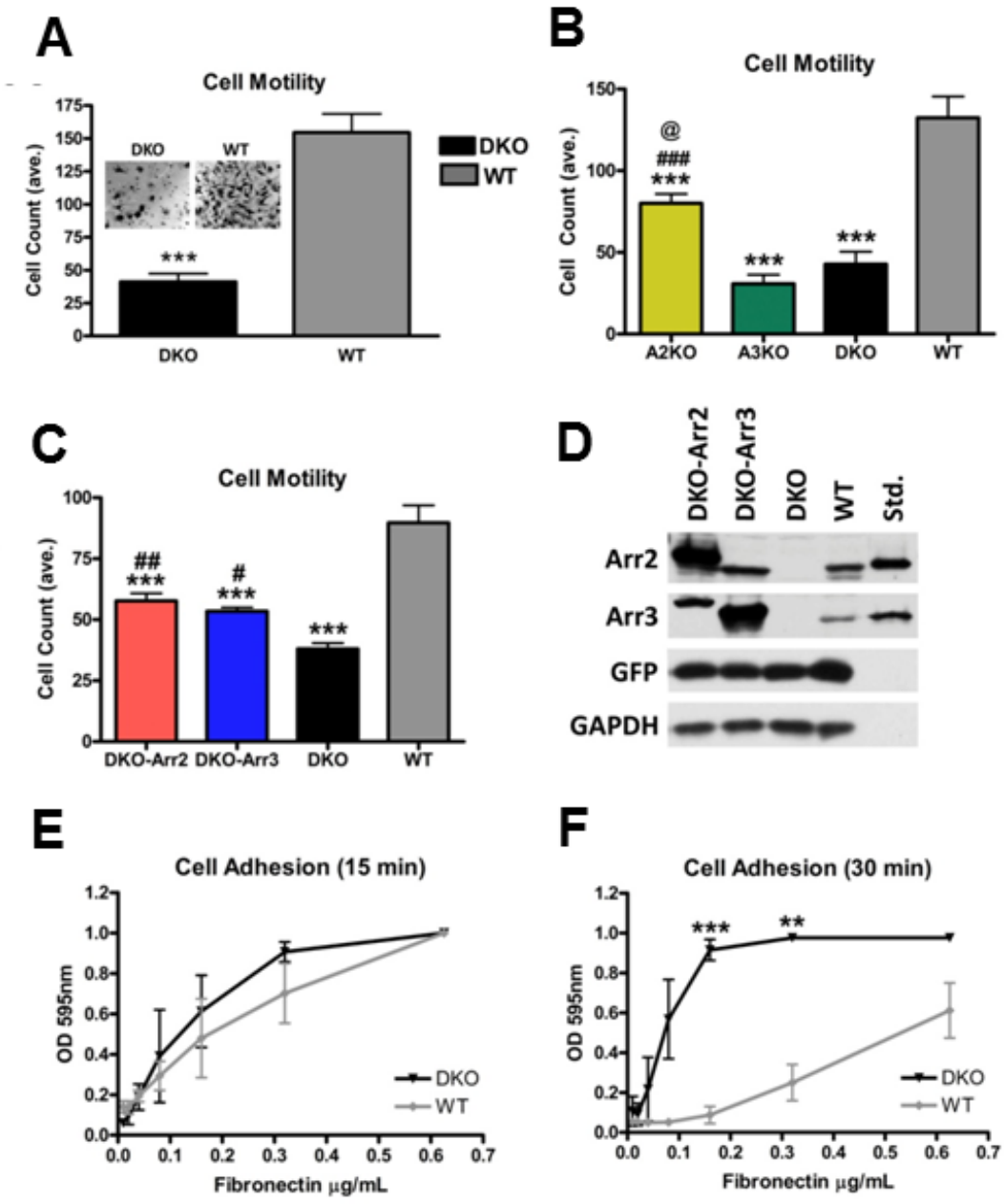
A
Cell Motility
Cell Count (ave.)
DKO
WT
***
DKO
WT
B
Cell Motility
Cell Count (ave.)
@
###
***
***
***
A2KO
A3KO
DKO
WT
C
Cell Motility
Cell Count (ave.)
##
***
#
***
***
DKO-Arr2
DKO-Arr3
DKO
WT
D
DKO-Arr2
DKO-Arr3
DKO
WT
Std.
Arr2
Arr3
GFP
GAPDH
E
Cell Adhesion (15 min)
OD 595nm
DKO
WT
Fibronectin μg/mL
F
Cell Adhesion (30 min)
***
**
OD 595nm
DKO
WT
Fibronectin μg/mL

Figure 3-6. Arrestins regulate cell migration and adhesion.
(A) Cells were plated in Transwell chambers coated with 0.32 µg/mL FN and allowed to migrate for 4 h. Cells were counted in 6 fields/chamber in each of four independent experiments. The data were analyzed by one-way ANOVA with cell type as the main factor, ***p= <0.001. Insets show representative membranes post migration. **(B)** Comparison of motility of single knock-out cell lines is also shown. The data were analyzed by one-way ANOVA with Genotype as the main factor. ***p <0.001 compared to WT, ###p<0.001 compared to A3KO, @ p<0.05 compared to DKO. **(C)** Migration rescue experiments were performed with DKO cells expressing arrestin-2 and GFP or arrestin-3 and GFP, or cells expressing GFP only (DKO and WT). Data from 5 fields/chamber from three independent experiments performed in duplicate were analyzed by one-way ANOVA with cell type as the main factor. ***p<0.001 compared to WT. DKO-Arr2 ##p<0.01 and DKO-Arr3 #p<0.05 compared to DKO. Arrestin expression in DKO cells was determined using arrestin-2 or arrestin-3-specific antibodies, with corresponding purified bovine arrestins (0.1 ng/lane) run as standards **(D)**. Adhesion was measured by plating cells on serial dilutions of fibronectin (0.01µg/mL to 1.25µg/mL) for 15 **(E)** or 30 min **(F)**. The data were analyzed by one-way ANOVA with Arrestin type as the main factor, which was highly significant at 30 min. DKO cells showed a dramatic increase in their ability to adhere, as compared to WT cells, ***p<0.001, **p<0.01. Data was taken from 3 experiments for each time point.

(Figure 3-6e), but they adhered significantly better than WT as cells began to spread (30 min) (Figure 3-6f). Thus, DKO cells form initial attachments similar to WT, but later demonstrate enhanced adhesion.

To determine whether the reversal of DKO morphology by arrestin-2 or -3 also rescues motility deficit, DKO cells were infected with arrestin-2 or -3 in constructs that drive GFP co-expression, with controls expressing only GFP. Cells were sorted for GFP expression (Figure 3-6d) and used in transwell migration assay. Arrestin-2 and -3 partially rescued the DKO migration defect (Figure 3-6c), suggesting that morphology and motility are regulated via the same arrestin-dependent mechanism(s), but both non-visual arrestins likely work in concert to yield WT behavior. Arrestin-2 and arrestin-3 single knockouts showed decreased migration, further proving this point (Figure 3-6b).

Focal adhesion number and size are increased in arrestin-deficient cells.

Focal adhesions (FAs) are key signaling hubs that recruit many proteins to the site of integrin activation (54, 138). Arrestins bind Src, ERK1/2, and JNK3 (18), all of which regulate FAs. Rapid assembly and disassembly of these complexes plays central role in cell adhesion and migration. Both decreased migration and increased adhesion of DKO cells suggest that FAs are likely affected. To test this idea, cells were stained with rhodamine-phalloidin and anti-paxillin antibody to visualize actin cytoskeleton and FAs, respectively. In WT MEFs we observed few FAs primarily at the edges of the cell on FN, and virtually none on PDL (Figure 3-7). Strikingly, in DKO cells the number of FAs was significantly increased. FAs in DKO MEFs demonstrate disordered localization throughout the cell on both FN and PDL (Figure 3-7a). The staining for two hallmarks of

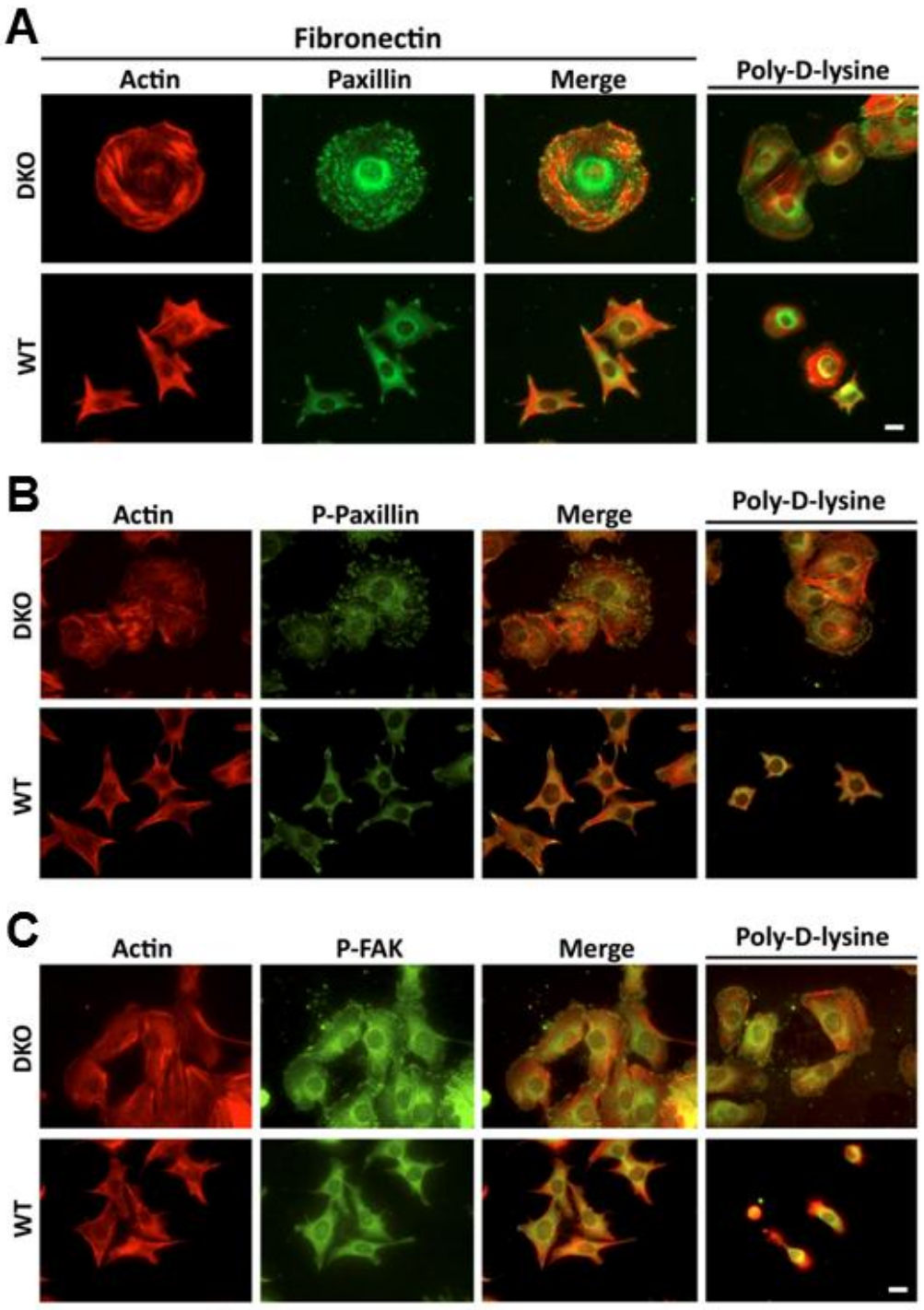

Figure 3-7. Arrestin knockout affects focal adhesion distribution.
(A) Focal adhesions were detected in DKO and WT cells after 2 h on FN or PDL with anti-paxillin antibody. (B) The distribution of phospho-paxillin was visualized with antibody specific for paxillin phosphorylated at Y118. (C) The distribution of focal adhesions stained with P-FAK (Y397) is similar to those visualized with P-paxillin (Y118) or total paxillin antibodies. Scale bar = 10μm.

FAs, active phospho-paxillin (P-Y118) and phospho-FAK (P-Y397) (Figure 3-7b,c) revealed similar differences between WT and DKO cells. Importantly, in single knockout cells the FA pattern was similar to WT (Figure 3-8). These data suggest that arrestin-2 and -3 participate in the regulation of FAs and cell size, and the magnitude of DKO phenotype reflects the absence of both arrestins.

To quantify this difference we measured FA number as a function of time in WT and DKO MEFs (Figure 3-9a). After 2 hours on FN DKO cells have ~5-fold more FAs than WT. After 24 hours the number of FAs in DKO cells doubled, whereas WT cells showed only a slight increase (Figure 3-9b). The difference in FA size distribution between DKO and WT cells increased over time, with DKO cells demonstrating an accumulation of very large FAs at 24 hours (Figure 3-9c).

Arrestins localize to focal adhesions and bind focal adhesion proteins

To determine whether FA phenotype of DKO cells can be rescued by arrestins, we expressed HA-tagged WT and Δ7 arrestin-2 and -3 and stained for paxillin and HA to determine FA number in arrestin-expressing DKO cells (Figure 3-10b). DKO and WT cells expressing GFP were used as controls (Figure 3-10a), and only the cells expressing GFP or HA-tagged arrestins were used for analysis. We found that the expression of any of the four arrestin proteins reduces FA number, although not to WT level ((Figure 3-10c). Interestingly, we detected co-localization of arrestin-2-Δ7 with FAs (Figure 3-10b). We also found that FAK co-immunoprecipitates with arrestin-2 (Figure 3-10d), suggesting that arrestins bind this key component of FAs. These data suggest that

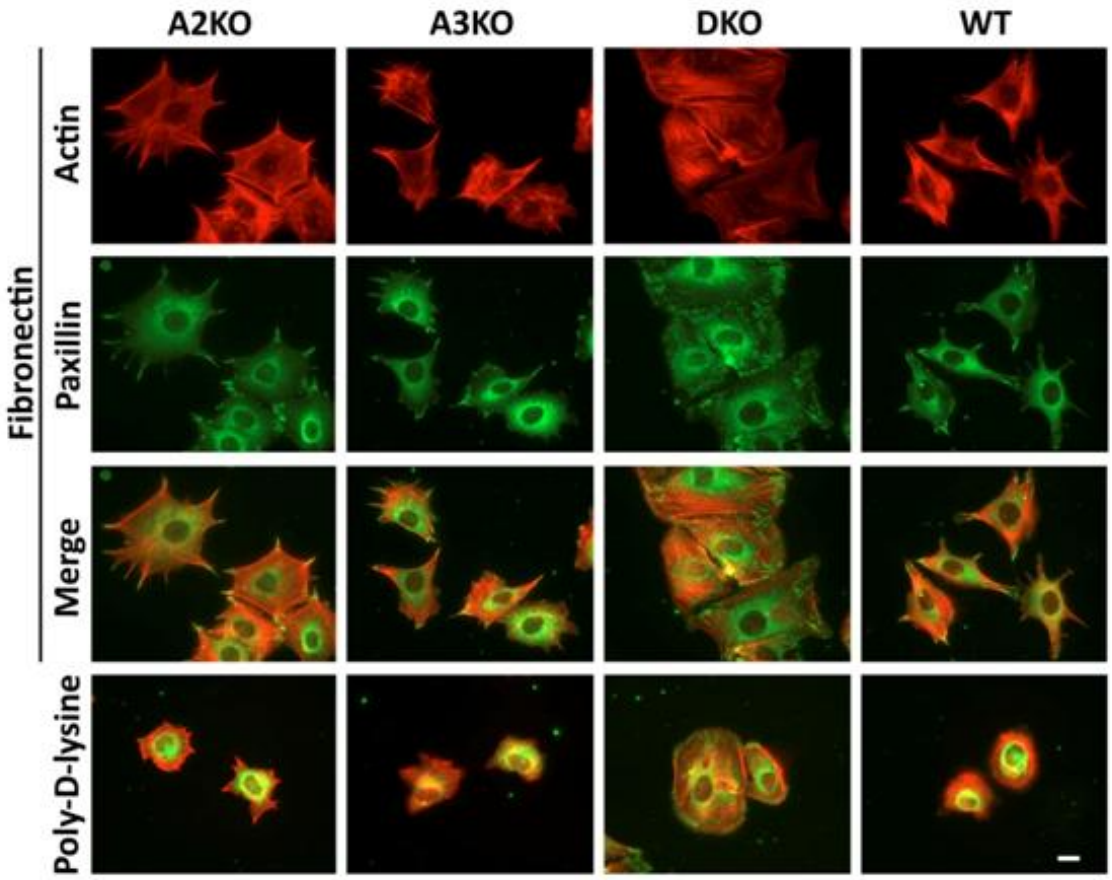

Figure 3-8. Arrestin single knock-out cells have focal adhesion intermediates between DKO and WT. Focal adhesions were detected in A2KO, A3KO, DKO and WT cells after 2 h on FN or PDL with anti-paxillin antibody. Scale bar = 10μm.

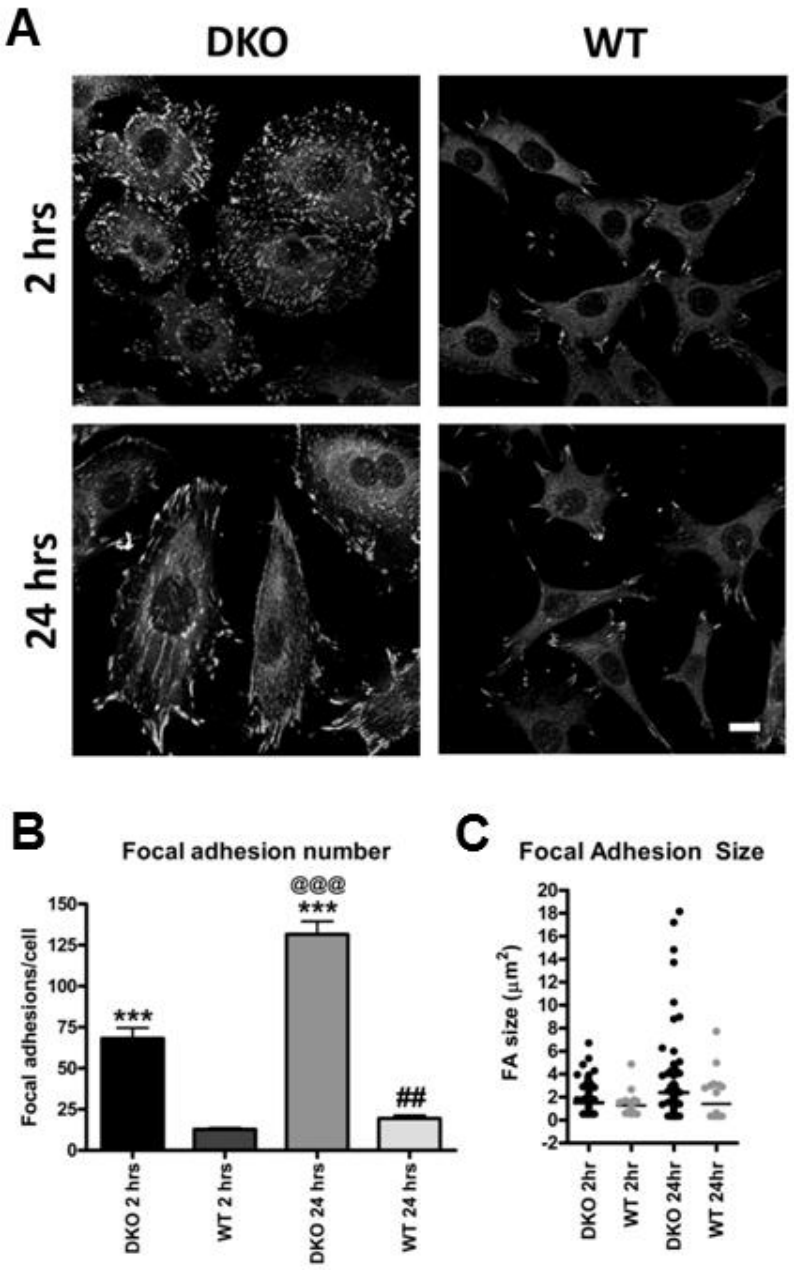

Figure 3-9. Both focal adhesion number and size are increased in DKO cells. **(A)** Cells were plated on fibronectin for either 2 h or 24 h and focal adhesions were visualized by paxillin staining. **(B)** The focal adhesions in DKO and WT cells plated on FN for 2 or 24 h were quantified and analyzed by two-way ANOVA with Genotype and Time as main factors. ***p<0.001 compared to WT, @@@p<0.001 DKO 24h compared to DKO 2 h, and ##p<0.01WT 24 h compared to WT 2h according to Bonferroni /Dunn *post hoc* test with correction for multiple comparisons. Measurements in 45-67 cells from 3 experiments were used. **(C)** Distribution of focal adhesion size is shown by scatter-plot. Focal adhesion size distributions were analyzed by nonparametric Kolmogorov Smirnov analysis, where DKO 2hr p=0.0023, DKO 24h p <0.0001, 24h p<0.0001 compared to WT 2h. Scale bar = 10µm.

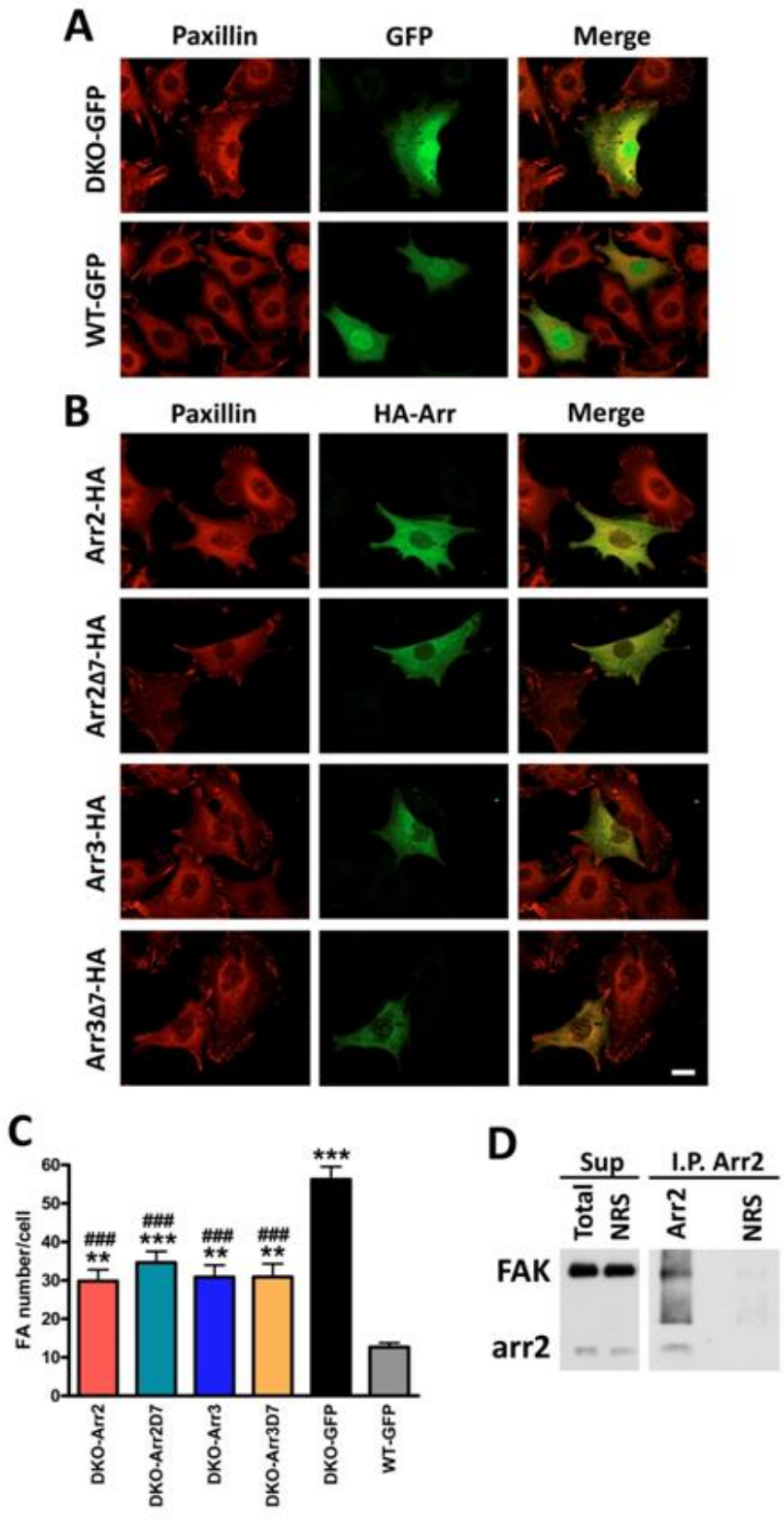
A
Paxillin
GFP
Merge
DKO-GFP
WT-GFP
B
Paxillin
HA-Arr
Merge
Arr2-HA
Arr2Δ7-HA
Arr3-HA
Arr3Δ7-HA
C
FA number/cell
60
50
40
30
20
10
0
**
***
**
**
***
DKO-Arr2
DKO-Arr2D7
DKO-Arr3
DKO-Arr3D7
DKO-GFP
WT-GFP
D
Sup
I.P. Arr2
Total
NRS
Arr2
NRS
FAK
arr2

Figure 3-10. Arrestins localize to focal adhesions and bind focal adhesion proteins. **(A)** Confocal images of DKO and WT cells expressing GFP or HA-tagged arrestins (B) and stained for paxillin. Focal adhesion number was calculated in rescued arrestin-expressing cells **(C)**. Data were analyzed by one-way ANOVA with arrestin type as the main factor **p<0.01 DKO-arrestin-2, DKO-arrestin-3, DKO-arrestin-3-Δ7 compared to WT, ***p<0.001 DKO-arrestin-2-Δ7 compared to WT, $^{###}$p=<0.001 compared to DKO-GFP according to Bonferroni /Dunn *post hoc* test with correction for multiple comparisons. Scale bar = 10μM. **(D)** Co-IP of endogenous arrestin-2 with FAK. Arrestin-2 was pulled down with FAK-specific antibody, but not with control rabbit serum (NRS).

arrestins directly regulate FA dynamics via binding to one or more of FA-associated proteins.

The absence of arrestins increases the activity of focal adhesion proteins.

To compare signaling in FAs in WT and DKO MEFs, we measured the activity of focal adhesion kinase (FAK) and paxillin after plating the cells for different times on FN (Figure 3-11a). DKO cells showed increased activity of both proteins over WT at every time point, even at time zero before the cells contacted extracellular substrate (Figure 3-11b,c). The total FAK was similar in WT and DKO cells (Figure 3-11e), while the total paxillin was even slightly lower in DKO (Figure 3-11d). Thus, higher percentage of paxillin and FAK was active in DKO cells than in WT.

Integrins serve as the anchoring points that link the extracellular matrix to the signaling complexes that promote cytoskeleton rearrangement inside the cell. To determine whether the increase in activity of FA proteins was due to an increase in integrin activity, cells were stained with antibodies recognizing total and active β1-integrin on the surface, and both were measured by FACs analysis (Figure 3-11f-h). Because integrins are activated by cations, staining for active β1-integrin was also performed in the presence of Mn^{2+} as a positive and EDTA as a negative control. We found no differences in active β1 integrin between DKO and WT cells (Figure 3-11h). However, we found that total (Figure 3-11f) and surface (Figure 3-11g) integrin in DKO cells was significantly higher than in WT. Collectively, these results along with the adhesion data (Figure 3-6e,f) suggest that DKO cells form initial attachments similar to WT, but have an advantage in spreading due to increased availability of integrins.

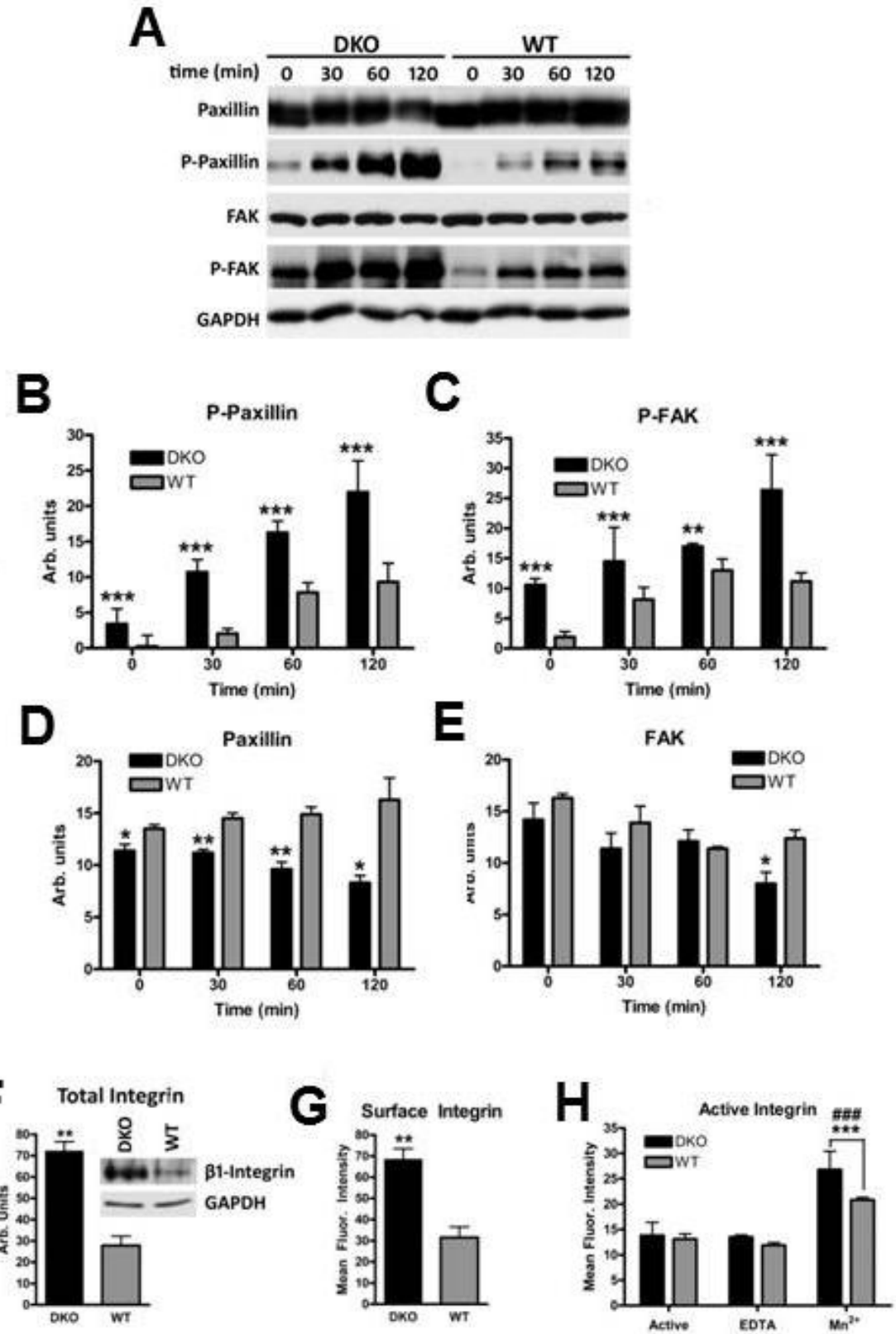
A
DKO
WT
time (min) 0 30 60 120 0 30 60 120
Paxillin
P-Paxillin
FAK
P-FAK
GAPDH
B
P-Paxillin
DKO
WT
Arb. units
Time (min)
C
P-FAK
DKO
WT
Arb. units
Time (min)
D
Paxillin
DKO
WT
Arb. units
Time (min)
E
FAK
DKO
WT
Time (min)
F
Total Integrin
DKO
WT
β1-Integrin
GAPDH
Arb. Units
G
Surface Integrin
Mean Fluor. Intensity
H
Active Integrin
DKO
WT
Mean Fluor. Intensity
Active
EDTA
Mn2+

Figure 3-11. The activity of focal adhesion proteins is altered in DKO cells.
(A) Lysates from cells plated on FN for indicated times were blotted for focal adhesion proteins paxillin, P-paxillin, FAK, and P-FAK. Blots from three experiments were analyzed by one way-ANOVA with cell type as the main factor **p<0.01 *p<0.05 **(B,C,D,E)** according to Bonferroni /Dunn *post hoc* test with correction for multiple comparisons. Data is from three experiments. **(F)** Total levels of integrin were measured in DKO and WT lysates in 3 experiments and analyzed by one-way ANOVA **p<0.01. **(G)** Surface integrin levels were measured by FACs with control IgG isotype control subtracted from the mean fluorescence intensity, **p<0.01. Data from 4 experiments (means $\pm$ SD) are shown. **(H)** Active integrins were measured on cells treated with 2 mM EDTA, 5 mM Mn^{2+}, or untreated controls. ###p=<0.001 compared to EDTA treated cells, ***p<0.001 compared to untreated cells. Data from 3 experiments (means $\pm$ SD) are shown.

The assembly and disassembly of FAs is affected by small GTPase signaling (67, 68). In particular, actin-myosin contractility mediated by ROCK activation via active RhoA provides tension within the cell that promotes the aggregation of integrins and an increase in associated FAs. If decreased RhoA activity in DKO cells is the main cause of increased FA number, the reduction of RhoA activity in WT cells should yield DKO-like phenotype. To test this idea, we expressed dominant-negative RhoN19 in WT cells and plated them on FN or PDL (Figure 3-12a). In contrast to DKO, FA number in cells expressing RhoN19 was lower than in WT controls (Figure 3-12b). Additionally, on PDL FAs were detected neither in WT-RhoN19 cells, nor control WT-GFP cells. Similar effects were observed when RhoA signaling was suppressed in WT cells by Rho inhibitor C3-transferase or ROCK inhibitor Y-27632. Under both conditions FAs were not decreased on FN and not detected on PDL (Figure 3-12b). Thus, increased number of FAs in DKO cells is not caused by reduced RhoA activity.

Arrestins are necessary for rapid FA disassembly

The accumulation and enlargement of FAs in DKO cells (Figure 3-9) along with increased activity of FA-associated proteins (Figure 3-11) suggests that the rate of FA disassembly might be reduced. To test this idea, we expressed GFP-paxillin in DKO and WT cells and measured FA lifetimes using live cell imaging (Figure 3-13a). Individual FAs at the leading edge of the cell were tracked from formation to disassembly (representative FAs are indicated by red arrows in Figure 3-13a). All FAs in WT cells formed and disassembled within 20-40 minutes (Figure 3-13b), with an average lifetime of ~25 minutes (Figure 3-13c). In contrast, lifetimes of FAs in DKO cells showed much

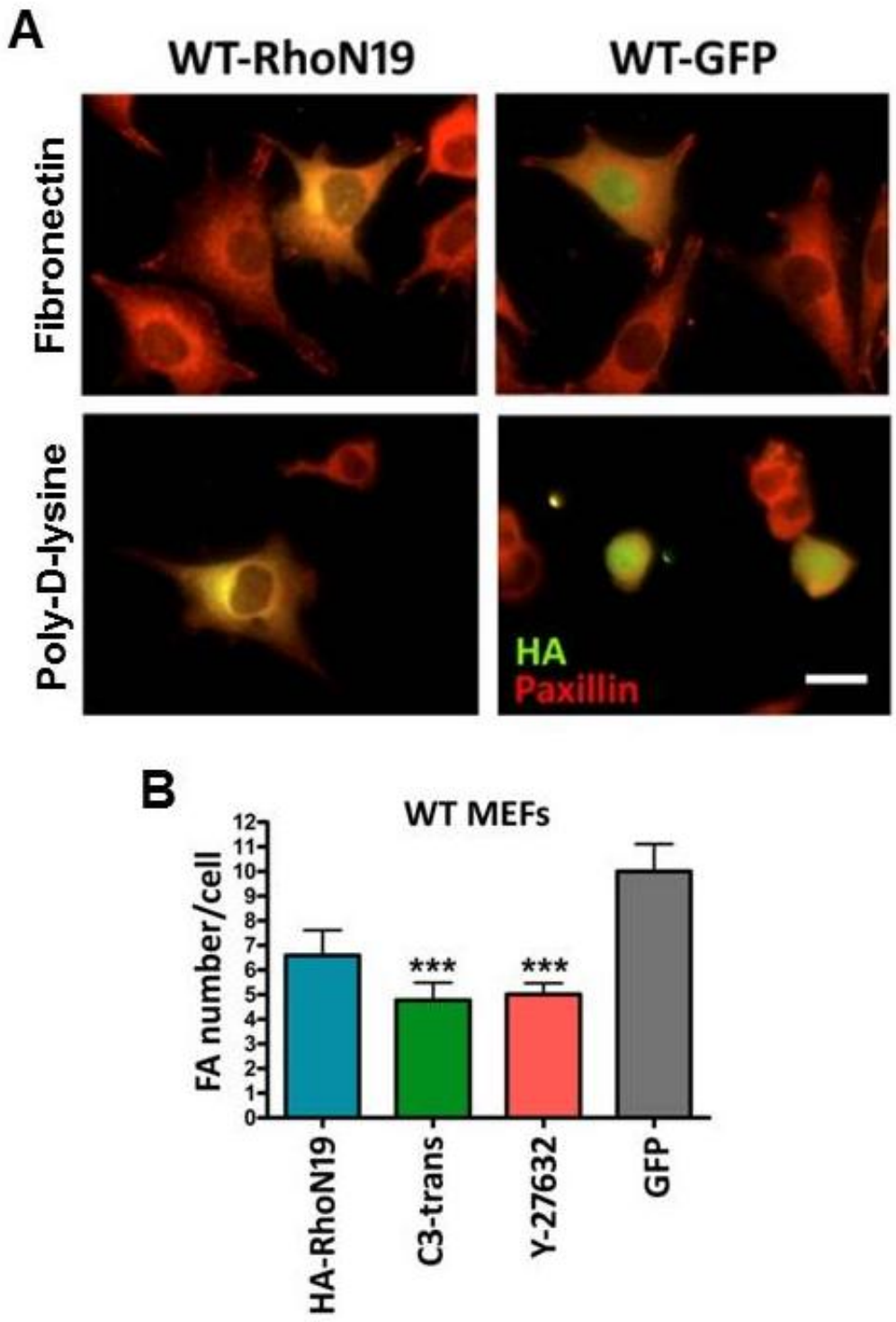

Figure 3-12. RhoA does not play an arrestin-dependent role in focal adhesion regulation. WT cells were infected with dominant-negative HA-RhoN19 or GFP. **(A)** Cells were plated on FN or PDL and stained for actin plus HA or actin plus paxillin. **(B)** Focal adhesion number was measured in 25 cells in three independent experiments and analyzed by one-way ANOVA, ***$p<0.001$ compared to WT-GFP.

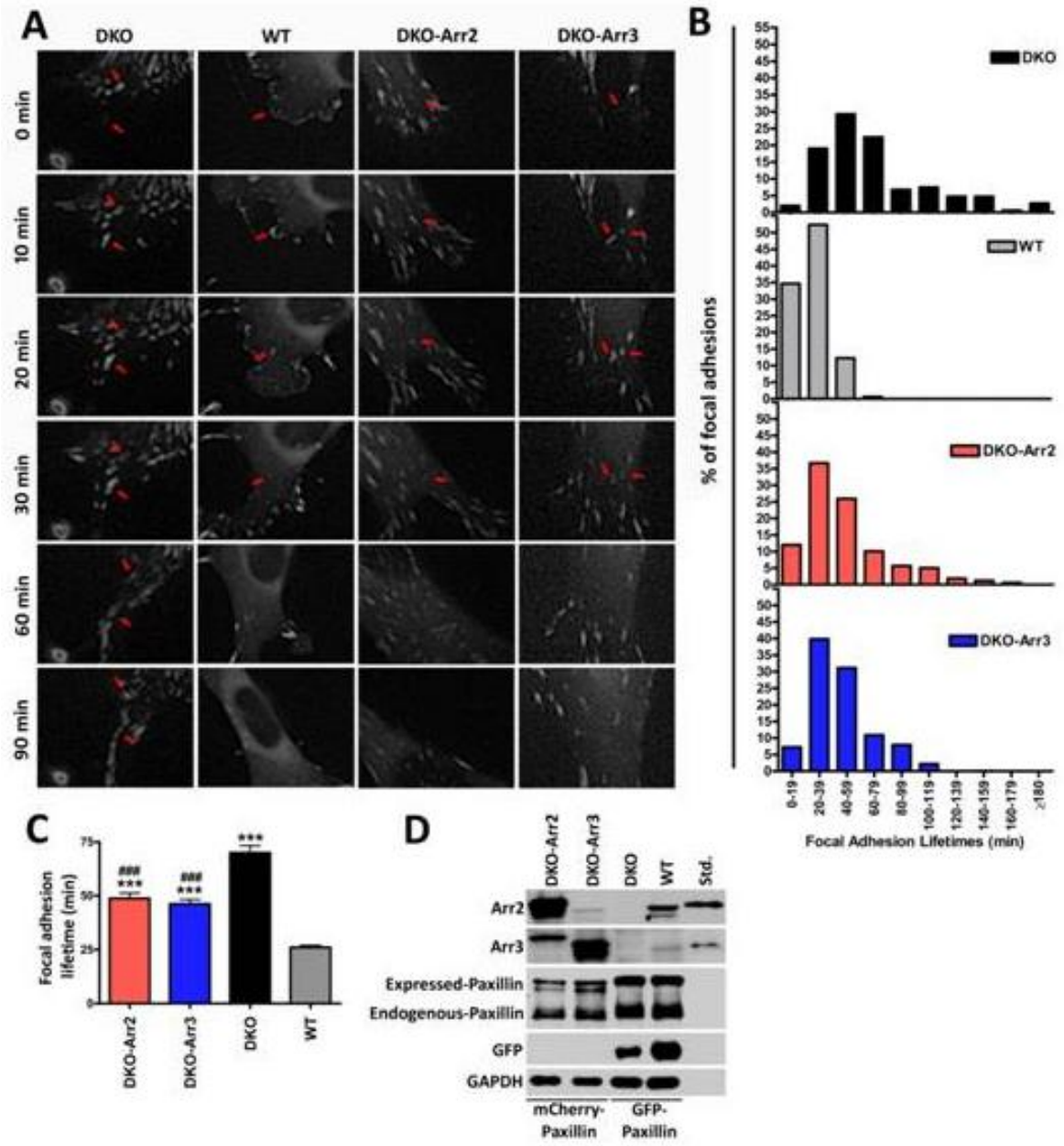
A
DKO
WT
DKO-Arr2
DKO-Arr3
0 min
10 min
20 min
30 min
60 min
90 min
B
% of focal adhesions
DKO
WT
DKO-Arr2
DKO-Arr3
0-19
20-39
40-59
60-79
80-99
100-119
120-139
140-159
160-179
≥180
Focal Adhesion Lifetimes (min)
C
Focal adhesion lifetime (min)
DKO-Arr2
DKO-Arr3
DKO
WT
D
DKO-Arr2
DKO-Arr3
DKO
WT
Std.
Arr2
Arr3
Expressed-Paxillin
Endogenous-Paxillin
GFP
GAPDH
mCherry-Paxillin
GFP-Paxillin

Figure 3-13. Arrestins regulate focal adhesion dynamics.
(A) DKO and WT cells expressing GFP-paxillin were viewed with DeltaVision Core microscope and images were captured at one-minute intervals. Representative images at 0, 10, 20, 30, 60, and 90 min are shown. Arrowheads indicate representative focal adhesions. Scale bar is 10 μM. FA lifetimes were determined by counting the number of sequential frames where individual FA (GFP-paxillin) is visible. Histogram distributions of FA lifetimes are shown 20 min intervals **(B)**. Data from 150 FAs in 15 cells for each cell type from 2-3 experiments. All distributions are significant from each other $p<0.0001$, except for DKO-Arr2 and DKO-Arr3 FA lifetimes, which are not significant according to nonparametric Kolmogorov Smirnov analysis. Insets show pre-images of cells used for still images, showing expression of GFP, indicative of arrestin expression, and mCherry-paxillin. **(C)** Mean FA lifetimes are shown. ***$p<0.001$ compared to WT, ###$p<0.001$ compared to DKO. **(D)** Expression of arrestins and tagged paxillin determined by Western blot with bovine arrestin-2 and arrestin-3 (0.1ng/lane) as standards (Std).

broader distribution, with ~72 minutes average. Notably, some FAs in DKO cells persisted longer than 3 h (Figure 3-13a). DKO cells also demonstrated a defect in leading edge formation and loss of polarity. To test whether the defect in FA disassembly is a result of the lack of arrestins, we transfected red mCherry-paxillin in cells co-expressing GFP with arrestins (Figure 3-13d). Live cell imaging revealed a shift in FA lifetimes towards WT (Figure 3-13b), with an average of ~48 and 46 minutes in cells expressing arrestin-2 and arrestin-3, respectively (Figure 3-13c). Thus, arrestins regulate FA turnover, and normal dynamics require the presence of both subtypes.

Microtubule targeting of focal adhesions is impaired in DKO cells

Decreased RhoA signaling (139) and increased FAK activity (140, 141) promote FA disassembly. However, DKO cells have a dramatic defect in disassembly despite having both of these conditions. Thus, arrestins regulate FA turnover via additional mechanisms. Microtubule targeting of FAs promotes disassembly (142, 143). To test whether microtubule-dependent FA disassembly is altered in DKO cells, we treated cells with nocodazole to destabilize microtubules, and then monitored FAs as the microtubules re-grew (Figure 3-14a). Upon nocodazole treatment of WT cells the number of FAs doubled. In agreement with FA lifetimes determined in live cell imaging (Figure 3-13b,c), after 30 min of nocodazole washout the number of FAs returned to baseline level, paralleling microtubule re-growth (Figure 3-14c). In contrast, DKO cells did not respond to microtubule destabilization, suggesting that microtubule loss has no effect on FAs in these cells (Figure 3-14b). Thus, arrestins likely participate in microtubule-dependent rapid FA disassembly.

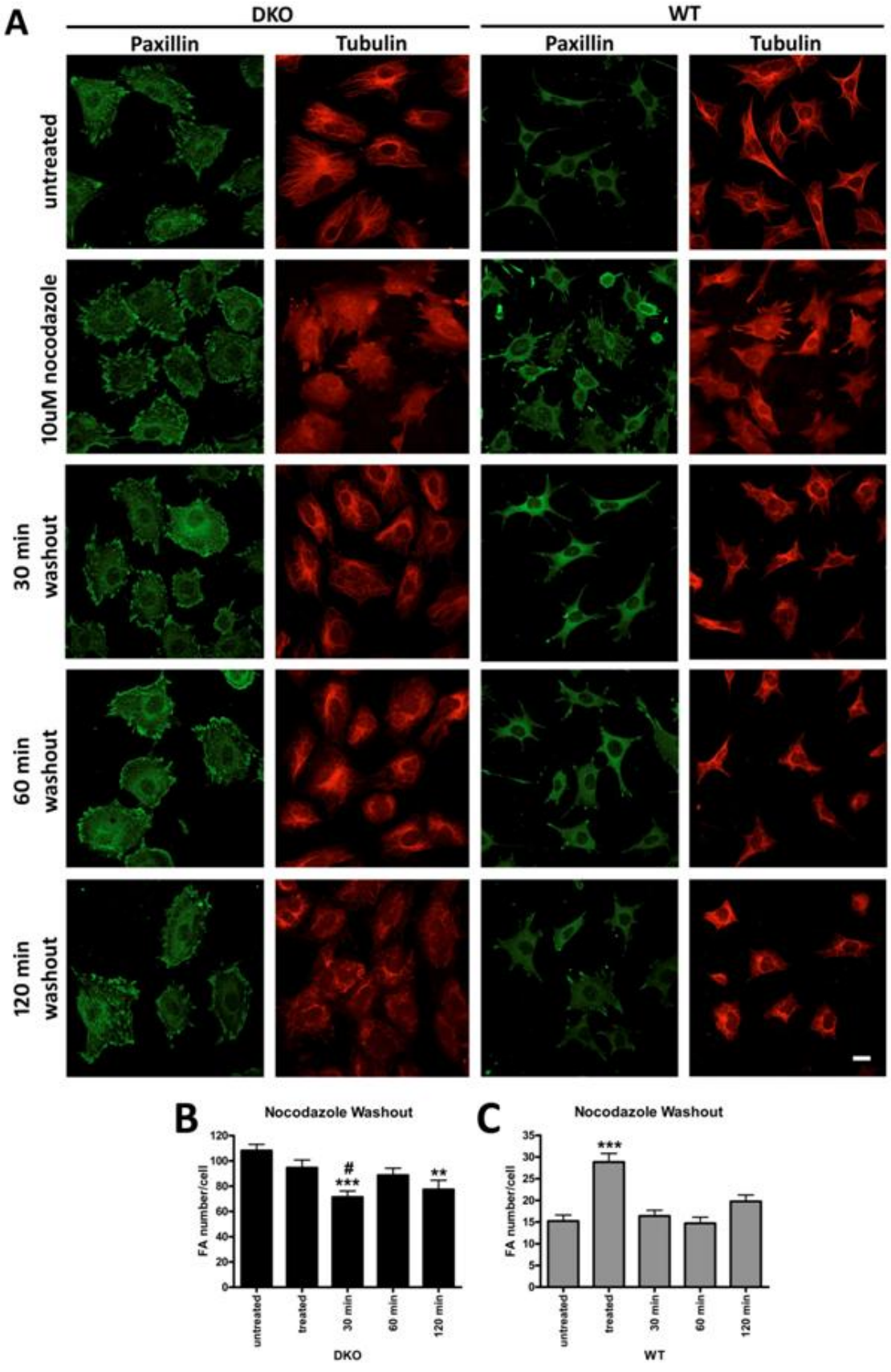
A
DKO
WT
Paxillin
Tubulin
Paxillin
Tubulin
untreated
10uM nocodazole
30 min washout
60 min washout
120 min washout
B
Nocodazole Washout
FA number/cell
120
100
80
60
40
20
0
#
***
**
untreated
treated
30 min
60 min
120 min
DKO
C
Nocodazole Washout
FA number/cell
35
30
25
20
15
10
5
0
***
untreated
treated
30 min
60 min
120 min
WT

Figure 3-14. Focal adhesion dynamics are altered in DKO cells with nocodazole treatment. (A) DKO and WT cells were plated for 24 h, and were treated with or without 10 µM nocodazole for 2 h. Nocodazole was washed-out and microtubules were allowed to re-grow for 30, 60 or 120 min. Paxillin or microtubules were visualized with respective antibodies. Focal adhesion number for each condition was calculated for DKO cells: **(B)** ***$p<0.001$, 30 min washout compared to untreated cells. #$p<0.05$ compared to treated cells. **$p<0.01$ 120 min washout compared to untreated cells. WT cells: **(C)** ***$p<0.001$ treated cells compared to all other conditions. Data were analyzed by one-way ANOVA with treatment as the main factor, and subjected to Bonferroni /Dunn *post hoc* test with correction for multiple comparisons. Data taken from 40-50 cells per condition. Scale bar = 10µM.

Discussion

Arrestins were first identified as terminators of GPCR signaling: arrestin binding to active phosphorylated receptors blocks G protein coupling (18). Subsequently, arrestins were shown to bind a variety of other proteins, including components of the endocytic machinery clathrin (144) and AP2 (145), MAP kinases (20, 41, 42, 44), ubiquitin ligases (146-148), and phosphodiesterase PDE4 (149). Arrestins have recently emerged as important players in cytoskeleton regulation via binding to microtubules (100), centrosome (150), and regulators of small GTPases (70, 72, 74). Despite clear interest in arrestin-dependent control of cytoskeleton (53, 151), very few mechanistic details have been established. Here we describe a dramatic phenotype of arrestin-2/3 DKO MEFs, and demonstrate that arrestins regulate cell morphology by altering the cytoskeleton in a receptor-independent fashion. Cells lacking both arrestins have a dramatic increase in cell size in both matrix-dependent (FN) and matrix-independent (PDL) conditions.

Small GTPases control cell shape by interacting with a variety of effectors that regulate the cytoskeleton. Dramatically altered morphology of DKO cells suggested that small GTPases are disregulated. Indeed, we found that basal activity of RhoA and Rac1 were significantly reduced. The expression of constitutively-active RhoA mutant returned DKO cell size back to WT, whereas the reduction of RhoA activity in WT cells resulted in an increase of cell spreading on PDL, similar to DKO. RhoA was previously identified as an arrestin-2 target. RhoA-induced stress fiber formation was shown to be dependent on arrestin-2, but not arrestin-3, following activation of the ATII1AR receptor (70). Arrestin-2 was shown to bind RhoGTPase activating protein, ARHGAP21, a known

inhibitor of RhoA activity (74). In both studies arrestin knockdown reduced RhoA activity, similar to our observations in DKO cells (Figure 3-3). Although arrestins were previously shown to promote RhoA activation, our study yielded several novel insights. First, we showed that both arrestin-2 and arrestin-3 regulate RhoA activity independently of receptor activation. Knockout of either arrestin individually does not change RhoA activity, whereas overexpression of individual non-visual arrestins in HEK293a increased RhoA activity. Thus, both arrestin-2 and arrestin-3 facilitate RhoA activation. Second, here we show for the first time that arrestin-dependent regulation of RhoA activity directly affects cell spreading.

Because the activity of signaling proteins that regulate the cytoskeleton is altered in DKO cells, we tested whether arrestins play a role in cell adhesion and migration. Arrestin-2/3 knockout decreased cell migration ~4-fold (Figure 3-6a), whereas the adhesion of DKO cells was enhanced (Figure 3-6f). Importantly, the rescue with individual arrestin-2 or arrestin-3 was partial, suggesting that both work together to control cell motility. A decrease in migration and an increase in adhesion suggest that FAs are altered in DKO cells. Indeed, we found that the numbers and sizes of FAs are dramatically increased in arrestin-null cells, and the difference with WT cells increases with time (Figure 3-9). Moreover, we found that arrrestin-2-Δ7 mutant co-localizes with FAs (Figure 3-10). In DKO cells we found higher levels of surface and total integrin, as well as increased activity of FAK and paxillin, even though total levels of these proteins were similar or even lower than in WT.

Rho-mediated myosin contractility promotes FA assembly by providing tension sufficient to cluster integrins (152). If higher RhoA activity increased the number of FAs,

one would expect increased RhoA activity in DKO cells, rather than the observed decrease (Figure 3-3b). We found that the reduction of RhoA activity by dominant-negative mutant or specific Rho inhibitors in WT cells leads to a decrease, rather than an increase of FAs. These data suggest that arrestin knockout acts via a novel mechanism, apparent slowing FA disassembly (Figure 3-13).

An increase in the activity of FA proteins and surface integrin both point to an impairment of FA turnover. Live cell imaging showed that FA lifetimes in DKO cells are dramatically longer than in WT. Importantly, the expression of arrestin-2 or -3 in DKO cells facilitates FA dynamics, although not to WT levels, suggesting that both are required for rapid FA turnover. A lot more is known about the assembly of FAs, than about their disassembly. Several studies showed that a decrease in RhoA and an increase in FAK promotes FA disassembly (139-141). However, DKO cells demonstrate impaired FA disassembly despite decreased RhoA and increased FAK activity, suggesting that arrestins regulate FA dynamics via other mechanisms.

Recently microtubule targeting has emerged as the predominant mediator of FA disassembly (142, 143). One study (153) revealed that the Rho family GTPases are not involved and that FA disassembly requires microtubules and dynamin, neither of which participates in FA assembly. FAs in DKO cells do not respond to nocodazole treatment: additional FAs do not form when microtubules are destroyed, and FA disassembly is abnormal during microtubule re-growth in these cells (Figure 3-14). It is tempting to speculate that arrestins, known to bind microtubules (100), might serve as a link between microtubules and FA dynamics. Consistent with this idea, DKO and WT cells stained for

focal adhesion marker paxillin and microtubules shows that microtubules are improperly targeted to focal adhesions in DKO cells (Figure 3-15).

The fact that dynamin is involved in microtubule-induced disassembly suggested that the rate-limiting step is endocytosis of integrins or other FA components (153). This was shown to be the case: integrin endocytosis mediated by clathrin and Dab2 is directly involved in microtubule-induced FA disassembly (153). It was suggested that microtubules deliver clathrin and Dab2 to FAs. Indeed, rapid accumulation of these proteins was documented when microtubules targeted FAs (154). Our data are compatible with this hypothesis. Higher proportion of β1-integrin on the surface of DKO cells is consistent with its impaired internalization. Arrestins participate in the endocytosis of GPCRs and other membrane receptors (27). Our finding that arrestin-2-Δ7 mutant with enhanced microtubule binding (100) shows subcellular localization similar to paxillin suggests that arrestins likely localize to FAs, which would place them in the proximity of integrins. The fact that this mutant, frozen in microtubule-bound conformation, shows stronger FA localization than WT (Figure 3-10b) suggests that binding to microtubules might facilitate arrestin localization to FAs. Upon GPCR binding arrestins undergo a distinct conformational change (27) that exposes binding sites for AP2 and clathrin (33) to initiate receptor endocytosis. Arrestins bind microtubules via the same interface as GPCRs (100), and AP2 and clathrin binding sites are exposed in the same manner (100). Thus, it is entirely possible that arrestins provide the link between microtubules and integrin endocytosis by recruiting clathrin to FAs, thereby promoting integrin internalization.

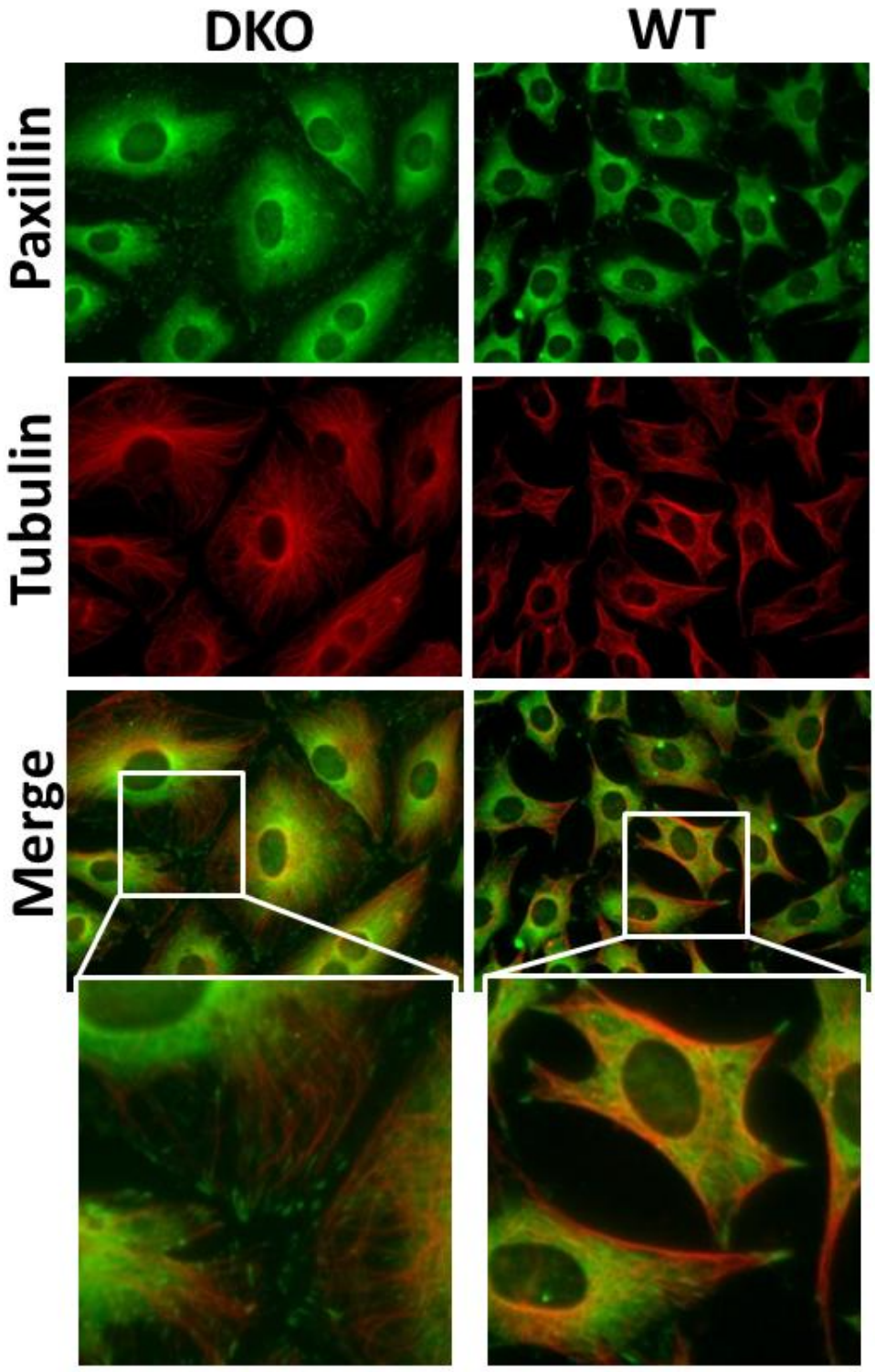

Figure 3-15. Microtubules are not properly targeted to focal adhesions in DKO cells. DKO and WT cells plated on fibronectin for 2 hours were stained with antibodies for α-tubulin and paxillin.

Arrestins can facilitate FA disassembly via several mechanisms. Arrestin-2 and -3 facilitate ERK1/2 activation (42, 155). Paxillin constitutively associates with MEK1 (156) and is phosphorylated by ERK1/2 on several serine residues upon growth factor stimulation (157). Activation of hepatocyte growth factor receptor promotes recruitment of cRaf1 and ERK1/2, leading to the phosphorylation of paxillin by ERK1/2 (158, 159). Thus, arrestins may recruit ERK1/2 to the leading edge of the cell in proximity of paxillin. FA turnover may be affected in three ways by ERK1/2 activated via arrestins. First, phosphorylation of paxillin by ERK may destabilize FAK-paxillin interaction, leading to localized disassembly of focal contacts. Second, ERK phosphorylates and activates myosin light chain kinase (MLCK), another key factor shown to promote FA disassembly (140). Third, filamin, which regulates the trafficking of β1-integrins (160, 161), binds arrestins and ERK1/2 (52). Interestingly, we recently found that Δ7 mutants of arrestin-2 and -3 bind ERK1/2 even better than parental WT proteins (162).

Our data reveal a completely novel function of arrestins. Arrestin-2 and arrestin-3 individually regulate RhoA independently of GPCR stimulation to promote proper cell spreading. Arrestins also directly affect FA disassembly and migration, and this function requires both non-visual arrestins and is not mediated by small GTPases. Thus, non-visual arrestins regulate cell spreading and migration via FA dynamics. Our results strongly suggest that non-visual arrestins might be the missing link between microtubules and FA disassembly.

CHAPTER IV

PROGRESSIVE REDUCTION OF ITS EXPRESSION IN RODS REVEALS TWO POOLS OF ARRESTIN-1 IN THE OUTER SEGMENT WITH DIFFERENT ROLES IN PHOTORESPONSE RECOVERY

This work was published in PLoS One in July 2011 (163).

The paper was a collaborative effort between the laboratories of Vsevolod V. Gurevich, Jeannie Chen, and Eugenia V. Gurevich

Introduction

Humans express ~800 different G-protein-coupled receptor (GPCR), among which rhodopsin is the best characterized (164). Rod phototransduction is the only GPCR-driven signaling cascade where the expression levels of all players are known with sufficient precision to model systems behavior of the cell (165-168). The biochemical mechanism of rod phototransduction serves as a model of GPCR-driven signaling cascade (164). Light activates rhodopsin by converting covalently linked 11-cis-retinal to all-trans-retinal. Active rhodopsin catalyzes GDP/GTP exchange on a heterotrimeric G protein transducin, which in turn activates cGMP phosphodiesterase. The hydrolysis of cGMP rapidly reduces its concentration, leading to the closure of cGMP-gated cation channels, which suppresses circulating current. Single photon sensitivity (169) and fine temporal resolution of the rod is ensured by the shutoff of rhodopsin signaling with sub-second kinetics (167, 170). Rhodopsin is turned off by a two-step mechanism. First,

GRK1 (also known as rhodopsin kinase) specifically binds activated rhodopsin and phosphorylates its C-terminus (171). When the number of rhodopsin-attached phosphates reaches three (85, 86), arrestin-1[a] binds the receptor with high affinity, sterically precluding further transducin activation (88, 172). Mouse rods express arrestin-1 and rhodopsin at ~0.8:1 ratio, making arrestin-1 the second most abundant protein in the rod photoreceptor (92, 173, 174). Using transgenic mice expressing arrestin-1 at levels ranging from 4% to 220% of WT, we recently found that supra-physiological arrestin-1 levels marginally improve the functional performance of rods (174). Reduced arrestin-1 levels are adequate at dim light, but impair functional performance at brighter illumination (174). Importantly, the reduction of arrestin-1 level in the OS to ~2.5% of WT dramatically slowed the recovery kinetics, as compared to mice with only twice as much arrestin-1 in the OS (174). Here we show that, while the recovery rates in all lines slow with the increased intensity of the desensitizing flash, the same "threshold" between 5% and 2.5% of arrestin-1 level in the OS is observed. These data indicate that ~2.5% of arrestin-1 content in the OS is not immediately available for rhodopsin quenching, suggesting that this separate pool of arrestin-1 resides relatively far from rhodopsin-containing discs. Slow diffusion of arrestin-1 across the OS in the lowest expressing line apparently delays the recovery by making rhodopsin inactivation rate-limiting, in contrast to WT and arrestin-1 hemizygous (Arr1+/-) animals where transducin inactivation is the slowest process that determines the speed of recovery (167, 170, 175).

Materials and Methods

Ethics Statement

Animal research was conducted in compliance with the NIH Guide for the Care and Use of Laboratory Animals and approved by the institutional Animal Care and Use Committee (protocol ID M/06/091).

Generation of transgenic mice expressing arrestin-1 at different levels.

Transgenic mice expressing different levels of arrestin-1 were described previously (92, 97, 174), and the arrestin-1 content in the dark-adapted OS of these mice was determined (174).

Electroretinography (ERG)

Electroretinograms were recorded from 6 to 8 week old mice reared in 12/12 light-dark cycle (90±10 lux in the cage during light period) and dark-adapted overnight, as described (174, 176). Briefly, under dim red light, mice were anesthetized by i.p. injection of (in μg/g body weight) 15-20 ketamine, 6-8 xylazine, 600-800 urethane in PBS. The pupils were dilated with 1% tropicamide in PBS. An eye electrode made with a coiled 0.2mm platinum wire was placed on the cornea, a tungsten needle reference electrode in the cheek, and ground needle electrode in the tail (177-179). ERG was recorded with the universal testing and electrophysiologic system UTAS E-3000 (LKC Technologies, Inc.). A Ganzfeld chamber was used to produce brief (from 20μs to 1ms) full field flash stimuli. The light intensity was calibrated by the manufacturer and

computer controlled. The mouse was placed on a heating pad connected to a temperature control unit to maintain the temperature at 37-38^{o}C throughout the experiment.

Double-flash protocol. The double flash recording was used to analyze the kinetics of recovery (177, 180). A test flash was delivered to suppress the circulating current of the rod photoreceptors. The recovery was monitored by delivering a second (probe) flash after time interval between the two flashes, which was varied from 200 to 120,000 ms. The intensity of the test flash was either -0.8, -0.4, 0, or +0.4 *log*cd*s/m^2, corresponding to ~160, ~400, ~ 1000, and ~2500 photoisomerizations per rod (179). The following probe flash was 0.65 *log*cd*s/m^2, corresponding to ~4,500 isomerizations per rod (179). Sufficient time for dark adaptation was allowed between trials, as determined by the reproducibility of the response to the test flash. Time-to-peak (implicit time) of the a-wave at the intensity of the probe flash was similar across different genotypes. This finding along with the shape of the a-wave indicates that the intrusion of b-wave and oscillation potentials (180, 181) did not differentially affect different genotypes. The normalized amplitude of the probe flash a-wave was plotted as a function of time between the two flashes. Instead of fitting the data points to a theoretical equation, which is inevitably based on certain assumptions that may not be correct for all of the genotypes used in this study, we fitted curves with polynomial nonlinear regression using GraphPad Prism (Version 4.0) and cosindered R^2>0.95 as a criterion for a good fit. The rate of recovery was characterized by the time interval necessary for half recovery (t_{half}).

Statistical Analysis

The data were analyzed by for each light level separately by one-way ANOVA with Genotype as main factor. To examine the change in recovery time with light intensity, the data for each genotype was analyzed separately with light as main factor. Means were compared using Bonferroni post hoc test with correction for multiple comparisons. In all cases, $p<0.05$ was considered significant.

Results

Arrestin-1, acting after GRK1 phosphorylation of rhodopsin (182, 183), is the key player in rapid photoresponse recovery in rods (184) and cones (185). In the dark, arrestin1 translocates out of OS and localizes primarily to cell bodies of rod photoreceptors, so the OS contains only a small proportion of arrestin-1 (92, 95, 173, 174, 186, 187). Dark-adapted rod OS of transgenic mice expressing arrestin-1 at 4% (Tr-$4^{Arr-/-}$), 12% (Tr-$12^{Arr-/-}$), 50% (Arr+/-), and 100% of WT contain ~ 7.6, 15, 180, and 300 μM arrestin-1, respectively (these calculations are based on 3 mM rhodopsin concentration in the OS (82, 174)), which constitutes 2.5%, 5%, 60%, and 100% of normal WT level, respectively. Rod function can be monitored non-invasively by ERG, where the suppression of rod circulating current is reflected by a negative a-wave response (177, 180, 188, 189). We used double-flash protocol, where an initial flash desensitizes rods, and the response to the second (probe) flash, delivered at varying time intervals after the initial flash, is measured to determine the extent of recovery. The time of half-recovery (t_{half}) is calculated by plotting the amplitude of the probe flash response as a function of time between flashes (177). Using desensitizing flash of -0.4 *log*cd*s/m^2

(400 photoisomerizations/rod), we previously found that recovery rates of the three lines with 100%, 60%, and 5% of WT arrestin-1 level in the OS are surprisingly similar, whereas rod recovery in mice with 2.5% of normal arrestin-1 content in the OS is dramatically slowed (Figure 4-1) (174). Considering that the pseudo-first-order rate of arrestin-1 binding to phosphorylated rhodopsin is the product of the on-rate constant (which was recently measured (190)) multiplied by the absolute arrestin-1 concentration near rhodopsin-containing discs, two mechanistic models could account for this "threshold"-like effect. If arrestin-1 is homogeneously distributed throughout OS cytoplasm, the threshold must depend on the intensity of the desensitizing flash, so that the activation of more than twice as many rhodopsins should place Tr-12$^{Arr-/-}$ mice with two-fold greater arrestin-1 content below the threshold. Alternatively, arrestin-1 distribution in the OS may be non-homogeneous, with immediately available and relatively unavailable pools. If the latter pool is roughly equal to arrestin-1 content in the lowest expressing animals, Tr-4$^{Arr-/-}$ mice would be below the threshold at all intensities of desensitizing flash, whereas all other lines would remain above it. To distinguish between these two possibilities, we used initial desensitizing flashes with intensities that vary ~16-fold, -0.8, -0.4, 0, and +0.4 *log*cd*s/m^2, corresponding to 160, 400, 1000, and 2500 photoisomerizations/rod (Figure 4-1,2; Table 4-1). Unexpectedly, we found no significant differences in the t_{half} of WT, Arr+/-, and Tr-12$^{Arr-/-}$ mice at any intensity of desensitizing flash tested, despite ~20-fold difference in the arrestin-1 content in the OS of WT and Tr-12$^{Arr-/-}$ animals. However, the magnitude of the recovery defect in Tr-4$^{Arr-/-}$ mice depended on flash intensity. At 160 photoisomerizations/rod, t_{half} of Tr-4$^{Arr-/-}$ mice was only ~1.8-fold longer than in other genotypes, but the difference increased to ~5.5-,

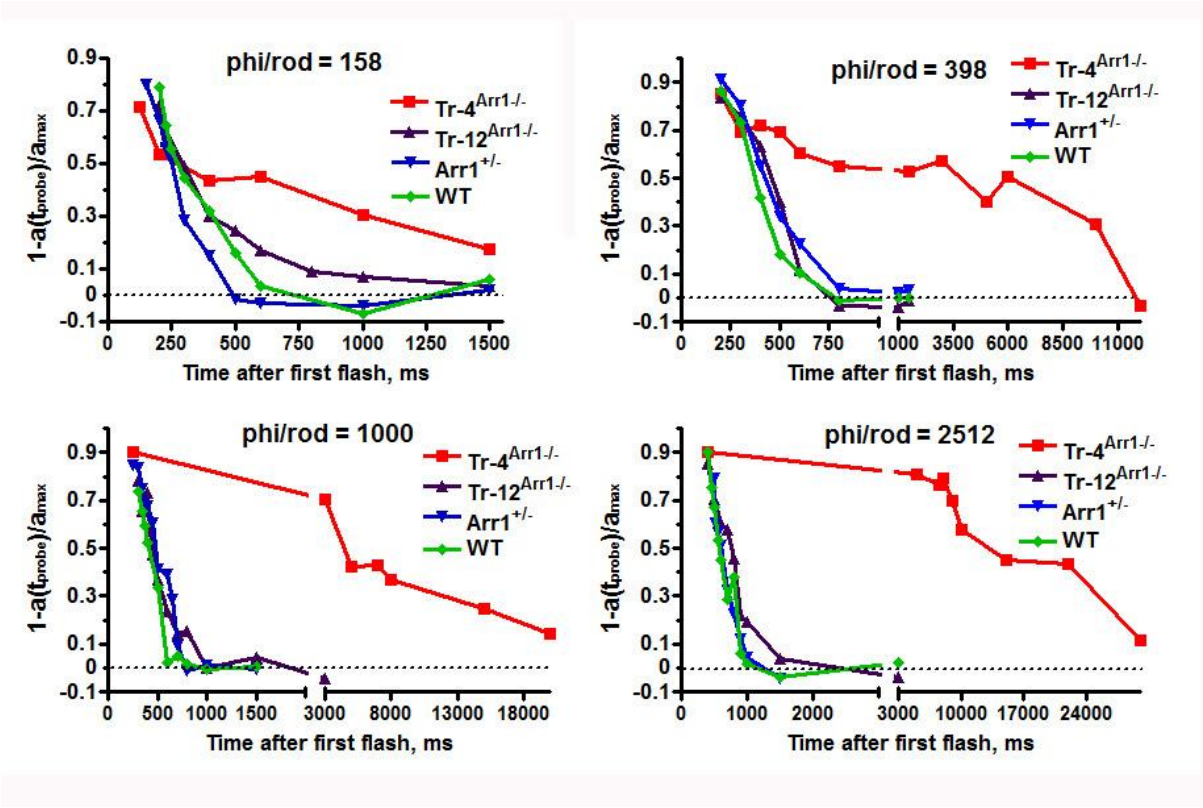

Figure 4-1. Reduced arrestin-1 expression slows down photoresponse recovery. The intensities of the first (desensitizing) flashes were -0.8, -0.4, 0, or +0.4 *log*cd*s/m^2 and second (probe) flash was 0.65 *log*cd*s/m^2. The a-wave elicited by the probe flash was plotted as a function of time elapsed after the first flash. Representative recovery curves for indicated genotypes and strengths of desensitizing flash are shown. The interval between the two flashes was varied from 200 to 120,000ms. Phi/rod, photoisomerizations/rod.

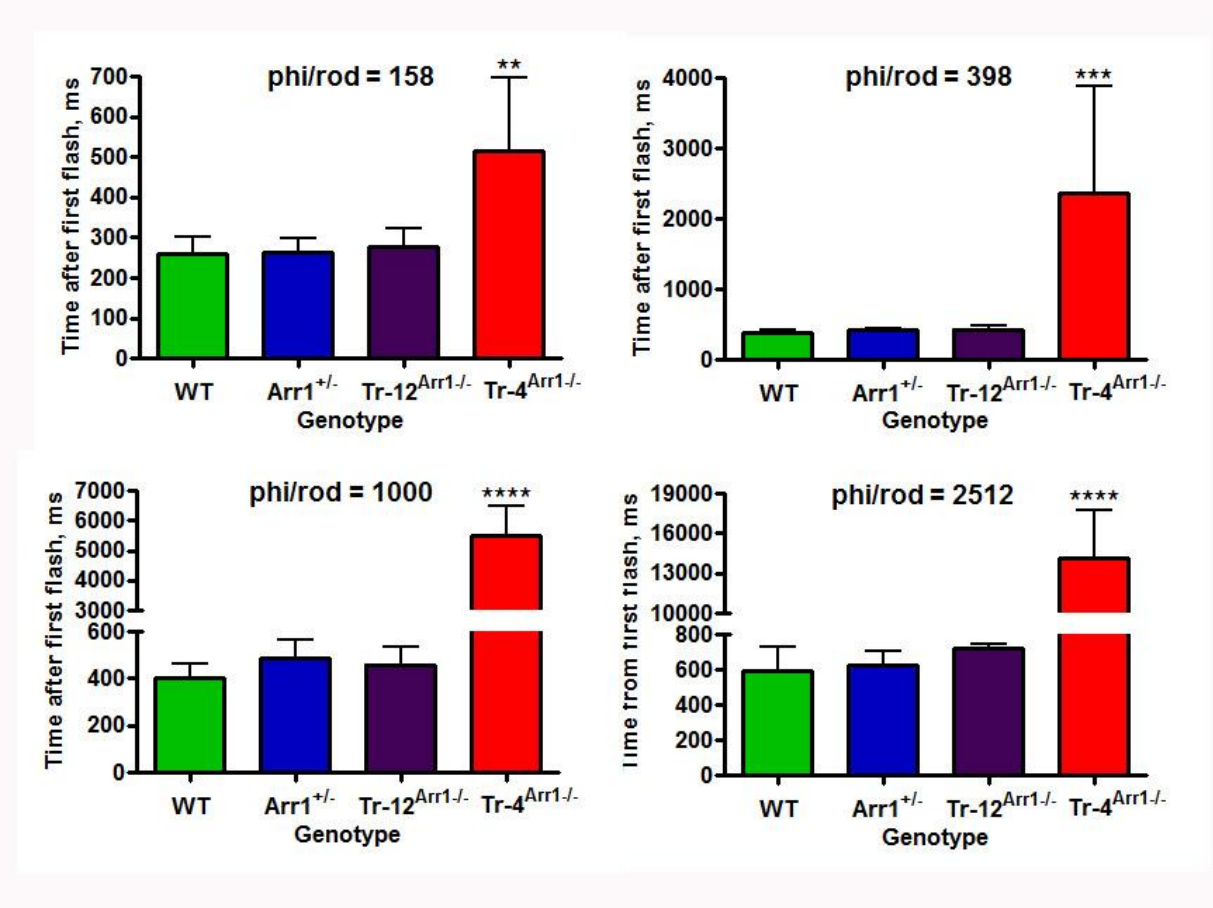

Figure 4-2. Animals with very low arrestin-1 in the OS show very long time of half recovery. To calculate the time of half recovery, recovery kinetics were fitted by polynomial nonlinear regression, with R^2>0.95, as described in methods. Means +/- SD for four animals per genotype are shown. The data were analyzed by one-way ANOVA with Genotype as main factor followed by Bonferroni post hoc comparison of means. * - p<0.05; ** - p<.001, *** - p<0.001 to WT; + - p<0.05, ++ - p<0.001, +++ - p<0.001 to Arr+/-, a – p<0.005, b – p<0.01, c – p<0.001 to Tr-12$^{Arr-/-}$. Phi/rod, photoisomerizations/rod.

Genotype	158 phi/rod	398 phi/rod	1000 phi/rod	2512 phi/rod	Arrestin-1 concentration (OS)
Wild type	258 ± 45 ms	376 ± 47 ms	405 ± 58 ms	646 ± 56 ms	300 μM
$Arr1^{+/-}$	262 ± 35 ms	426 ± 26 ms	486 ± 82 ms	626 ± 79 ms	180 μM
$Tr\text{-}12^{Arr1\text{-}/\text{-}}$	278 ± 46 ms	433 ± 45 ms	460 ± 75 ms	718 ± 27 ms	15 μM
$Tr\text{-}4^{Arr1\text{-}/\text{-}}$	514 ± 183 ms	2368 ± 1515 ms	5515 ± 999 ms	14137 ± 3595 ms	7.6 μM

Table 4-1. The rates of photoresponse recovery in mice with different arrestin-1 expression. Initial desensitizing flashes with intensities that vary ~16-fold, -0.8, -0.4, 0, and +0.4 *log*cd*s/m^2, corresponding to 160, 400, 1000, and 2500 photoisomerizations/rod were used. The magnitude of the recovery defect in $Tr\text{-}4^{Arr\text{-}/\text{-}}$ mice depended on flash intensity. At 160 photoisomerizations/rod, t_{half} of $Tr\text{-}4^{Arr\text{-}/\text{-}}$ mice was only ~1.8-fold longer than in other genotypes, but the difference increased to ~5.5-, 12-, and 23-fold at 400, 1000, and 2500 photoisomerizations/rod, respectively. In WT, Arr+/-, and $Tr\text{-}12^{Arr\text{-}/\text{-}}$ mice, t_{half} increased ~2.5-fold with the desensitizing flash inducing 2,500 instead of 160 photoisomerizations/rod. In sharp contrast, the increase in recovery time from the dimmest to brightest desensitizing flash for $Tr\text{-}4^{Arr\text{-}/\text{-}}$ mice was ~28 fold.

12-, and 23-fold at 400, 1000, and 2500 photoisomerizations/rod, respectively (Figure 4-2; Table 4-1).

Importantly, WT, Arr+/-, and Tr-12$^{Arr-/-}$ mice demonstrated a gradual slowing of the recovery with increasing intensity of the desensitizing flash, and the slope of the slowing was the same in these three genotypes, as evidenced by lack of interaction between Genotype and Light factors in two-way-ANOVA ($F(6,41)$-1.12, p=0.37 n.s.). In these genotypes t_{half} increased ~2.5-fold with desensitizing flash inducing 2,500 instead of 160 photoisomerizations/rod (Table 4-1). In sharp contrast, the increase in recovery time from the dimmest to brightest desensitizing flash for Tr-4$^{Arr-/-}$ mice was ~28 fold (Table 4-1). Virtually identical slowing of the recovery in WT, Arr+/-, and Tr-12$^{Arr-/-}$ animals likely reflects the increased time that it takes guanylyl cyclase to replenish hydrolyzed cGMP necessary to open cGMP-gated channels and restore circulating current, whereas much more dramatic increase of t_{half} in Tr-4$^{Arr-/-}$ animals must reflect additional processes that do not operate in the other three genotypes.

Discussion

Comprehensive understanding of systems behavior of rod photoreceptors requires precise knowledge of the concentration, localization, and activity of every signaling protein in the cell. While the functional role of many signaling proteins in rod phototransduction have been qualitatively established using genetically modified mice (reviewed in (83)), the biological significance of the specific level of each protein is rarely addressed. The studies where rods with different expression levels of rhodopsin (191, 192), RGS9 (170, 175), GRK1 (193), and arrestin (174, 175, 193) were functionally

characterized yielded seminal, often unanticipated, results. Here we report an unexpected finding that 20-fold reduction of arrestin-1 content in the dark-adapted rod OS from 100% to 5% of WT level has no appreciable effect on photoresponse recovery, whereas further 2-fold reduction to 2.5% dramatically slows this process (Figure 4-1,2; Table 4-1). This remarkable difference in recovery kinetics is unlikely to be simply the result of depletion of arrestin-1 in the OS. The calculated amount of arrestin-1 present in the OS for Tr-$4^{Arr-/-}$ mice is approximately 7.6 μM, which corresponds to about 200,000 molecules per OS (174). Mouse OS contains ~10^8 rhodopsins in ~800 disks (82), or ~125,000 rhodopsins per disc. In the case of even arrestin-1 distribution in the OS there would be ~250 arrestin-1 molecules per disc available to quench rhodopsin. However, even at the dimmest desensitizing flash used, which generates only 160 Rh*/rod (0.2 Rh*/disc), we observed a 1.8-fold slowing of the recovery, which increases to >20-fold at 3 Rh*/disc (Table 4-1). Arrestin-1 concentration in the WT mouse OS is ~300 μM (174). Taking into account known constants of mouse arrestin-1 self-association (194), this yields ~ 50 μM active monomer. This results in estimated pseudo-first-order on-rate of 50 s^{-1}, enabling arrestin-1 to "check" the state of each rhodopsin molecule every 20 msec. This is consistent with recent estimates of an active rhodopsin lifetime of <60 ms (170), or possibly even ~30 ms (167, 175). Average arrestin-1 concentration in the OS of Tr-$4^{Arr-/-}$ mice is ~ 7.6 μM (174), so that arrestin-1 would be able to encounter each rhodopsin every 200 ms. This difference is sufficient to account for ~200 ms delay, but cannot explain the multi-second times of half-recovery observed (Figure 4-2; Table 4-1). Thus, our data suggest that most of arrestin-1 in the OS of Tr-$4^{Arr-/-}$ animals is not immediately available for rhodopsin quenching.

Self-association could potentially limit arrestin-1 availability. Arrestin-1 forms dimers and tetramers at physiological concentrations (195-197), yet only the monomer is capable of binding rhodopsin (197, 198), because the well-defined rhodopsin-binding surface of each molecule (25, 106, 194, 199-204) is occluded by other subunits in the solution tetramer (198). Recent measurements of self-association constants of mouse arrestin-1 yielded $K_{d\ dimer}$ = 57.5 μM and $K_{d\ tetramer}$ = 63.1 μM (194). These values allow the calculation of the half-life of the dimer and tetramer (205), both of which turn out to be on the order of 12 ms. Thus, arrestin-1 self-association also cannot account for the multi-second times of half-recovery in Tr-$4^{Arr-/-}$ mice (Table 4-1).

Sub-cellular distribution of arrestin-1 in rods is strictly light dependent. In the dark, arrestin-1 is predominantly located in the inner segment, perinuclear layer, and synaptic terminals, with relatively small fraction, estimated at 2-4% (92, 97), 9% (173), or ~15% (174), residing in the OS. Prolonged bright illumination triggers the translocation of the majority of arrestin-1 to the OS (97, 186, 206). Different lines of evidence suggest that arrestin-1 movement is either energy-independent, driven by diffusion (97), or may involve active transport (207), or possibly diffusion with active gating in the cilium (173). Considering that in the light and dark arrestin-1 in the rod is at disequilibrium (208), it is clear that, regardless of the mode of transportation, its distribution must be determined by the interactions with non-mobile partners: otherwise the diffusion would quickly ruin concentration gradients created by any mechanism (209). Arrestin-1 binds rhodopsin at 1:1 ratio (89, 90), and the molar amount of arrestin-1 that can translocate to the OS in the light is limited by the amount of rhodopsin present in this compartment (92), indicating that rhodopsin is the immobile binding partner that holds arrestin-1 in the

OS in the light. Arrestin-1 binds several proteins present in the cell body, including polymerized tubulin (microtubules) (210, 211), c-Jun N-terminal kinase (39), ubiquitin ligase Mdm2 (39), calmodulin (35), N-ethylmaleimide-sensitive factor (212), and enolase1 (213). Among these, however, tubulin appears to be the only sufficiently abundant protein to serve as an "anchor" for arrestin-1 expressed at 0.8:1 ratio to rhodopsin (92, 173, 174). High concentration of arrestin-1 in the compartments particularly rich in microtubules (the inner segment, perinuclear area, and synaptic terminals (214)) in the dark supports this notion. Arrestin-1 translocation is a relatively slow process that takes many minutes (97, 173, 206). Thus, in dark-adapted animals used in this study arrestin-1 already present in the OS must be responsible for signal shutoff. Microtubules are not abundant in the OS, but several bundles near the outer membrane extend along the full length of the OS and the axoneme (95, 214). The diameter of mouse rod OS is ~1.4 μm (165), so that arrestin-1 bound to these microtubules would need to diffuse for up to 0.7 μm before reaching rhodopsin. This would take seconds (165), which matches the observed delay of photoresponse recovery in Tr-4$^{Arr-/-}$ mice, as compared to the Tr-12$^{Arr-/-}$ animals (Table 4-1), fairly well. Thus, the simplest model that accounts for our data is that there are two distinct pools of arrestin-1 in the OS. At least 2.5% is bound to the microtubules at the plasma membrane, whereas the rest is distributed throughout OS cytoplasm, with only the latter being available to quench rhodopsin signaling on the millisecond timescale. In Tr-4$^{Arr-/-}$ animals microtubules take up most of the arrestin-1 present, leaving relatively little immediately available to rhodopsin. This slows down shutoff by the time necessary for arrestin-1 diffusion across the OS. In contrast, in Tr-12$^{Arr-/-}$ mice and higher expressors the microtubules in the OS

apparently saturate by the amount of arrestin-1 roughly equal to that present in Tr-4$^{Arr-/-}$ animals, allowing the rest of arrestin-1 to freely distribute in the cytoplasm to be immediately available for rhodopsin shutoff (Figure 4-3).

In summary, our data suggest the existence of two distinct pools of arrestin-1 in dark-adapted mouse outer segments. To the best of our knowledge, so far only one genetically modified mouse line where rhodopsin shutoff was made rate-limiting was described: mice with low expression of GRK1/2 chimera (215). In Tr-4$^{Arr-/-}$ mice we made rhodopsin shutoff the rate-limiting stage of photoresponse recovery by low expression of arrestin-1. Collectively, these results strongly support the idea that both phosphorylation and arrestin binding are necessary steps in rhodopsin shutoff.

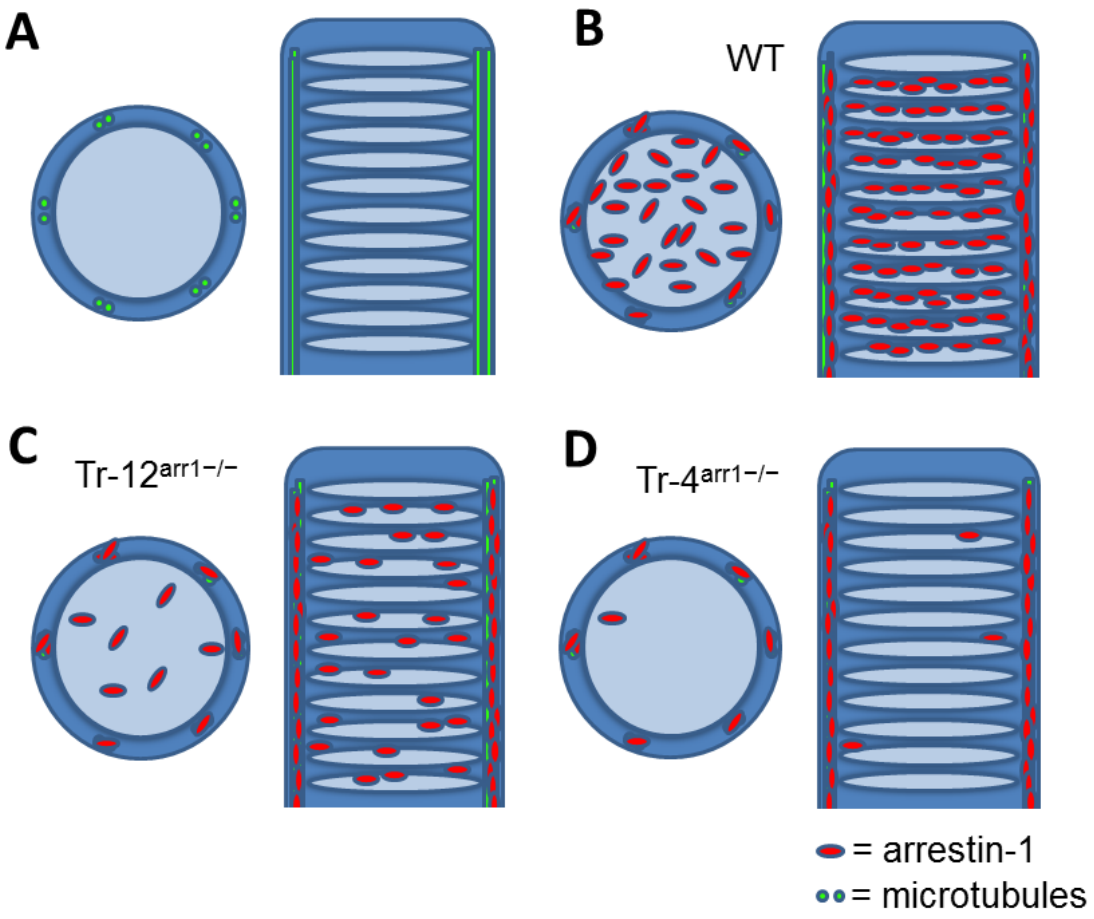

Figure 4-3. There are two distinct pools of arrestin in the OS in the dark: microtubule bound, and cytoplasmic.
Because arrestin translocation happens on the order of minutes, arrestin already in the OS must be available to quench rhodopsin signaling with sub-second kinetics in dim light. The simplest model that accounts for our data is that there are two distinct pools of arrestin-1 in the OS in the dark. **(A)** Rod photoreceptors have microtubules that extend along the axoneme of the OS. **(B)** In WT animals, at least 2.5% is bound to the microtubules at the plasma membrane, whereas the rest is distributed throughout OS cytoplasm, with only the latter being available to quench rhodopsin signaling on the millisecond timescale. **(C)** In Tr-12$^{Arr-/-}$ animals, the level of arrestin in the OS is reduced, however there is enough arrestin to saturate the microtubules, with protein left over to quench rhodopsin singling. **(D)** In Tr-4$^{Arr-/-}$ animals, however, microtubules take up most of the arrestin-1 present, leaving relatively little immediately available to rhodopsin. This slows down shutoff by the time necessary for arrestin-1 diffusion across the OS.

CHAPTER V

THE CONFORMATION OF RECEPTOR-BOUND ARRESTIN

Introduction

Arrestin was first discovered in the visual system as a protein that blocks the signaling of the prototypical G protein-coupled receptor (GPCR) rhodopsin (Rh) via specific binding to P-Rh* (216). The discovery of non-visual arrestins (16) showed that phosphorylation followed by arrestin binding is the common mechanism of GPCR regulation. Crystal structures of all four arrestin subtypes (30, 217-219) in their basal state revealed similar topology: the two cup-like domains linked by an inter-domain hinge (Fig. 1).

Arrestin-1 shows a remarkable selectivity for P-Rh*. Its binding to inactive phosphorylated (P-Rh) or active unphosphorylated rhodopsin (R*) is less than 10% of the binding to P-Rh*, whereas its binding to inactive unphosphorylated rhodopsin (R) is barely detectable (220, 221). A sequential multi-site binding model was proposed to explain arrestin-1 selectivity. This model suggests that arrestin-1 has sensors that recognize rhodopsin-attached phosphates and active rhodopsin conformation. Simultaneous engagement of both sensors, which only P-Rh* can achieve, triggers a global conformational change, allowing arrestin-1 transition into a conformation that results in high-affinity receptor-binding (222). This activation mechanism appears to be conserved in the non-visual arrestins (223, 224) that initiate a second round of signaling upon receptor binding (126, 225). Thus, the arrestin-receptor complex serves as a

signalosome (126), where the shape of the receptor-bound arrestin apparently determines its interactions with multiple signaling proteins (226).

To obtain a comprehensive picture of receptor-induced conformational changes in arrestin-1, we used DEER to perform long-range (~ 17 to 60 Å) measurements of intra-molecular distances in free and P-Rh* bound arrestin-1. DEER is a great tool to monitor the motion of a protein backbone through interspin distance changes, which can be resolved by less than 1 Å difference (227, 228). In addition, it can provide valuable information on multiple conformations and dynamics of proteins from multiple distances and the widths of distance distributions. For these experiments, pairs of R1 nitroxide side chains were introduced into arrestin-1, targeting the four loops on the receptor-binding surface that were expected to be flexible based on crystal structure. Additionally, multiple positions were targeted in the cores of both domains, where the rigid β-strand sandwich provides useful reference points. A total of 25 distances were measured in the absence and presence of P-Rh* (Figure 5-1). The proteins specifically purified or cloned by me are detailed in Figure 5-2 and Figure 5-3. Our data revealed receptor binding-induced movements of multiple arrestin elements. The model based on these data is the first description of the active receptor-bound arrestin. This structural information will improve our understanding of the molecular mechanism of arrestin-mediated regulation of GPCR signaling.

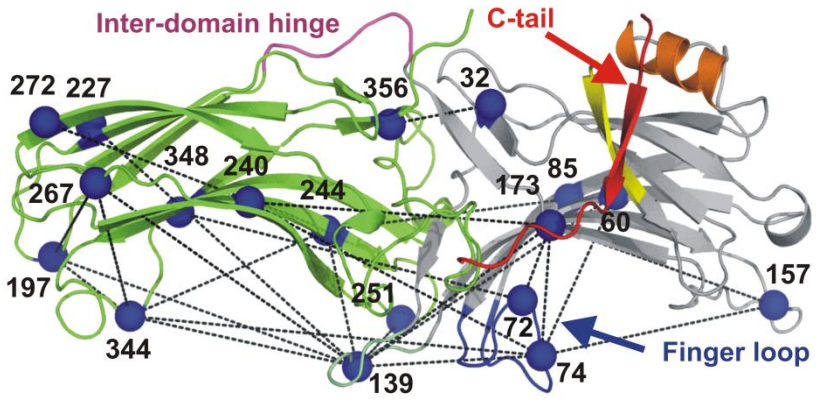

Figure 5-1. The 25 interspin distances measured by DEER.
Ribbon model of arrestin-1 (PDB ID 1CF1, Chain D) (30) composed of two main domains (N-, and C- domains in gray and green, respectively). Inter-domain hinge is colored magenta and the finger loop is colored blue. The very flexible C-tail (red) forms a strong intra-molecular interaction with adjacent α-helix I (orange) and β-strand I (yellow), which is crucial for the stability of the inactive state. Spin-labeled sites are shown as blue spheres at their α-carbons and black dotted lines represent 25 interspin distances measured using DEER.

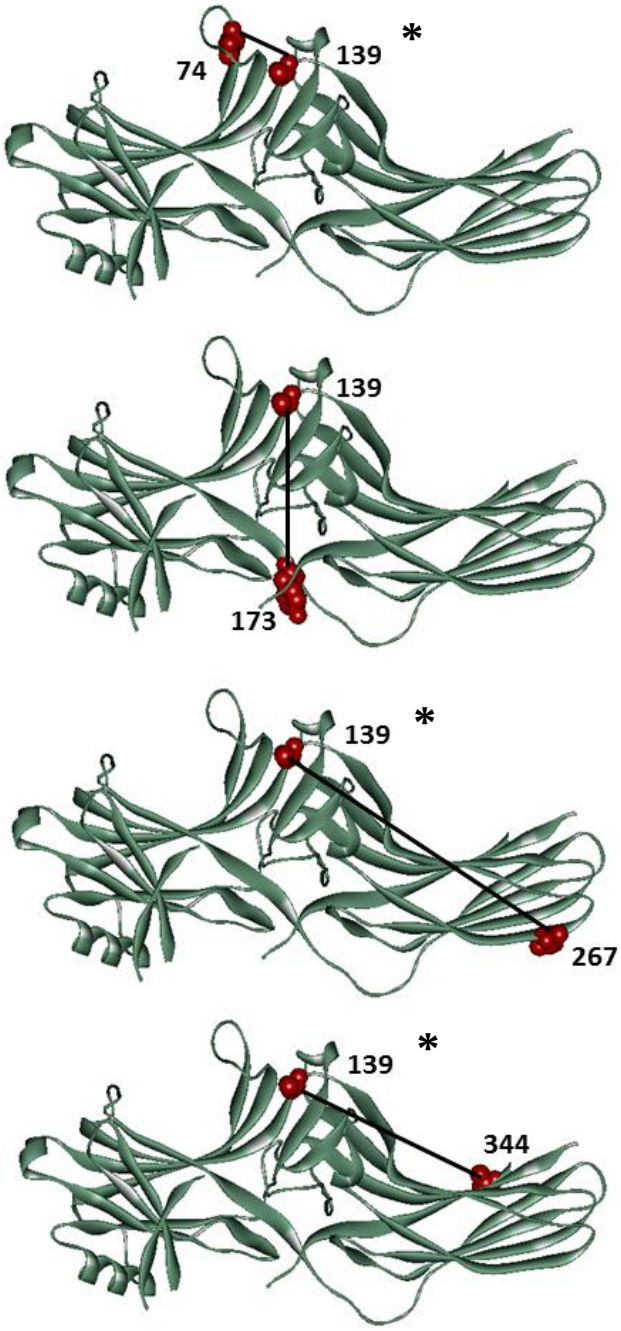

Figure 5-2. 139 loop movement pairs. Cysteines were introduced on cysteine-less base background in two positions on arrestin-1. * Indicate those I purified, the rest are mutants I created and cloned.

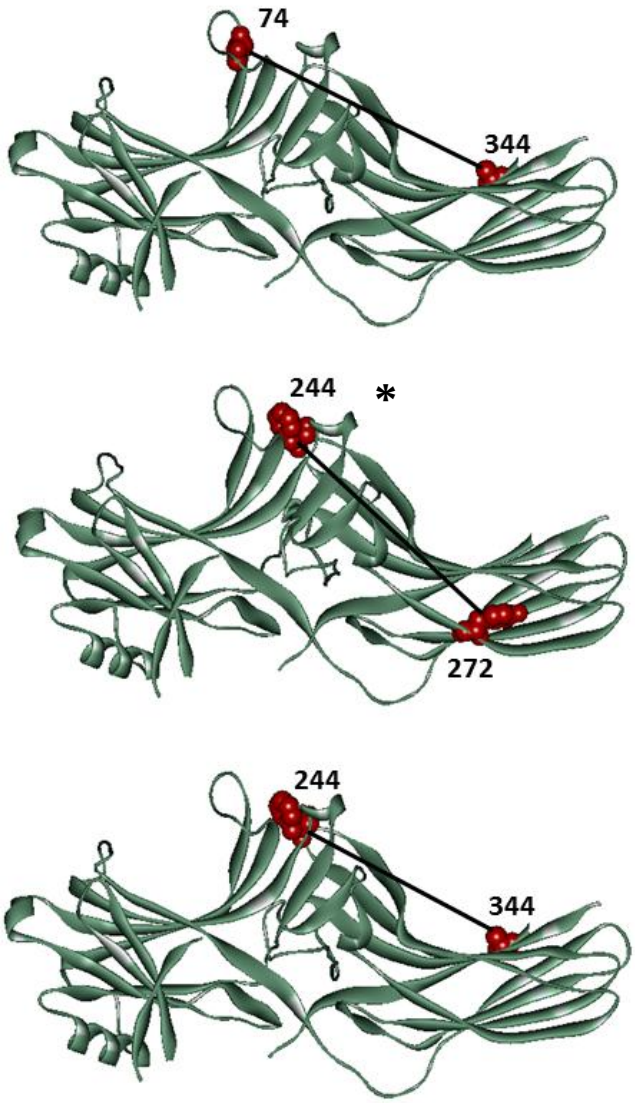

Figure 5-3. Additional cysteine mutants used to measure arrestin movement with DEER. * Indicate those I purified, the rest are mutants I created and cloned.

Materials and Methods

Preparation of Arrestin Double Mutants and Phosphorylated Rhodopsin

Site-directed mutagenesis, expression, and purification of arrestin were performed as previously described (229). All mutations were introduced on the fully functional cysteine-less base mutant, VSV-CL (C63V, C128S, and C143V) (230). Rhodopsin in ROS membranes was phosphorylated with rhodopsin kinase after illumination and fully regenerated by 11-cis-retinal, as previously described (231). The stoichiometry of phosphorylation for the rhodopsin preparations used in this study was higher than 2.5 mol phosphates/mol rhodopsin to ensure arrestin-1 binding to P-Rh* (232).

Spin Labeling and Sample Preparation

For spin labeling, arrestin-1 cysteine mutants in 50 mM MOPS and 100 mM NaCl (pH 7.2) buffer were mixed with 10-fold molar excess of 1-oxyl-2,2,5,5-tetramethyl-3-pyrroline-3-methyl methanethiosulfonate spin label (MTSL) overnight at 4 °C. Removal of excess spin labels and concentration were performed using Amicon Ultra centrifugal filter device (Millipore). During concentration, 20% of glycerol was added to the final samples as a cryoprotectant. For receptor-free arrestin samples, the doubly-labeled arrestin-1 mutants were mixed with cysteine-less arrestin-1 WT (unlabeled) samples at a ratio of 1:3 prior to the concentration in order to get rid of undesired inter-molecular distances within the solution tetramer. For measurements with P-Rh*, two to four molar excess of P-Rh in native ROS membranes was pelleted at 100,000 g for 10 min and then resuspended in the dark with the doubly-labeled arrestin-1 mutants in the buffer. P-Rh was light-activated by illumination for 2 min at room temperature before the DEER

measurement. Continuous wave EPR spectra were collected for each pair in free and P-Rh* bound forms to check binding.

DEER Spectroscopy and Data Analysis

For DEER measurements, 15 μL of samples (~ 200 μM) were loaded into sealed quartz capillaries (1.5 mm i.d. × 1.8 mm o.d.) and flash-frozen using liquid nitrogen. Data were collected at 80 K on a Bruker Elexys 580 spectrometer fitted with an MS-2 split ring resonator as previously described (231). Data analysis to obtain distance distribution including phase correction, background subtraction, and fitting the dipolar evolution function with Tikhonov regularization was performed using the DeerAnalysis 2011 software (233). Selected background corrected dipolar evolution data are shown. In order to estimate the median distance, the obtained distance distribution was integrated followed by normalization of the integrated plot by maximum amplitude. The normalized integrated plot is useful for estimating relative populations of the distances. The median distance was estimated from the midpoint of the transition where the population is equally divided into half.

Results

Introduced pairs of spin labels allowed us to determine three types of distances: 12 inter-domain, 8 within the N-domain, and 5 within the C-domain. The distances for each pair were measured in free arrestin-1 upon binding to P-Rh* in native disk membranes. Representative distance distribution profiles are shown in Figure 5-4a, from which the most probable and median distances were obtained. Median distances

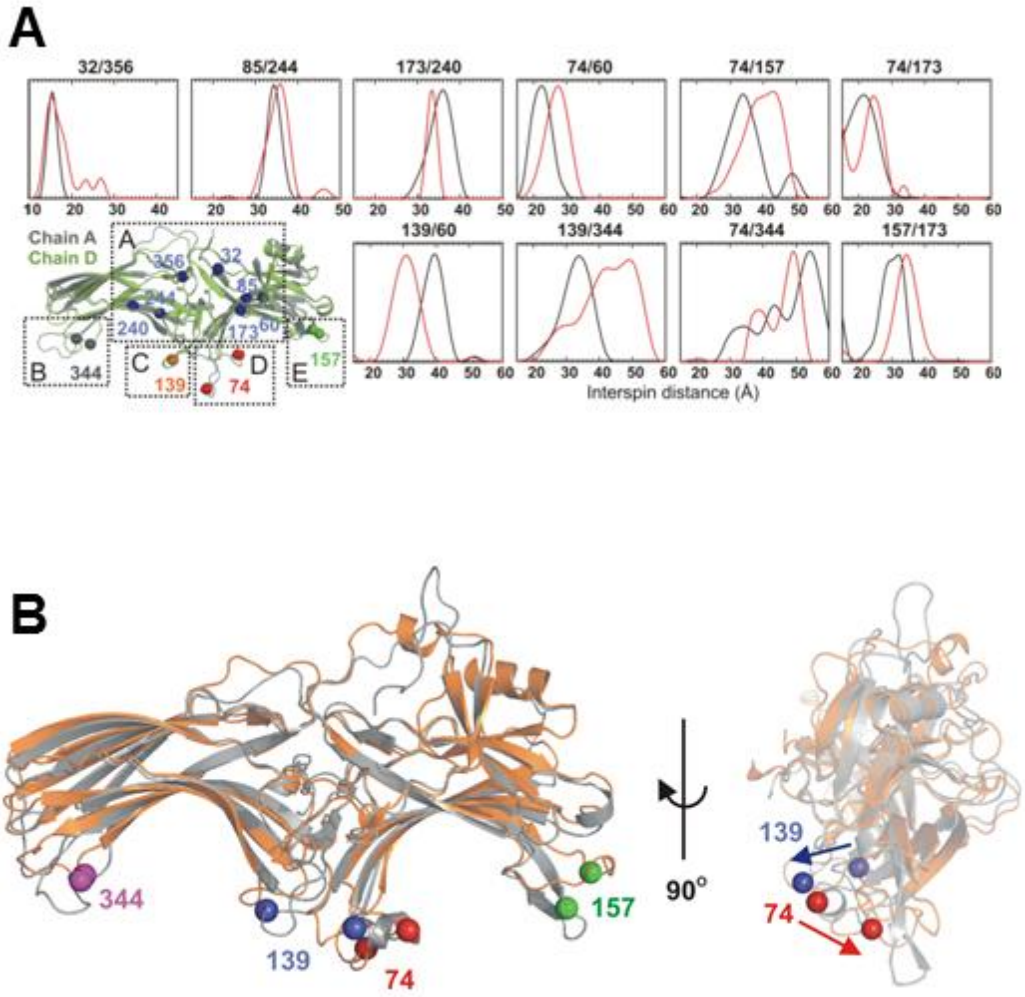

Figure 5-4. The movement of 139 loop of arrestin upon P-Rh* binding is dramatic. **(A)** DEER data of doubly-labeled arrestin-1 mutants in free (black traces) and P-Rh* bound (red traces) states. Spin-labeled sites are indicated as spheres in the overlaid two chains from the crystal structure of arrestin-1 (PDB ID 1CF1, chain A and D). Due to conformational plasticity, the alpha carbon positions of certain residues are different in two chains as indicated. In particular, the finger loop is shown in both extended (chain A) and bent (chain D) conformation. Spin-labeled pairs were designed to look at inter-domain movement *(A)* and the conformational changes in four flexible loops on the receptor-binding sites *(B to E)*. **(B)** Two proposed structural models of arrestin-1 determined by RosettaEPR using DEER distance constraints. Free (gray) and P-Rh* bound (orange) structures are overlaid showing the front view *(A)* and side view *(B)*. Cα locations of four residues of interest which are in the flexible loops on the receptor-binding surface are shown as spheres. Arrows in *(B)* indicate the direction of conformational change upon binding to P-Rh*.

(Table 5-1) were used for modeling to take into account broad distance distributions, which reflect the plasticity of the region. The distances were used as geometric constraints to predict the conformations of free and bound arrestin-1using Rosetta EPR tool (234, 235). All spin-labeled arrestins retained the ability to bind P-Rh*.

Conformational Changes in Arrestin-1 upon Binding to P-Rh*.

Despite accumulated indirect evidence for conformational changes in arrestin-1 upon binding to P-Rh*, the actual movements of specific regions in arrestin-1 were never determined experimentally. Therefore, to determine the conformation of receptor-bound arrestin-1, we measured 25 inter-spin distances to identify possible movement of the two domains, finger loop, and four flexible loops on the receptor-binding surface.

The N- and C- domains in all arrestins are connected by a 12-residue "hinge" (Figure 5-1). The addition of extra residues to the hinge does not affect P-Rh* binding, whereas increasing deletions progressively reduces the ability of arrestin-1 to bind P-Rh* (26). This suggests that the transition of arrestin into the active receptor-bound state requires an extended hinge. Additionally, strong evidence shows that the concave sides of both arrestin domains are engaged by the receptor (230, 236-238). Arrestins in their basal state have relatively large (~70 Å) "wingspan" (30, 217-219), as compared to a more compact cytoplasmic tip of the receptor (35~40 Å) in their inactive state (239). These data taken together lead to the idea that the domains must move relative to each other, closing in on the receptor (the clam-shell model) (222). However, the

	Arrestin	Median distance (Å)		
	Mutant	Free (d1)	+ P-Rh* (d2)	d2-d1
1	32/356	15.5	16.5	1
2	72/173	19	21.5	2.5
3	72/348	39	37	-2
4	74/60	22.5	27	4.5
5	74/139	27	23	-4
6	74/157	34	40	6
7	74/173	21.5	24	2.5
8	74/240	36	37	1
9	74/344	50	47	-3
10	85/244	34.5	35.5	1
11	139/60	39	31	-8
12	139/173	28	18	-10
13	139/197	43	55	12
14	139/227	45.5	49	3.5
15	139/244	23	35	12
16	139/251	16	34	18
17	139/267	41	45	4
18	139/344	33	44	11
19	157/173	30	34.5	4.5
20	173/240	36	33	-3
21	197/267	27.5	27.5	0
22	197/344	22	21	-1
23	244/272	37.5	37	-0.5
24	244/344	32	25	-7
25	267/344	21	24.5	3.5

Table 5-1. Interspin distances measured using DEER in both free and P-Rh* bound arrestin For each pair, two distance profiles were obtained and median distances were estimated from them as described in Materials and Methods.

measurement of three inter-domain distances revealed only slight changes (<3 Å) upon binding to P-Rh* (Figure 5-4a and Table 5-1), which rule out this model.

In the basal state of arrestin-1, the finger loop is bent towards the N-domain. We investigated possible conformational changes induced by P-Rh* binding, using two reference points at positions 72 and 74 (Figure 5-1). Upon P-Rh* binding the distance distribution generally becomes smaller, unless the other site is in a very plastic region such as residues 157 and 344, suggesting that the finger loop is near the binding interface where the motion is more restricted (Figure 5-4a). All the pairs with the finger loop show distance changes up to 6 Å (Table 5-1), indicating that the finger loop dislocates when in complex with P-Rh*. The best receptor-bound model shows that it moves towards the binding interface with P-Rh* (Figure 5-4b). Interestingly, 7 out of 10 models show a propensity of the finger loop to form a-helix upon P-Rh* binding, similar to its helical state in free form.

The most striking movement observed was that of the loop containing residue 139 (139 loop). Although this loop is adjacent to the finger loop (Figure 5-1), EPR studies revealed that residue 139 is immobilized in the presence of inactive P-Rh. However in contrast to the finger loop, its mobility is dramatically increased in free and P-Rh*-bound arrestin-1 (230, 240). This suggests that 139 loop is not directly involved in P-Rh* binding. Upon P-Rh* binding interspin distances involving position 139 show remarkably large changes up to ~20 Å (Figure 5-4a, Table 5-1). Notably, most of the pairs show broad distance distributions both in the absence and presence of P-Rh*, indicating that the 139 loop remains flexible in the complex. This model is consistent

with all of the data shows that the 139 loop moves away from the the receptor-binding surface (Figure 5-4b), and is also consistent with previous findings (230).

Discussion

Light absorption converts rhodopsin into an active form (Rh*), which activates visual G protein, transducin (5, 227). This signaling is switched off by two sequential steps: Rh* is phosphorylated by rhodopsin kinase, and then arrestin-1 specifically binds to P-Rh*, precluding further G protein activation. Indirect evidence accumulating for more than 20 years suggests that arrestin-1 binding to P-Rh* involves a significant conformational change (26, 241-243). For example, the release of the arrestin C-tail upon receptor binding was demonstrated by an increased accessibility of this element in the P-Rh*-associated form (242, 243) and higher mobility of C-terminal residues in the presence of phosphorylated receptor mimics (244). However, the first direct proof that the C-tail moves away from the β-strand I and α-helix, with which it interacts in the basal conformation (30), was obtained only recently by measuring P-Rh* binding-induced changes in distances between the C-tail residues and the body of the molecule using CW EPR and DEER (230, 240). Here we report direct evidence of conformational changes accompanying arrestin-1 binding to P-Rh* in other parts of the molecule, using intra-molecular distance measurements in free and P-Rh*-bound arrestin-1.

We used 25 different pairs of spin labels to systematically study multiple regions in arrestin-1. In view of strong experimental support for one-to-one arrestin-receptor interaction, binding-induced conformational changes in arrestin were expected to make the receptor-binding surface more compact, largely by the proposed movement of the two

arrestin domains relative to each other (245). This model was supported by the findings that progressive deletions in the inter-domain hinge reduced the ability of all arrestins to bind receptors (26, 246). We detected only subtle changes in the inter-domain distances, ruling out large domain movement. Thus, hinge deletions likely perturb site-to-site allosteric coupling, which distorts the conformation of arrestin-1 necessary for P-Rh* binding (247). Among the four vertebrate subtypes, arrestin-1 shows the highest receptor specificity (218, 248) and selectivity for P-Rh* (199). However, the mechanism of arrestin activation by GPCRs is conserved in all subtypes (132, 223, 224), suggesting that receptor binding induces similarly small domain movement in non-visual arrestins. This would leave a large portion of the molecule essentially unchanged. This can readily explain why many non-receptor signaling proteins bind comparably to free and GPCR-associated arrestins (20, 39, 47, 132, 249, 250).

We detected two major rearrangements in the central "crest" on the receptor-binding side of arrestin-1. The finger loop was implicated in rhodopsin binding by several groups (230, 251, 252). We found no proof for the predicted transition of the finger loop from folded to extended conformation (252): this loop is partially bent in free arrestin and moves by less than 5 Å upon binding, bringing it closer to the binding interface. Recently, it has been shown by NMR that an arrestin peptide corresponding to the finger loop becomes α-helical upon binding to P-Rh* (251). Restraining this α-helix formation by disulfide linkage inhibits arrestin binding to P-Rh*, indicating that the conformational flexibility is required for arrestin transition to P-Rh*-bound state. Our data showed its tendency to form a helix in both free and bound state. Interestingly, members of three protein families that preferentially bind active GPCRs: G proteins, G-

protein-coupled receptor kinases (GRKs), and arrestins all show a similar helical conformation when bound to GPCRs. The unstructured C-terminus of the G protein α-subunit interacts with the cavity that opens between the receptor helices upon activation, assumes α-helical conformation upon binding (253, 254). Similarly, the unstructured N-terminus of GRKs implicated in binding active receptor (255, 256) also assumes helical conformation as revealed by crystal structure of GRK6 in an active-like state (257). Therefore, the N-terminal helix of GRKs was proposed to bind in the same active GPCR cavity as the C-terminus of Gα (257). If the finger loop of arrestin binds in the same cavity, as appears likely based on 1:1 interaction stoichiometry (258, 259) and localization of receptor-binding elements on the concave sides of both arrestin domains (230, 238, 248, 260), that would mean that all three types of proteins specifically recognizing active receptors use flexible loops that fold into an α-helix in the binding pocket of GPCRs.

Notably, the pairs involving "139 loop" showed the largest distance change upon binding. Our data are consistent with a dramatic displacement of139 loop, with its tip swinging out by ~15 Å, apparently out of the receptor-binding surface. This explains our previous finding that residue 139 comes into contact with phosphorylated inactive rhodopsin, but reverts to high basal mobility in complex with P-Rh* (230). Our data suggest that the observed large movement of the 139 loop facilitates receptor binding. In fact, the deletions in this region increase P-Rh* binding. Collectively our data suggest that 139 loop stabilizes the basal conformation of arrestin-1 and serves as a "brake", preventing its binding to dark P-Rh and Rh*. This would increase arrestin-1 selectivity

for P-Rh*. This loop is located next to the finger loop, and both are conserved in all arrestins, indicative of its biological importance.

In summary, we present direct evidence of the conformational changes in arrestin-1 upon binding to P-Rh*. A model based on our data is the first low-resolution structure of the active-receptor bound state of any arrestin (figure 5-4b). We identified two large receptor-induced conformational changes, the release of the C-tail and the movement of 139 loop. Additionally we identified the smaller-scale movement of the finger loop and several other arrestin elements. Importantly, this is the first demonstration that the movement of 139 loop is important for receptor selectivity. The shape of the receptor-bound arrestin provides firm structural basis for the mechanistic studies of arrestin-mediated signaling. Our data identify arrestin elements that change upon receptor binding, which likely determine preferential interactions of receptor-bound or free arrestin with certain partners (226). Disruption of the binding sites for individual partners can be used to re-channel arrestin-mediated signaling to desired pathways for therapeutic purposes (225). While the crystal structure of the complex would yield higher resolution, EPR and NMR provide dynamic information that cannot be supplied by crystallography, which is particularly important for obtaining information about the high plasticity of most proteins, including arrestins.

This data chapter was adapted from a manuscript in preparation: "The conformation of the receptor-bound visual" by Miyeon Kim, Sergey A. Vishnivetskiy, Ned Van Eps, Whitney M. Cleghorn, Xuanzhi Zhan, Nathan Alexander, Susan M. Hanson, Jens Meiler, Vsevolod V. Gurevich, and Wayne L. Hubbell.

CHAPTER VI

CONCLUSIONS

Arrestins regulate cell spreading and motility via focal adhesion dynamics

Arrestins are ubiquitous regulators of cell signaling and are expressed in all cells types. They were first shown to bind and terminate signaling through cognate GPCRs, and were later shown to link these receptors to different signaling pathways. In an "unstimulated" state arrestins are fairly diffuse throughout the cytoplasm where they are either free or bound to signaling proteins (Figure 6-1) (35, 39, 261, 262). In addition, arrestins are able to bind microtubules at physiological concentrations, but a small fraction is also present in the nucleus (39, 122, 263) or anchored to the plasma membrane via interactions with other proteins (37).

One of the key features of arrestin is its ability to translocate to the plasma membrane to quench receptor signaling. Arrestins recruitment to GPCRs occurs within minutes (264). They may be recruited to the receptor to terminate G protein signaling alone, or may bring one or more signaling proteins already bound to it (Figure 6-1) (39). Some arrestin binding partners bind to both receptor-bound and free arrestin, whereas some prefer one form to the other (33, 34). Many studies have described a vast number of non-receptor binding partners that are localized by arrestin to receptors such as as AP2, clathrin, c-Src, PDE4, ARNO, Arf6, etc., and serves as a scaffold for MAP kinase cascades facilitating the activation of JNK3 and ERK1/2 (reviewed in (1, 34, 265)). The

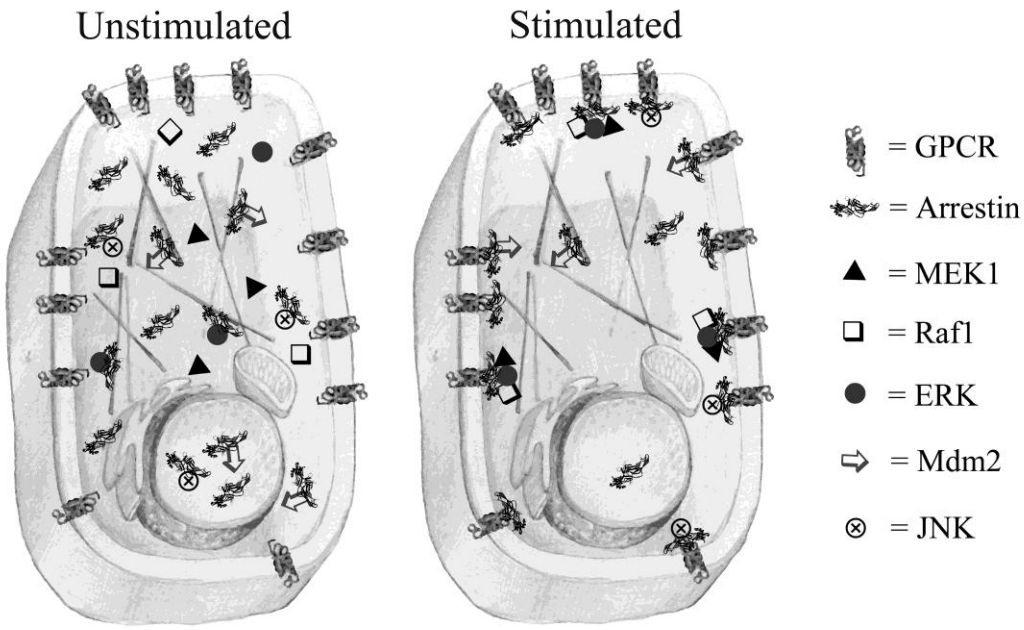

Figure 6-1. The functional cycle of arrestin proteins.
Left panel. In a cell where most GPCRs are silent arrestin is distributed throughout the cytoplasm. Some of the cytoplasmic arrestin is bound to microtubules. The extent of nuclear localization depends on arrestin subtype (arrestin2 >> arrestin3) and cell type. Free cytoplasmic and nuclear arrestin interacts with several non-receptor binding partners: JNK3, Mdm2, and likely many others. Microtubule-bound arrestin mobilizes ERK1/2 and Mdm2 to the cytoskeleton. **Right panel.** Upon stimulation of one or more GPCR subtypes a significant proportion of arrestin is mobilized to the receptor(s), so that the abundance of free and microtubule-bound arrestin decreases. Receptor-bound arrestin serves as an organizer of signalosome, mobilizing numerous signaling proteins to the receptor and scaffolding c-Raf-1->MEK1-.ERK1/2 and ASK1->MKK4-.JNK3 MAP kinase cascades.

number of known non-receptor binding partners of arrestin proteins has been continually growing; it exceeded thirty at the last count (1).

Arrestins were recently shown to bind to microtubules (98). Binding sites for GPCRs and microtubules on the arrestin molecule largely overlap which means that the non-receptor binding elements of arrestin are exposed in both cases (266, 267). Indeed we showed that arrestins recruit ERK1/2 and Mdm2 to the microtubules with different functional outcomes (100). First, arrestin brings ERK1/2 to the MTs but not its upstream kinases cRaf1 and MEK1. This results in a decrease in the active levels of ERK in the cytoplasm suggesting that arrestins bring ERK1/2 to the microtubules to keep it away from compartments of the cell where it can be activated. Conversely, recruitment of Mdm2 to microtubules by arrestin channels Mdm2 activity toward cytoskeleton-associated proteins, significantly increasing their ubiquitination. This was the first study to show that arrestins interaction with microtubules has a direct functional outcome. However the biological relevance of this interaction was still poorly understood.

We described for the first time a dramatic phenotype of arrestin-2/3 DKO MEFs, and demonstrate that arrestins regulate cell morphology by two different mechanisms. First, arrestins regulate RhoA to promote proper cell spreading. Second, arrestins regulate focal adhesion activity and disassembly.

The Rho family of GTPases is comprised of signaling proteins that control cell shape by interacting with a variety of different effectors that regulate the cytoskeleton. RhoA was previously identified as an arrestin-2 target. RhoA-induced stress fiber formation was shown to be dependent on arrestin-2, but not arrestin-3, following activation of the AT1AR receptor (70). Arrestin-2 was shown to bind RhoGTPase

activating protein, ARHGAP21, a known inhibitor of RhoA activity (74). In both studies arrestin knockdown was shown to reduce RhoA activity, similar to what we found in arrestin-2/3 DKO cells. These studies implicate the main function of arrestins regulation of RhoA is to promote its activity. However the functional outcomes of this regulation were not addressed. Here we show for the first time that arrestins regulate RhoA activity to promote proper cell spreading. Rescue with a constitutively-active RhoA mutant, but not Rac1, returned the cell size back to WT. Furthermore, reducing RhoA activity in WT cells resulted in an increase of cell spreading similar to DKO when plated on poly-D-lysine. We also show that, both arrestin-2 and arrestin-3 are able to regulate RhoA activity independently, and in the absence of receptor activation. Knock-down of either arrestin does not change RhoA activity, however knock-down of both dramatically reduces it. Overexpression of either non-visual arrestin in Hek293a results in similar activation of RhoA. Thus arrestin-2 and arrestin-3 are both able to regulate RhoA activation.

Focal adhesions are key signaling modules that link extracellular stimulus to signaling components inside the cell. The rapid assembly and disassembly of focal adhesions is essential for migration and adhesion. Here we show that arrestin DKO cells have a defect in focal adhesion turnover and that rescue with either non-visual arrestin is partial. These data suggest that contrary to arrestins regulation of RhoA, regulation of focal adhesion dynamics requires both arrestins. The number and size of focal adhesions are dramatically increased in the absence of arrestins, and this number increases over time. Importantly, surface integrin levels were also increased in DKO cells and the activity of signaling proteins FAK and paxillin were increased.

The functional importance of arrestins regulation of small GTPases and focal adhesion dynamics became clear when arrestin2/3 knock-down decreased the cells ability to migrate nearly 4-fold, however the cells were able to adhere significantly better. Interestingly, rescue of the defect in cell migration with either arrestin was also partial, suggesting that focal adhesion disassembly is likely the reason.

While much is known about how focal adhesions assemble, not much is known about how they disassemble. Some studies implicated that a decrease in RhoA and an increase in FAK promotes FA disassembly. However, our cells have impaired focal adhesion disassembly despite both decreased RhoA activity and an increase in FAK activity, suggesting that arrestins regulate dynamics upstream of these signaling proteins. Recently microtubule targeting has emerged as the predominant mediator of disassembly (142, 143). One key study (153) revealed several facts about this mechanism. First, that the Rho family GTPases are not involved. Second, that FA disassembly requires microtubules and dynamin, two players not involved in FA assembly. We showed that FAs in DKO cells do not respond to nocodazole treatment: additional FAs do not form when microtubules are destroyed, and FA disassembly is abnormal during microtubule regrowth in these cells. These data suggest that arrestins, known to bind microtubules (100), likely serve as a link between microtubules and FA dynamics.

Our data reveal a completely novel function of arrestin proteins. For the first time we demonstrate that arrestins regulate the cytoskeleton through two mechanisms. First arrestins regulate small GTPases of Rho family independently of GPCR stimulation to promote proper cell spreading. Secondly, we discovered direct arrestin effect on FA disassembly, which is not mediated by small GTPases. Thus, here we demonstrate two

new arrestin functions that regulate processes involved in cell spreading, adhesion, and migration.

Future directions

Arrestin-dependent internalization is not limited to GPCRs. Other receptors such as insulin-like growth factor I receptor (IGF-IR) are also internalized by arrestins. However whether arrestins internalize integrins has never been addressed. To determine this experimentally, integrin internalization in DKO cells should be compared to WT using tagged integrin and TIRF microscopy. To determine if this is arrestin specific, rescue experiments should be performed with DKO cells expressing either arrestin-2 or arrestin-3, or both. It is expected that if a defect in integrin internalization is the cause of the focal adhesion turnover defect, that both arrestin proteins would be required.

The next step would be to determine the mechanism of arrestin-dependent integrin internalization. Arrestins are capable of binding to AP-2 and clathrin to endocytosis GPCRs. To determine whether the mechanism for integrin internalization is similar, the first experiment would be to monitor whether clathrin accumulates at focal adhesions during microtubule targeting in DKO cells using live cell TIRF microscopy. Additionally, arrestin mutants where clathrin sites have been mutated on arrestin C-tail could be infected into DKO cells. If arrestins recruitment of clathrin is required, integrin internalization would still be impaired. If arrestins promote internalization through another mechanism, DKO cells expressing this mutant would internalize like WT.

To further characterize this mechanism, experiments to determine if other proteins that regulate integrin endocytosis are involved in arrestin-dependent focal adhesion

disassembly. FAK has been shown to be required, and we showed that arrestins bind to FAK and regulate its activity. To determine if this interaction promotes disassembly, binding sites for FAK on arrestin could be determined, and small peptides used to block this interaction. Additionally, it is unknown whether arrestins interact with dynamin or clathrin adapter Dab2, both involved in clathrin-mediated integrin internalization. Co-immunoprecipitation experiments and subsequent co-localization experiments via TIRF could be done.

To determine whether arrestin-dependent integrin internalization is a result of microtubule targeting, first look at surface integrin level by FACs before and during MT-induced focal adhesion disassembly. Additionally, experiments could be done to look at arrestin/clathrin targeting to focal adhesions during nocodazole washout and microtubule regrowth using TIRF microscopy. Thirdly, determine whether arrestin-Δ7 mutants, with enhanced microtubule binding alter dynamics during microtubule regrowth. And lastly, binding elements on arrestin important for microtubule binding have already been identified. Mutations of these residues to determine the most critical can be made to render an arrestin protein deficient in microtubule binding. If integrin internalization and focal adhesion dynamics are still altered in DKO cells, arrestins likely serve as a link between microtubules and focal adhesions.

It is entirely possible that arrestins regulate focal adhesion dynamics by a mechanism not involving direct integrin endocytosis. First, arrestins bind to FAK, and may promote focal adhesion turnover by regulating FAK activity. Additionally, paxillin phosphorylation is also increased in the absence of arrestins. However, the relationship between the activity of these proteins and arrestins has not been addressed. We show that

arrestin-2 binds to FAK, however, the biological importance of this interaction is unknown. Interaction sites on arrestin or FAK important for their binding can be determined through EPR, or by mutation of specific residues and subsequent binding assays. Small peptides can be used to block the interaction between the two, and focal adhesion disassembly can be monitored.

Paxillin has been shown to be phosphorylated by a well-known arrestin scaffold: the cRaf1-MEK1-ERK1/2 cascade (42, 155). Localization of ERK1/2 to focal adhesions could be mediated by arrestins. Arrestin-dependent recruitment of ERK1/2 to focal adhesions could be monitored experimentally by TIRF. It is also entirely possible that arrestins link paxillin to the ERK cascade and these interactions could be determined biochemically.

Progressive reduction of its expression in rods reveals two pools of arrestin-1 in the outer segment with different roles in photoresponse recovery

Comprehensive understanding of systems behavior of rod photoreceptors requires precise knowledge of the concentration, localization, and activity of every signaling protein in the cell. While the functional role of many signaling proteins in rod phototransduction have been qualitatively established using genetically modified mice (reviewed in (83)), the biological significance of the specific level of each protein is rarely addressed. Here we report an unexpected finding that 20-fold reduction of arrestin-1 content in the dark-adapted rod OS from 100% to 5% of WT level has no appreciable effect on photoresponse recovery, whereas further 2-fold reduction to 2.5% dramatically

slows this process. Our data suggest that most of arrestin-1 in the OS of Tr-4$^{Arr-/-}$ animals is not immediately available for rhodopsin quenching.

In summary, our data suggest the existence of two distinct pools of arrestin-1 in dark-adapted mouse outer segments. To the best of our knowledge, so far only one genetically modified mouse line where rhodopsin shutoff was made rate-limiting was described: mice with low expression of GRK1/2 chimera (215). In Tr-4$^{Arr-/-}$ mice we made rhodopsin shutoff the rate-limiting stage of photoresponse recovery by low expression of arrestin-1. Collectively, these results strongly support the idea that both phosphorylation and arrestin binding are necessary steps in rhodopsin shutoff.

Future Directions

One sure way to ascertain whether a proportion of arrestin comparable to the concentration of arrestin in the OS of Tr-4$^{Arr-/-}$ mice is localized to microtubules, is to look at arrestin localization in these cells in the dark. Simple immunofluorescence experiments staining for arrestin-1 and tubulin would not be informative because the concentration of arrestin-1 is undetectable in the OS of these mice. Therefore, arrestin-1 localization would have to be determined by electron microscopy.

The conformation of receptor bound arrestin

We present direct evidence of the conformational changes in arrestin-1 upon binding to P-Rh*. We identified two large receptor-induced conformational changes: the release of the C-tail, and the movement of 139 loop. The incredible movement of this loop is a completely novel discovery, and sheds light into arrestins selectivity for GPCRs.

We also showed smaller-scale movement of the finger loop and several other arrestin elements. A model based on our data is the first low-resolution structure of the active-receptor bound state of any arrestin. Our data identify arrestin elements that change upon receptor binding, which likely determine preferential interactions of receptor-bound or free arrestin with certain partners (226). While the crystal structure of the complex would yield higher resolution, EPR and NMR provide dynamic information that cannot be supplied by crystallography, which is particularly important in view of high plasticity of most proteins, including arrestins.

Future Directions

Arrestins recruitment and binding to GPCRs has many functional outcomes, and its conformation is the key determinant of its functional capabilities (33). The flexibility of the loops may allow arresitn to assume different conformations, and could explain why the non-visual arrestins accommodate hundreds of structurally divers GPCRs. A better understanding of this complex would allow investigators to explore the binding elements for both GPCRs and non-receptor bidning partners. Additional studies to better understand the dynamic nature of these proteins, and a crystal structure of this complex are essential. Knowing exactly how these two proteins interact would allow investigators to create mutations in arrestin that affect the flexibility of the molecule and potentially limit the conformational space it can inhabit. In this way, one could alter arrestins ability to interact with some partners without affecting the binding to others, thereby dramatically shifting arrestin-mediated signaling. Because arrestins play a role in so many different cellular functions, the therapeutic implications of this are vast.

Thesis Conclusions

Arrestins are diverse signaling molecules that regulate a variety of proteins in the cell. There are four arrestins subtypes, two expressed in the retina, arrestin-1 and arrestin-4, and two that are ubiquitously expressed, arrestin-2 and arrestin-3. While the functional requirements of arrestins expressed in the retina vary from the arrestins expressed in all cell types, several functions are the same. First, all arrestins terminate GPCR signaling. Second, all arrestins bind to microtubules. It is my hope that the findings in this thesis provide a better global understanding of arrestin signaling at the receptor and cytoskeletal level in both visual and non-visual systems.

APPENDIX A

Robust self-association is a common feature of mammalian visual arrestin-1

Much of the work in this chapter was published in Biochemistry in February 2011 (268). The paper was a collaborative effort between the laboratories Vsevolod V. Gurevich and Wayne L. Hubbell.

My contribution to this work was purification of human arrestin-1.

Arrestin-1 binds light-activated phosphorhodopsin and ensures rapid signal termination. Its deficiency in humans and mice results in prolonged signaling and rod degeneration. However, most of the biochemical studies were performed on bovine arrestin-1, which was shown to self-associate forming dimers and tetramers, although only the monomer binds rhodopsin. It is unclear whether self-association is a property of arrestin-1 in all mammals, or a specific feature of bovine protein. To address this issue, we compared self-association parameters of purified human and mouse arrestin-1 with those of bovine counterpart using multi-angle light scattering. We found that mouse and human arrestin-1 also robustly self-associate, existing in monomer-dimer-tetramer equilibrium. Interestingly, the combination of dimerization and tetramerization constants in these three species is strikingly different. While tetramerization of bovine arrestin-1 is highly cooperative, with $K_{D,dim}^4 > K_{D,tet}$, in mouse $K_{D,dim} \sim K_{D,tet}$, whereas in human $K_{D,dim} << K_{D,tet}$. Importantly, in all three species at very high physiological concentrations

of arrestin-1 in rod photoreceptors, most of it is predicted to exist in oligomeric form, with relatively low concentration of free monomer. Thus, it appears that maintenance of low levels of active monomer is the biological role of arrestin-1 self-association.

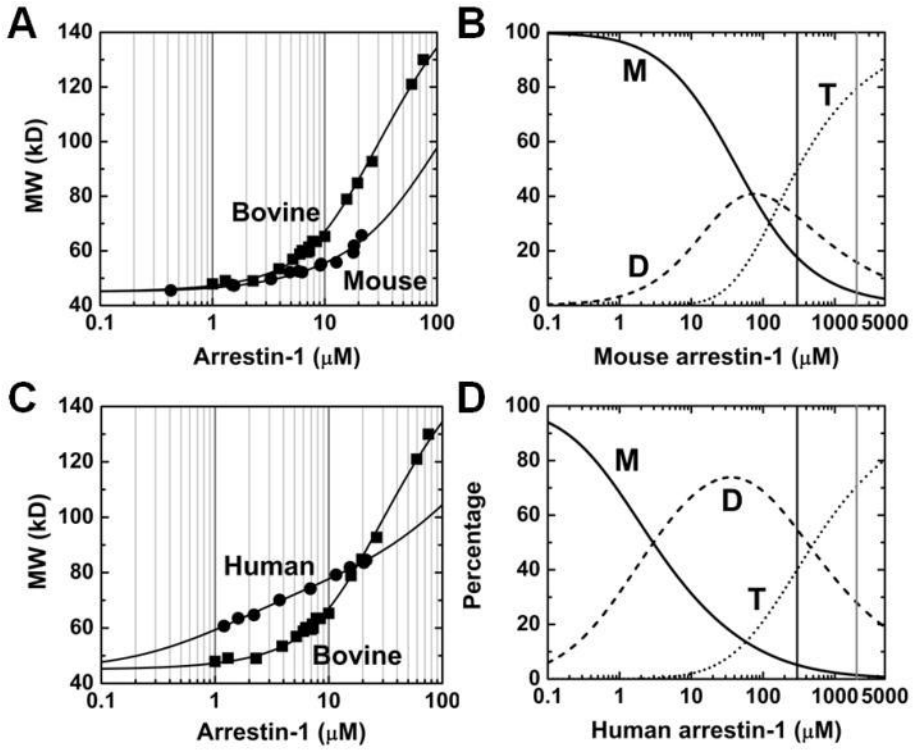

Figure A. Mouse and human arrestin-1 form dimers and tetramers at physiological concentrations. (A) The average molecular weight of wild type mouse arrestin-1 as a function of total concentration (black circles) was determined from the light scattering data as described in the Methods. The solid curve is a least-squares fit of the data to the MDT model with $K_{D,dim}$ = 57.5±0.6 μM and $K_{D,tet}$ = 63.1±2.6 μM. The data for bovine arrestin-1 are shown as squares for comparison. **(B)** The percentage of mouse arrestin-1 molecules in monomer (M, straight line), dimer (D, dashed line), and tetramer (T, dotted line) as a function of total arrestin-1 concentration computed for the MDT model and the data in panel A. **(C)** The average molecular weight of wild type human arrestin-1 as a function of total concentration (black circles) was determined from the light scattering data. The solid curve is a least-squares fit of the data to the MDT model with $K_{D,dim}$ = 2.95±0.02 μM and $K_{D,tet}$ =224±5 μM. **(D)**. The percentage of human arrestin-1 molecules in monomer (M, straight line), dimer (D, dashed line), and tetramer (T, dotted line) as a function of total arrestin-1 concentration computed for the MDT model and the data in panel **(C).** Vertical lines in **(B)** and **(D)** correspond to arrestin-1 concentrations in the outer segment (300 μM, black) and cell body (2,000 μM, gray) of dark-adapted rod.

Table A-1
Equilibrium constants characterizing self-association of WT and mutant mouse, human, and bovine arrestin-1.

Protein	**log K_{dim}[a]**	**log K_{tet}[a]**	**$K_{D,dim}$, μM**	**$K_{D,tet}$, μM**
Mouse arrestin-1	4.24±0.04	4.20±0.17	57.5±0.6	63.1±2.6
Mouse arrestin-1-(F86A,F198A)	3.27±0.05	-	537±9	-
Mouse arrestin-1-(F86A,F198A, A349V)	3.14±0.11	-	724±26	-
Human arrestin-1	5.53±0.03	3.65±0.08	2.95±0.02	224±5
Bovine arrestin-1	4.43±0.02	5.13±0.03	37.2±0.2	7.4±0.1
Bovine arrestin-1-(F85A,F197A)	3.28±0.10	-	525±16	-

[a]K_{dim} and K_{tet} are the *association* constants determined from light scattering analysis.

Table A-2
Predicted concentrations of monomer, dimer, and tetramer of mouse, human, and bovine arrestin-1 at concentrations in the outer segment (300 μM) and cell body (2,000 μM) of dark-adapted rods.

Arrestin-1	**Total, μM**	**Monomer, μM (%)**	**Dimer, μM (%)**	**Tetramer, μM (%)**
Bovine	300	27.6 (9.2%)	20.8 (13.9%)	57.7 (76.9%)
Mouse	300	52.8 (17.6%)	48.8 (32.5%)	37.4 (49.9%)
Human	300	15.5 (5.2%)	82.1 (54.7%)	30.1 (40.1%)
Bovine	2,000	46 (2.3%)	59 (5.9%)	459 (91.8%)
Mouse	2,000	95 (4.7%)	159 (15.9%)	397 (79.4%)
Human	2,000	29 (1.5%)	281 (28.1%)	352 (70.4%)

APPENDIX B

Caspase-cleaved arrestin-2 and BID cooperatively facilitate cytochrome C release and cell death

This work is in review and is a collaboration between the laboratories of Eugenia V. Gurevich, Vsevolod V. Gurevich, and Jeffery L. Benovic.

My contribution to this work was caspase inhibition assay to determine caspases that cleave arrestin-2, and purification of arrestin2 (1-380) and caspase resistant arrestin2-D380/408E for direct study of cytochrome C release from mitochondria.

Arrestins are multi-functional regulators of cell signaling that interact with hundreds of G protein-coupled receptors and numerous other proteins. Here we demonstrate that arrestin2 is specifically cleaved at Asp380 and Asp408 by caspases during apoptosis induced by a variety of stimuli in different cell types. Caspase-generated arrestin2(1-380) translocates to mitochondria facilitating cytochrome C release and apoptotic cell death. At physiological concentrations, arrestin2(1-380) directly enhances cytochrome C release from isolated mitochondria induced by cleaved N/C-BID. In contrast, caspase-resistant arrestin2-D380/408E increases cell survival. Arrestin2-D380/408E does not affect the action of N/C-BID on isolated mitochondria and demonstrates strong cytoprotective effect in cells lacking endogenous arrestins, which rules out its competition with the fragment. Thus, caspases convert cytoprotective full-

length arrestin2 into pro-apoptotic arrestin2(1-380) fragment, creating a positive feedback loop with a built-in threshold determined by the level of arrestin2 expression in the cell. This earlier unappreciated mechanism significantly contributes to the progression of apoptosis.

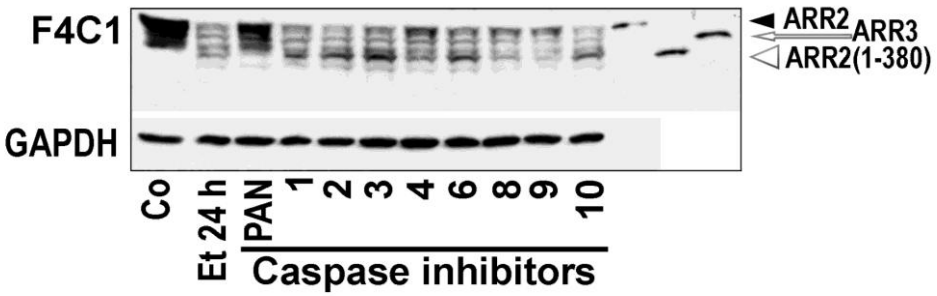

Figure B-1. Arrestin-2 is cleaved by specific caspases.
In etoposide-treated rat-1 cells we found that inhibitors of caspases-4, -8, and -9 reduce the accumulation of the arrestin2 fragment, whereas the inhibitors of initiator caspases-2 and -10 and executioner caspases-3 and -6 do not. Rat-1 cells were pre-treated with 100 μM of indicated caspase inhibitors for 2 h and exposed to 40μM etoposide for 24 h. The number below indicates caspase specificity of the inhibitors: PAN, pan-caspase zVAD-fmk; 1, zWEHD-fmk; 2, zVDVAD-fmk; 3, zDEVD-fmk; 4, zYVAD-fmk; 6, zVEID-fmk; 8, zIETD-fmk; 9, zLEHD-fmk; 10, z-AEVD-fmk. Upper panel: endogenous arrestins were detected with F4C1 antibody and identified by running purified arrestin2, arrestin2(1-380), and arrestin3 as standards. The band between arrestin3 and arrestin2(1-380) present in all lanes is non-specific. Lower panel: GAPDH (loading control). In some samples in panels B and C the combined intensity of full-length arrestin2 and its (1-408) and (1-380) products is consistently lower than that of arrestin2 band in control, possibly due to generation of smaller fragments not detectable by the antibody.

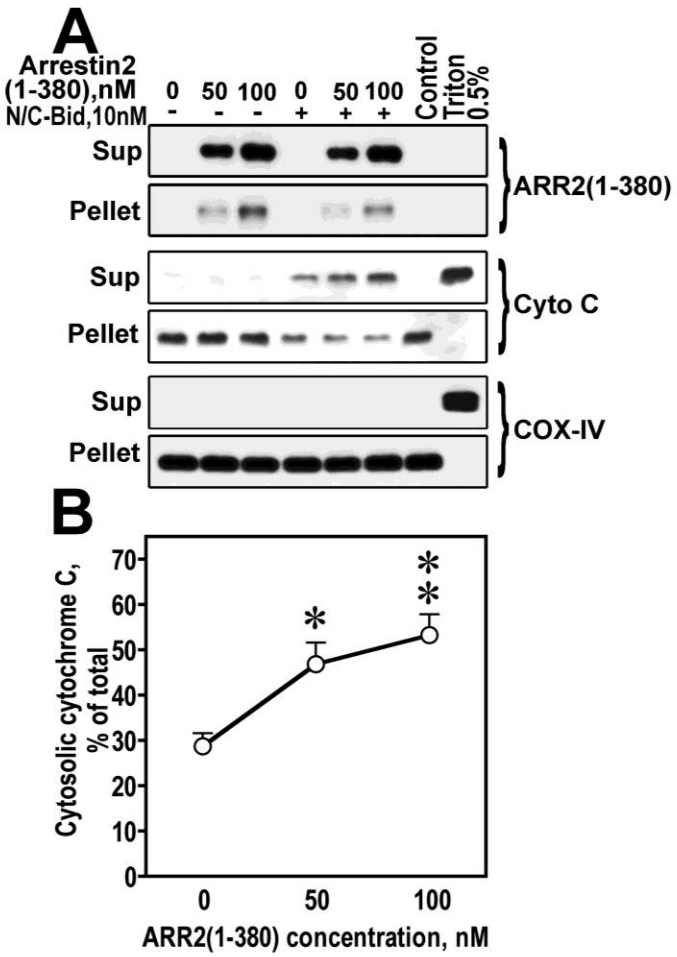

Figure B-2. Arrestin2(1-380) binds isolated mitochondria and facilitates cytochrome C release induced by caspase-cleaved Bid. (**A**) Isolated mouse liver mitochondria (20 μg) were incubated in 50 μl WHAT buffer with or without 10 nM N/C-Bid and indicated concentrations of purified arrestin2(1-380) for 20 min at room temperature. Mitochondria were pelleted by centrifugation at 16,000xg for 10 min at 4°C. The distribution of cytochrome C, arrestin2(1-380), and COX-IV in the pellet and supernatant is shown. COX-IV serves as loading control, as well as control of mitochondria integrity and completeness of mitochondria solubilization by Triton X-100. (**B**) The fraction of cytochrome C released by 10 nM N/C-Bid without (0 nM) or with arrestin2(1-380) (50 and 100 nM) is shown as the percent of the total cytochrome C (released by Triton X-100). Mean +/- SD of four independent experiments is shown. *, $p<0.05$; **, $p<0.01$, as compared to 10 nM N/C-Bid alone according to one-way ANOVA with Concentration as main factor ($F(2,9)=8.84$, $p=0.0075$) followed by Bonferroni/Dunn *post hoc* comparison.

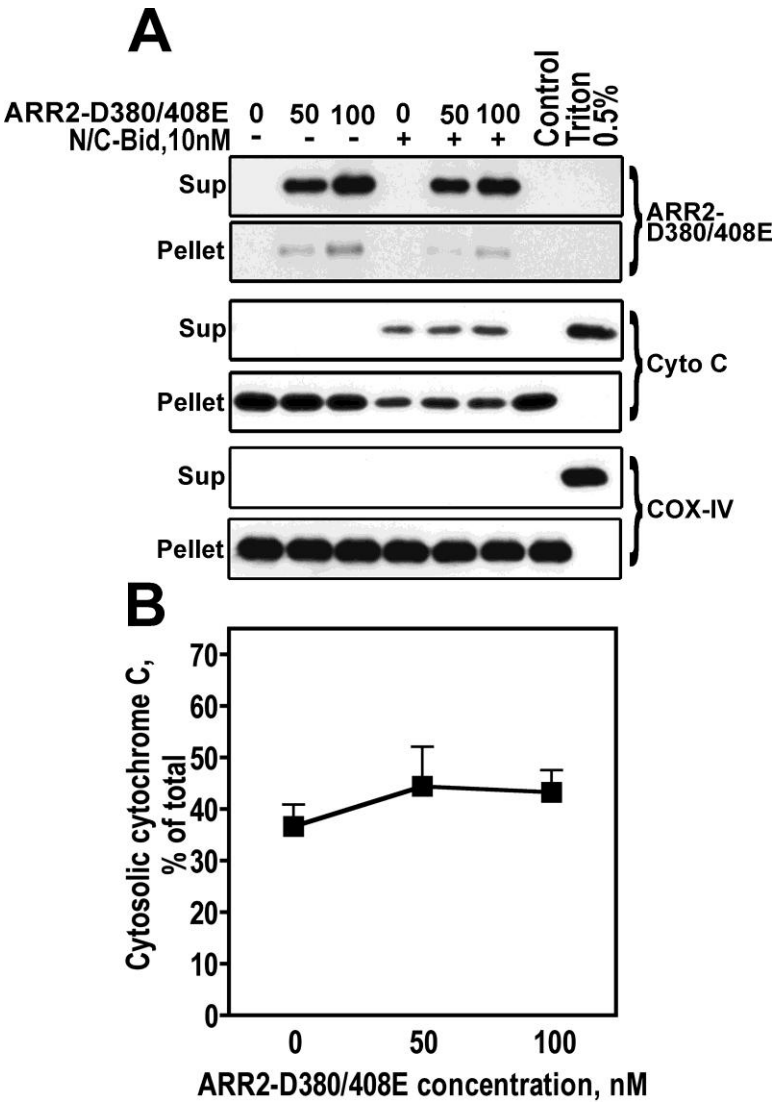

Figure B-3 . Caspase-resistant arrestin2-D380/408E does not affect the integrity of isolated mitochondria or cytochrome C release induced by caspase-cleaved Bid. (**A**) Isolated mouse liver mitochondria (20 μg) were incubated in 50 μl with or without 10 nM N/C-Bid and indicated concentrations of purified arrestin2-D380/408E for 20 min at room temperature. Mitochondria were pelleted by centrifugation at 16,000xg for 10 min at 4°C. The distribution of cytochrome C, arrestin2-D380/408E, and COX-IV in the pellet and supernatant is shown. COX-IV serves as loading control, as well as control of mitochondria integrity and completeness of mitochondria solubilization by Triton X-100. (**B**) The fraction of released cytochrome C released by 10 nM N/C-Bid without (0 nM) or with arrestin2-D380/408E (50 and 100 nM) is shown as the percent of the total cytochrome C (released by Triton X-100). Mean +/- SD of four independent experiments is shown. N/C-Bid induces the release of ~40% of cytochrome C, and caspase-resistant arrestin2-D380/408E does not affect cytochrome C release with ($F(2,9)=0.56$ $p=0.59$) or without N/C-Bid

APPENDIX C

LIST OF PUBLICATIONS

1. Hanson SM, **Cleghorn WM**, Francis DJ, Vishnivetskiy SA, Raman D, Song X, Nair KS, Slepak VZ, Klug CS, Gurevich VV. Arrestin Mobilizes Signaling Proteins to the Cytoskeleton and Redirects their Activity. J Mol Biol. 2007 Apr 27;368(2):375-87

2. Gurevich VV, Gurevich EV, **Cleghorn WM**. Arrestins as Multi-functional Signaling Adaptors. Handb Exp Pharmacol. 2008;(186): 15-37. Review.

3. Kim M, Hanson, SM, Vishnivetskiy SA, Song X, **Cleghorn WM**, Hubbell WL, Gurevich VV. Robust self-association is a common feature of mammalian visual arrestin-1. Biochemistry. 2011 Mar 29;50(12):2235-42.

4. **Cleghorn WM**, Tsakem EL, Song X, Vishnivetskiy SA, Seo J, Chen J, Gurevich EV, Gurevich VV. Progressive reduction of its expression in rods reveals two pools of arrestin-1 in the outersegment with different roles in photoresponse recovery. PLoS One. 2011;6(7):e22797

5. **Cleghorn WM**, Branch KM, Kook S, Bulus N, Gurevich EV, Zent R, Weaver AM, Gurevich VV. Arrestins regulate cell spreading and motility via focal adhesion dynamics. In preparation.

6. Kim M, Vishnivetskiy SA, Van Eps N, **Cleghorn WM**, Zhan X, Alexander N, Hanson SM, Meiler J, Gurevich VV, Hubell WL. The conformation of the receptor-bound arrestin. In preparation.

7. Kook S, Zhan X, Baameur F, **Cleghorn WM**, Benovic JL, Gurevich VV, Gurevich EV. Caspase-cleaved arrestin-2 and BID cooperatively facilitate cytochrome C release and cell death. Mol Cell, In revision.

REFERENCES

1. Gurevich EV & Gurevich VV (2006) Arrestins are ubiquitous regulators of cellular signaling pathways. *Genome Biol* 7:236.

2. Gurevich VV & Gurevich EV (2008) GPCR monomers and oligomers: it takes all kinds. *Trends Neurosci* 31:74-81.

3. Pierce KL, Premont RT, & Lefkowitz RJ (2002) Seven-transmembrane receptors. *Nat Rev Mol Cell Biol* 3:639-650.

4. Lefkowitz RJ (1998) G protein-coupled receptors. III. New roles for receptor kinases and b-arrestins in receptor signaling and desensitization. *J Biol Chem* 273:18677-18680.

5. Carman CV & Benovic JL (1998) G-protein-coupled receptors: turn-ons and turn-offs. *Curr Opin Neurobiol* 8:335-344.

6. Goodman OB, Jr., *et al.* (1996) Beta-arrestin acts as a clathrin adaptor in endocytosis of the beta2-adrenergic receptor. *Nature* 383(6599):447-450.

7. Laporte SA, *et al.* (1999) The b2-adrenergic receptor/b-arrestin complex recruits the clathrin adaptor AP-2 during endocytosis. *Proc Nat Acad Sci USA* 96:3712-3717.

8. Ferguson SS, *et al.* (1996) Role of beta-arrestin in mediating agonist-promoted G protein-coupled receptor internalization. *Science* 271:363-366.

9. Krueger KM, Daaka Y, Pitcher J, & Lefkowitz RJ (1997) The role of sequestration in G protein-coupled receptor resensitization. Regulation of b2-adrenergic receptor dephosphorylation by vesicular acidification. *J Biol Chem* 272:5-8.

10. Pippig S, Andexinger S, & Lohse MJ (1995) Sequestration and recycling of b2-adrenergic receptors permit receptor resensitization. *Mol Pharmacol* 47:666-676.

11. Pfister C, *et al.* (1985) Retinal S antigen identified as the 48K protein regulating light-dependent phosphodiesterase in rods. *Science* 228:891-893.

12. Kuhn H, Hall SW, & Wilden U (1984) Light-induced binding of 48-kDa protein to photoreceptor membranes is highly enhanced by phosphorylation of rhodopsin. *FEBS Lett.* 176:473-478.

13. Wilden U & Kuhn H (1982) Light-dependent phosphorylation of rhodopsin: number of phosphorylation sites. *Biochemistry* 21:3014-3022.

14. Kuhn H (1978) Light-regulated binding of rhodopsin kinase and other proteins to cattle photoreceptor membranes. *Biochemistry* 17:4389-4395.

15. Murakami A, Yajima T, Sakuma H, McLaren MJ, & Inani G (1993) X-Arrestin: a new retinal arrestin mapping to the X chromosome. *FEBS Lett.* 334:203-209.

16. Lohse MJ, Benovic JL, Codina J, Caron MG, & Lefkowitz RJ (1990) beta-Arrestin: a protein that regulates beta-adrenergic receptor function. *Science* 248:1547-1550.

17. Sterne-Marr R, *et al.* (1993) Polypeptide variants of b-arrestin and arrestin3. *J Biol Chem* 268:15640-15648.

18. Gurevich VV & Gurevich EV (2006) The structural basis of arrestin-mediated regulation of G protein-coupled receptors. *Pharm Ther* 110:465-502.

19. Dawson TM, *et al.* (1993) b-adrenergic receptor kinase-2 and b-arrestin2 as mediators of odorant-induced desensitization. *Science* 259:825-829.

20. Song X, Coffa S, Fu H, & Gurevich VV (2009) How does arrestin assemble MAPKs into a signaling complex? (Translated from eng) *J Biol Chem* 284(1):685-695 (in eng).

21. Kohout TA, Lin FS, Perry SJ, Conner DA, & Lefkowitz RJ (2001) beta-Arrestin 1 and 2 differentially regulate heptahelical receptor signaling and trafficking. *Proc Nat Acad Sci USA* 98:1601-1606.

22. Oakley RH, Laporte SA, Holt JA, Caron MG, & Barak LS (2000) Differential affinities of visual arrestin, barrestin1, and barrestin2 for G protein-coupled receptors delineate two major classes of receptors. *J Biol Chem* 275:17201-17210.

23. Sutton RB, *et al.* (2005) Crystal Structure of Cone Arrestin at 2.3Å: Evolution of Receptor Specificity. *J Mol Biol* 354:1069-1080.

24. Gurevich VV & Benovic JL (1997) Mechanism of phosphorylation-recognition by visual arrestin and the transition of arrestin into a high affinity binding state. *Mol Pharmacol* 51:161-169.

25. Gurevich VV & Benovic JL (1993) Visual arrestin interaction with rhodopsin: Sequential multisite binding ensures strict selectivity towards light-activated phosphorylated rhodopsin. *J. Biol. Chem.* 268:11628-11638.

26. Vishnivetskiy SA, Hirsch JA, Velez MG, Gurevich YV, & Gurevich VV (2002) Transition of arrestin into the active receptor-binding state requires an extended interdomain hinge. *J Biol Chem* 277(46):43961-43967.

27. Gurevich VV & Gurevich EV (2004) The molecular acrobatics of arrestin activation. *Trends Pharmacol Sci* 25:59-112.

28. Vishnivetskiy SA, Hirsch JA, Velez M-G, Gurevich YV, & Gurevich VV (2002) Transition of arrestin in the active receptor-binding state requires an extended interdomain hinge. *J. Biol. Chem.* 277(46):43961-43968.

29. Sutton RB, *et al.* (2005) Crystal Structure of Cone Arrestin at 2.3Å: Evolution of Receptor Specificity. *Structure* in press.

30. Hirsch JA, Schubert C, Gurevich VV, & Sigler PB (1999) The 2.8 A crystal structure of visual arrestin: a model for arrestin's regulation. *Cell* 97(2):257-269.

31. Han M, Gurevich VV, Vishnivetskiy SA, Sigler PB, & Schubert C (2001) Crystal structure of beta-arrestin at 1.9 A: possible mechanism of receptor binding and membrane translocation. *Structure* 9(9):869-880.

32. Luttrell LM, *et al.* (1999) Beta-arrestin-dependent formation of beta2 adrenergic receptor-Src protein kinase complexes. *Science* 283:655-661.

33. Gurevich VV & Gurevich EV (2003) The new face of active receptor bound arrestin attracts new partners. *Structure* 11:1037-1042.

34. Lefkowitz RJ & Shenoy SK (2005) Transduction of receptor signals by beta-arrestins. *Science* 308:512-517.

35. Wu N, *et al.* (2006) Arrestin binding to calmodulin: a direct interaction between two ubiquitous signaling proteins. *J Mol Biol* 364:955-963.

36. Baillie GS, *et al.* (2003) beta-Arrestin-mediated PDE4 cAMP phosphodiesterase recruitment regulates beta-adrenoceptor switching from Gs to Gi. *Proceedings of the National Academy of Sciences* 100:940-945.

37. Hunzicker-Dunn M, Gurevich VV, Casanova JE, & Mukherjee S (2002) ARF6: a newly appreciated player in G protein-coupled receptor desensitization. *FEBS Lett.* 521:3-8.

38. Shenoy SK, McDonald PH, Kohout TA, & Lefkowitz RJ (2001) Regulation of receptor fate by ubiquitination of activated beta 2-adrenergic receptor and beta-arrestin. *Science* 294:1307-1313.

39. Song X, Raman D, Gurevich EV, Vishnivetskiy SA, & Gurevich VV (2006) Visual and both non-visual arrestins in their "inactive" conformation bind JNK3 and Mdm2 and relocalize them from the nucleus to the cytoplasm. *J Biol Chem* 281:21491-21499.

40. Gurevich VV, Gurevich EV, & Cleghorn WM (2008) Arrestins as multi-functional signaling adaptors. *Handb Exp Pharmacol* (186):15-37.

41. McDonald PH, *et al.* (2000) Beta-arrestin 2: a receptor-regulated MAPK scaffold for the activation of JNK3. *Science* 290:1574-1577.

42. Luttrell LM, *et al.* (2001) Activation and targeting of extracellular signal-regulated kinases by beta-arrestin scaffolds. *Proc Natl Acad Sci U S A* 98(5):2449-2454.

43. DeFea KA, *et al.* (2001) beta-arrestin-dependent endocytosis of proteinase-activated receptor 2 is required for intracellular targeting of activated ERK1/2. *J Cell Biol* 148:1267-1281.

44. Bruchas MR, Macey TA, Lowe JD, & Chavkin C (2006) Kappa opioid receptor activation of p38 MAPK is GRK3- and arrestin-dependent in neurons and astrocytes. *J Biol Chem* 281:18081-18089.

45. Davis RJ (2000) Signal Transduction by the JNK group of MAP kinases. *Cell* 103:239-252.

46. Willoughby EM & Collins MK (2005) Dynamic Interaction between the Dual Specificity Phosphatase MKP7 and the JNK3 Scaffold Protein β- Arrestin 2. *The Journal of Biological Chemistry* 280:25651-25658.

47. Seo J, Tsakem EL, Breitman M, & Gurevich VV (2011) Identification of arrestin-3-specific residues necessary for JNK3 kinase activation. *J Biol Chem* 286:27894-27901.

48. Scott MG, *et al.* (2002) Differential nucleocytoplasmic shuttling of beta-arrestins. Characterization of a leucine-rich nuclear export signal in beta-arrestin2. *J Biol Chem* 277:37693-37701.

49. Wang P, Wu Y, Ge X, Ma L, & Pei G (2003) Subcellular localization of beta-arrestins is determined by their intact N domain and the nuclear export signal at the C terminus. *J Biol Chem* 278:11648-11653.

50. Hunton DL, *et al.* (2005) Beta-arrestin 2-dependent angiotensin II type 1A receptor-mediated pathway of chemotaxis. *Molecular Pharmacology* 67:1229-1236.

51. Ge L, Y. L, Hollenberg M, & DeFea KA (2003) A β-arrestin-dependent scaffold is associated with prolonged MAPK activation in pseudopodia during protease-activated receptor-2-induced chemotaxis. *The Journal of Biological Chemistry* 278:34418-34426.

52. Scott MGH, *et al.* (2006) Cooperative Regulation of Extracellular Signal-Regulated Kinase Activation and Cell Shape Change by Filamin A and β-Arrestins. *Molecular and Cellular Biology* 26:3432-3445.

53. Min J & DeFea KA (2011) β-Arrestin-Dependent Actin Reorganization: Bringing the Right Players Together at the Leading Edge. *Molecular Pharmacology* 80:760-768.

54. Sastry SK & Burridge K (2000) Focal Adhesions: A Nexus for Intracellular Signaling and Cytoskeletal Dynamics. *Experimental Cell Research* 261:25-36.

55. Ridley AJ, *et al.* (2003) Cell migration: integrating signals from front to back. *Science* 302:1704-1709.

56. Weiner OD, *et al.* (1999) Spatial control of actin polymerization during neutrophil chemotaxis. *Nature Cell Biology* 1:75-81.

57. Proudfoot AEI (2002) Chemokine receptors: multifaceted therapeutic targets. *Nat Rev Immunol* 2:106-115.

58. Fong AM, *et al.* (2002) Defective lymphocyte chemotaxis in beta-arrestin2- and GRK6-deficient mice. *Proceedings of the National Academy of Sciences* 99:7478-7483.

59. Kraft K, *et al.* (2001) Characterization of sequence determinants within the carboxyl-terminal domain of chemokine receptor CCR5 that regulate signaling and receptor internalization. *J Biol Chem* 276:34408-34418

60. Lagane B, *et al.* (2005) Mutation of the DRY motif reveals different structural requirements for the CC chemokine receptor 5-mediated signaling and receptor endocytosis. *Mol. Pharmacol.* 67:1966-1976.

61. Su Y, *et al.* (2005) Altered CXCR2 signaling in β-arrestin-2-deficient mouse models. *J. Immunol.* 175:5396-5402.

62. Richardson RM, Marjoram RJ, Barak LS, & Snyderman R (2003) Role of the cytoplasmic tails of CXCR1 and CXCR2 in mediating leukocyte migration, activation, and regulation. *J Immunol* 170:2904-2911.

63. Fan GH, Yang W, Wang XJ, Qian Q, & Richmond A (2001) Identification of a motif in the carboxyl terminus of CXCR2 that is involved in adaptin 2 binding and receptor internalization. *Biochemistry* 40:791-800.

64. Barlic J, *et al.* (1999) β-Arrestins regulate interleukin-8-induced CXCR1 internalization. *J Biol Chem* 274:16287-16294.

65. Colvin RA, Campanella GSV, Sun J, & Luster AD (2004) Intracellular domains of CXCR3 that mediate CXCL9, CXCL10, and CXCL11 function. *J Biol Chem* 279:30219-30227

66. Hall A (1998) Rho GTPases and the Actin Cytoskeleton. *Science* 279:509-514.

67. Nobes CD & Hall A (1995) Rho, rac, and cdc42 GTPases regulate the assembly of multimolecular focal complexes associated with actin stress fibers, lamellipodia, and filopodia. *Cell* 81:53-62.

68. Ridley AJ & Hall A (1992) The small GTP-binding protein rho regulates the assembly of focal adhesions and actin stress fibers in response to growth factors. *Cell* 70:389-399.

69. Raftopoulou M & Hall A (2003) Cell migration: Rho GTPases lead the way. *Developmental Biology* 265:23-32.

70. Barnes WG, *et al.* (2004) β-Arrestin 1 and $G_{\alpha q/11}$ Coordinately Activate RhoA and Stress Fiber Formation following Receptor Stimulation. *The Journal of Biological Chemistry* 280:8041-8050.

71. Veeman MT, Axelrod JD, & Moon RT (2003) A second canon. Functions and mechanisms of beta-catenin-independent Wnt signaling. *Developmental Cell* 5:367-377.

72. Kim GH & Han JK (2007) Essential role for β-arrestin 2 in the regulation of *Xenopus* convergent extension movements. *The EMBO Journal* 26:2513-1526.

73. Jaffe AB & Hall A (2005) Rho GTPases: biochemistry and biology. *Annu Rev Cell Dev Bio* 21:247-269.

74. Anthony DF, *et al.* (2011) β−Arrestin 1 Inhibits the GTPase-Activating Protein Function of ARHGAP21, Promoting Activation of RhoA following Angiotensin II Type 1A Receptor Stimulation. *Molecular and Cellular Biology* 31:1066-1075.

75. Bhattacharya M, *et al.* (2002) Beta-arrestins regulate a Ral-GDS Ral effector pathway that mediates cytoskeletal reorganization. *Nature Cell Biology* 4:547-555.

76. Gohla A, Birkenfeld J, & Bokoch GM (2005) Chronophin, a novel HAD-type serine protein phosphatase, regulates cofilin-dependent actin dynamics. *Nature Cell Biology* 7:21-29.

77. Bamburg JR & Wiggan OP (2002) ADF/cofilin and actin dynamics in disease. *Trends Cell Biol* 12:598-605

78. Zoudilova M, *et al.* (2007) β−Arrestin-dependent Regulation of the Cofilin Pathway Downstream of Protease-activated Receptor-2. *The Journal of Biological Chemistry* 282:20634-20646.

79. Claing A, *et al.* (2001) beta-Arrestin-mediated ADP-ribosylation factor 6 activation and beta 2-adrenergic receptor endocytosis. *J Biol Chem* 276( ):42509-42513.

80. Santy LC, Ravichandran KS, & Casanova JE (2005) The DOCK180/Elmo complex couples ARNO-mediated Arf6 activation to the downstream activation of Rac1. *Curr Biol* 15:1749-1754.

81. Bouschet T, Martin S, Kanamarlapudi V, Mundell S, & Henley JM (2007) The calcium-sensing receptor changes cell shape via a β–arrestin-1-ARNO-ARF6-ELMO protein network. *Journal of Cell Science* 120:2489-2497.

82. Pugh EN, Jr. & Lamb TD (2000) Phototransduction in vertebrate rods and cones: molecular mechanisms of amplification, recovery and light adaptation. *In: Handbook of biological physics. Molecular mechanisms in visual transduction (Stavenga, D.G., et al., eds)*:183-255. Amsterdam: Elsevier.

83. Makino CL, Wen XH, & Lem J (2003) Piecing together the timetable for visual transduction with transgenic animals. *Curr Opin Neurobiol* 13:404-412.

84. Burns ME & Arshavsky VY (2005) Beyond counting photons: trials and trends in vertebrate visual transuction. *Neuron* 48:387-401.

85. Mendez A, *et al.* (2000) Rapid and reproducible deactivation of rhodopsin requires multiple phosphorylation sites. *Neuron* 28(1):153-164.

86. Vishnivetskiy SA, *et al.* (2007) Regulation of arrestin binding by rhodopsin phosphorylation level. *J Biol Chem* 282:32075-32083.

87. Wilden U, Hall SW, & Kuhn H (1986) Phosphodiesterase activation by photoexcited rhodopsin is quenched when rhodopsin is phosphorylated and binds the intrinsic 48-kDa protein of rod outer segments. *Proceedings of the National Academy of Sciences of the United States of America* 83(5):1174-1178.

88. Krupnick JG, Gurevich VV, & Benovic JL (1997) Mechanism of quenching of phototransduction: binding competition between arrestin and transducin for phosphorhodopsin. *J Biol Chem* 272:18125-18131.

89. Bayburt TH, *et al.* (2011) Rhodopsin monomer is sufficient for normal rhodopsin kinase (GRK1) phosphorylation and arrestin-1 binding. *J Biol Chem* 286:1420-1428.

90. Tsukamoto H, Sinha A, Dewitt M, & Farrens DL (2010) Monomeric Rhodopsin Is the Minimal Functional Unit Required for Arrestin Binding. *J Mol Biol* 399:501-511.

91. Mendez A, Lem J, Simon MI, & Chen J (2003) Light-dependent translocation of arrestin in the absence of rhodopsin phosphorylation and transducin signaling. *J Neurosci* 23:3124-3129.

92. Hanson SM, *et al.* (2007) Each rhodopsin molecule binds its own arrestin. *Proc Natl Acad Sci* 104(9):3125-3128.

93. Hamm HE & Bownds MD (1986) Protein complement of rod outer segments of frog retina. *Biochemistry* 25:4512-4523.

94. Nair KS, *et al.* (2004) Direct binding of visual arrestin to microtubules determines the differential subcellular localization of its splice variants in rod photoreceptors. *J. Biol. Chem.* 279:41240-41248.

95. McGinnis JF, Matsumoto B, Whelan JP, & Cao W (2002) Cytoskeleton participation in subcellular trafficking of signal transduction proteins in rod photoreceptor cells. *J Neurosci Res* 67:290-297.

96. Nir I & Ransom N (1993) Ultrastructural analysis of arrestin distribution in mouse photoreceptors during dark/light cycle. *Exp Eye Res* 57:307-318.

97. Nair KS, *et al.* (2005) Light-dependent redistribution of arrestin in vertebrate rods is an energy-independent process governed by protein-protein interactions. *Neuron* 46:555-567.

98. Nair KS, *et al.* (2004) Direct binding of visual arrestin to microtubules determines the differential subcellular localization of its splice variants in rod photoreceptors. *J Biol Chem* 279:41240-41248.

99. Sutton RB, *et al.* (2005) Crystal structure of cone arrestin at 2.3 Å: evolution of receptor specificity. *J Mol Biol* 354:1069-1080.

100. Hanson SM, *et al.* (2007) Arrestin mobilizes signaling proteins to the cytoskeleton and redirects their activity. *J Mol Biol* 368:375-387.

101. Hanson SM, *et al.* (2006) Differential interaction of spin labeled arrestin with inactive and active phosphorhodopsin. *Proc Natl Acad Sci USA* 103:4900-4905.

102. Hanson SM & Gurevich VV (2006) The differential engagement of arrestin surface charges by the various functional forms of the receptor. *J Biol Chem* 281:3458-3462.

103. Gurevich VV & Gurevich EV (2004) The molecular acrobatics of arrestin activation. *Trends Pharmacol Sci* 25:105-112.

104. Vishnivetskiy SA, Hirsch JA, Velez MG, Gurevich YV, & Gurevich VV (2002) Transition of arrestin in the active receptor-binding state requires an extended interdomain hinge. *J. Biol. Chem.* 277(46):43961-43968.

105. Hanson SM, *et al.* (2006) Differential interaction of spin labeled arrestin with inactive and active phosphorhodopsin. *Proc Natl Acad Sci USA* 103:4900-4905.

106. Vishnivetskiy SA, Hosey MM, Benovic JL, & Gurevich VV (2004) Mapping the arrestin-receptor interface: structural elements responsible for receptor specificity of arrestin proteins. *J. Biol. Chem.* 279(2):1262-1268.

107. Nair KS, *et al.* (2005) Light-dependent redistribution of arrestin in vertebrate rods is an energy-independent process governed by protein-protein interactions. *Neuron* 46:555-567.

108. Gurevich VV & Gurevich EV (2006) The structural basis of arrestin-mediated regulation of G protein-coupled receptors. *Pharmacol Ther* 110:465-502.

109. Lefkowitz RJ & Shenoy SK (2005) Transduction of receptor signals by beta-arrestins. *Science* 308:512-517.

110. Xiao K, Shenoy SK, Nobles K, & Lefkowitz RJ (2004) Activation-dependent conformational changes in beta-arrestin 2. *J Biol Chem* 279:55744-55753.

111. Marchese A, Chen C, Kim YM, & Benovic JL (2003) The ins and outs of G protein-coupled receptor trafficking. *Trends Biochem Sci* 28(7):369-376.

112. Gurevich VV & Gurevich EV (2003) The new face of active receptor bound arrestin attracts new partners. *Structure (Camb)* 11:1037-1042.

113. McDonald PH, *et al.* (2000) Beta-arrestin 2: a receptor-regulated MAPK scaffold for the activation of JNK3. *Science* 290:1574-1577.

114. Luttrell LM, *et al.* (2001) Activation and targeting of extracellular signal-regulated kinases by beta-arrestin scaffolds. *Proc Natl Acad Sci U S A* 98:2449-2459.

115. Luttrell LM (2003) "Location, location, location": activation and targeting of MAP kinases by G protein-coupled receptors. *J Mol Endocrinol* 30:117-126.

116. Shenoy SK & Lefkowitz RJ (2003) Trafficking patterns of beta-arrestin and G protein-coupled receptors determined by the kinetics of beta-arrestin deubiquitination. *J Biol Chem* 278:14498-14506.

117. Wang P, *et al.* (2003) Beta-arrestin 2 functions as a G-protein-coupled receptor-activated regulator of oncoprotein Mdm2. *J Biol Chem* 278:6363-6370.

118. Song X, Raman D, Gurevich EV, Vishnivetskiy SA, & Gurevich VV (2006) Visual and both non-visual arrestins in their "inactive" conformation bind JNK3 and Mdm2 and relocalize them from the nucleus to the cytoplasm. *J Biol Chem* 281:21491-21499.

119. Shenoy SK, McDonald PH, Kohout TA, & Lefkowitz RJ (2001) Regulation of receptor fate by ubiquitination of activated beta 2-adrenergic receptor and beta-arrestin. *Science* 294:1307-1313.

120. Hupfeld CJ, Resnik JL, Ugi S, & Olefsky JM (2005) Insulin-induced beta-arrestin1 Ser-412 phosphorylation is a mechanism for desensitization of ERK activation by Galphai-coupled receptors. *J Biol Chem* 280:1016-1023.

121. Hanson SM, Francis DF, Vishnivetskiy SA, Klug CS, & Gurevich VV (2006) Visual arrestin binding to microtubules involves a distinct conformational change. *J Biol Chem* 281:9765-9772.

122. Scott MG, *et al.* (2002) Differential nucleocytoplasmic shuttling of beta-arrestins. Characterization of a leucine-rich nuclear export signal in beta-arrestin2. *J Biol Chem* 277:37693-37701.

123. Song X, Raman D, Gurevich EV, Vishnivetskiy SA, & Gurevich VV (2006) Visual and both non-visual arrestins in their "inactive" conformation bind JNK3 and Mdm2 and relocalize them from the nucleus to the cytoplasm. *J Biol Chem*:[Epub ahead of print; May 31, 2006].

124. Gundersen GG & Cook TA (1999) Microtubules and signal transduction. *Curr Opin Cell Biol* 11:81-94.

125. Xiao K, *et al.* (2007) Functional specialization of beta-arrestin interactions revealed by proteomic analysis. *Proc Natl Acad Sci U S A* 104:12011-12016.

126. DeWire SM, Ahn S, Lefkowitz RJ, & Shenoy SK (2007) Beta-arrestins and cell signaling. *Annu Rev Physiol* 69:483-510.

127. Hanson SM, Francis DJ, Vishnivetskiy SA, Klug CS, & Gurevich VV (2006) Visual arrestin binding to microtubules involves a distinct conformational change. *J Biol Chem* 281:9765-9772.

128. Mundell SJ, Loudon RP, & Benovic JL (1999) Characterization of G protein-coupled receptor regulation in antisense mRNA-expressing cells with reduced arrestin levels. *Biochemistry* 38:8723-8732.

129. Orsini MJ & Benovic JL (1998) Characterization of dominant negative arrestins that inhibit beta2-adrenergic receptor internalization by distinct mechanisms. *The Journal of Biological Chemistry* 273:34616-34622.

130. Goodwin AE & Pauli BU (1995) A new adhesion assay with buoyancy to remove nonadherent cells. *J. Immunol. Methods* 187:213-219.

131. Benard V & Bokoch GM (2002) Assay of Cdc42, Rac, and Rho GTPase Activation by Affinity Methods. *Methods in Enzymology* 345:349-359.

132. Breitman M, *et al.* (2012) Silent scaffolds: inhibition of JNK3 activity in the cell by a dominant-negative arrestin-3 mutant. *J Biol Chem* 287:in press.

133. Benard V, Bohl BP, & Bokoch GM (1999) Characterization of Rac and Cdc42 Activation in Chemoattractant-stimulated Human Neutrophils Using a Novel Assay for Active GTPases. *The Journal of Biological Chemistry* 274:13198-13204.

134. Arthur WT, Ellerbroek SM, Der CJ, Burridge K, & Wennerberg K (202) XPLN, a guanine nucleotide exchange factor for RhoA and RhoB, but not RhoC. *The Journal of Biological Chemistry* 277:42964-42972.

135. Ren XD, Kosses WB, & Schwartz MA (1999) Regulation of the small GTP-binding protein Rho by cell adhesion and the cytoskeleton. *EMBO Journal* 18:578-585.

136. Kamakura S, Moriguchi T, & Nishida E (1999) Activation of the Protein Kinase ERK5/BMK1 by Receptor Tyrosine Kinases: Identification and Characterization of a Signaling Pathway to the Nucleus. *The Journal of Biological Chemistry* 274:26563-26571.

137. Wennerberg K & Burridge K (2004) Rho and Rac Take Center Stage. *Cell* 116:167-179.

138. Gieger B, Spatz JP, & Bershadsky AD (2009) Environmental sensing through focal adhesions. *Nature Review Molecular Cell Biology* 10:21-33.

139. Huveneers S & Danen EHJ (2009) Adhesion signaling - crosstalk between integrins, Src, and Rho. *Journal of Cell Science* 122:1059-1069.

140. Webb DJ, *et al.* (2004) FAK-Src signalling through paxillin, ERK, and MLCK regulates adhesion disassembly. *Nature Cell Biology* 6:154-161.

141. Bechara A, *et al.* (2008) FAK–MAPK-dependent adhesion disassembly downstream of L1 contributes to semaphorin3A-induced collapse. *EMBO J* 27:1549–1562.

142. Kaverina I, Krylyshkina O, & Small JV (1999) Microtubule targeting of substrate contacts promotes their relaxation and dissociation. *Journal of Cell Biology* 146:1033-1044.

143. Small JV, Geiger B, Kaverina I, & Bershadsky A (2002) How do microtubules guide migrating cells? *Nature Review Molecular Cell Biology* 3:957-964.

144. Goodman OB, *et al.* (1996) Beta-arrestin acts as a clathrin adaptor in endocytosis of the beta2-adrenergic receptor. *Nature* 383(6599):447-450.

145. Laporte SA, Oakley RH, Holt JA, Barak LS, & Caron MG (2000) The interaction of beta-arrestin with the AP-2 adaptor is required for the clustering of beta 2-adrenergic receptor into clathrin-coated pits. *J Biol Chem* 275(30):23120-23126.

146. Shenoy SK, McDonald PH, Kohout TA, & Lefkowitz RJ (2001) Regulation of receptor fate by ubiquitination of activated beta 2-adrenergic receptor and beta-arrestin. *Science* 294:1307-1313.

147. Bhandari D, Trejo J, Benovic JL, & Marchese A (2007) Arrestin-2 interacts with the ubiquitin-protein isopeptide ligase atrophin-interacting protein 4 and mediates endosomal sorting of the chemokine receptor CXCR4. *J Biol Chem* 282:36971-36979.

148. Ahmed MR, *et al.* (2011) Ubiquitin ligase parkin promotes Mdm2-arrestin interaction but inhibits arrestin ubiquitination. *Biochemistry* 50:3749-3763.

149. Perry SJ, *et al.* (2002) Targeting of cyclic AMP degradation to beta 2-adrenergic receptors by beta-arrestins. *Science* 298(5594):834-836.

150. Shankar H, *et al.* (2010) Non-visual arrestins are constitutively associated with the centrosome and regulate centrosome function. *J Biol Chem* 285:8316-8329.

151. DeFea KA (2007) Stop That Cell! β-Arrestin-Dependent Chemotaxis: A Tale of Localized Actin Assembly and Receptor Desensitization. *Annual Review of Physiology* 69:535-560.

152. Chrzanowska-Wodnicka M & Burridge K (1996) Rho-stimulated contractility drives the formation of stress fibers and focal adhesions. *Journal of Cell Biology* 133:1403-1415.

153. Ezratty EJ, Partridge MA, & Gundersen GG (2005) Microtubule-induced focal adhesion disassembly is mediated by dynamin and focal adhesion kinase. *Nature Cell Biology* 7:581-590.

154. Ezratty EJ, Bertaux C, Marcantonio EE, & Gundersen GG (2009) Clathrin mediates integrin endocytosis for focal adhesion disassembly in migrating cells. *The Journal of Cell Biology* 187:733-747.

155. Coffa S, Breitman M, Spiller BW, & Gurevich VV (2011) A single mutation in arrestin-2 prevents ERK1/2 activation by reducing c-Raf1 binding. *Biochemistry* 50:6951-6958.

156. Ishibe S, Joly D, Zhu X, & Cantley LG (2003) Phosphorylation-dependent paxillin-ERK association mediates hepatocyte growth factor-stimulated epithelial morphogenesis. *Mol Cell* 12:1275-1285.

157. Cai X, Li M, Vrana J, & Schaller MD (2006) Glycogen synthase kinase 3- and extracellular signal-regulated kinase-dependent phosphorylation of paxillin regulates cytoskeletal rearrangement. *Molecular and Cellular Biology* 26:2857-2868.

158. Ishibe S, Joly D, Liu ZX, & Cantley LG (2004) Paxillin serves as an ERK-regulated scaffold for coordinating FAK and Rac activation in epithelial morphogenesis. *Molecular Cell* 16:257-267.

159. Liu ZX, Yu CF, Nickel C, Thomas S, & Cantley LG (2002) Hepatocyte growth factor induces ERK-dependent paxillin phosphorylation and regulates paxillin-focal adhesion kinase association. *The Journal of Biological Chemistry* 277:10452-10458.

160. Meyer SC, Sanan DA, & Fox JE (1998) Role of actin-binding protein in insertion of adhesion receptors into the membrane. *Journal of Biological Chemistry* 273:3013-3020.

161. Kim H, *et al.* (2010) Filamin A is required for vimentin-mediated cell adhesion and spreading. *Am. J. Physiol. Cell Physiology* 298:C221-C236.

162. Coffa S, *et al.* (2011) The Effect of Arrestin Conformation on the Recruitment of c-Raf1, MEK1, and ERK1/2 Activation. *PLoS One* 6:e28723.

163. Cleghorn WM, *et al.* (2011) Progressive Reduction of its Expression in Rods Reveals Two Pools of Arrestin-1 in the Outer Segment with Different Roles in Photoresponse Recovery. *PLoS One* 6:e22797.

164. Luo DG, Xue T, & Yau KW (2008) How vision begins: an odyssey. *Proc Natl Acad Sci U S A* 105:9855-9862.

165. Shen L, *et al.* (2010) Dynamics of mouse rod phototransduction and its sensitivity to variation of key parameters. *IET Syst Biol* 4:12-32.

166. Burns ME & Pugh EN, Jr. (2010) Lessons from photoreceptors: turning off g-protein signaling in living cells. *Physiology (Bethesda)* 25:72-84.

167. Burns ME & Pugh EN, Jr. (2009) RGS9 concentration matters in rod phototransduction. *Biophys J* 97:1538-1547.

168. Caruso G, *et al.* (2010) Kinetics of rhodopsin inactivation and its role in regulating recovery and reproducibility of rod photoresponse. *PLoS Computational Biology* 6:e1001031.

169. Baylor DA, Lamb TD, & Yau KW (1979) Responses of retinal rods to single photons. *J Physiol* 288:613-634.

170. Krispel CM, *et al.* (2006) RGS expression rate-limits recovery of rod photoresponses. *Neuron* 51:409-416.

171. Palczewski K, Buczylko J, Kaplan MW, Polans AS, & Crabb JW (1991) Mechanism of rhodopsin kinase activation. *J Biol Chem* 266:12949-12955.

172. Wilden U (1995) Duration and amplitude of the light-induced cGMP hydrolysis in vertebrate photoreceptors are regulated by multiple phosphorylation of rhodopsin and by arrestin binding. *Biochemistry* 34:1446-1454.

173. Strissel KJ, Sokolov M, Trieu LH, & Arshavsky VY (2006) Arrestin translocation is induced at a critical threshold of visual signaling and is superstoichiometric to bleached rhodopsin. *J Neurosci* 26:1146-1153.

174. Song X, *et al.* (2011) Arrestin-1 expression level in rods: Balancing functional performance and photoreceptor health. *Neuroscience* 174:37-49.

175. Gross OP & Burns ME (2010) Control of rhodopsin's active lifetime by arrestin-1 expression in mammalian cells. *J Neurosci* 30:3450-3457.

176. Song X, *et al.* (2009) Enhanced Arrestin Facilitates Recovery and Protects Rods Lacking Rhodopsin Phosphorylation. *Current Biology* 19(700-705).

177. Lyubarsky ALaP, E.N. Jr. (1996) Recovery phase of the murine rod photoresponse reconstructed from electroretinographic recordings. *Journal of Neuroscience* 16:563-571.

178. Lyubarsky AL, *et al.* (2002) Functionally rodless mice: transgenic models for the investigation of cone function in retinal disease and therapy. *Vision Res* 42:401-415.

179. Lyubarsky AL, Daniele LL, & Pugh EN, Jr. (2004) From candelas to photoisomerizations in the mouse eye by rhodopsin bleaching in situ and the light-rearing dependence of the major components of the mouse ERG. (Translated from eng) *Vision Res* 44(28):3235-3251 (in eng).

180. Hetling JR & Pepperberg DR (1999) Sensitivity and kinetics of mouse rod flash responses determined *in vivo* from paired-flash electroretinograms. *J Physiol* 516:593-609.

181. Pepperberg DR, Birch DG, & Hood DC (1997) Photoresponses of human rods *in vivo* derived from paired-flash electroretinograms. *Vis Neurosci* 14:73-82.

182. Chen CK, *et al.* (1999) Abnormal photoresponses and light-induced apoptosis in rods lacking rhodopsin kinase. *Proc Nat Acad Sci USA* 96:3718-3722.

183. Chen J, Makino CL, Peachey NS, Baylor DA, & Simon MI (1995) Mechanisms of rhodopsin inactivation in vivo as revealed by a COOH-terminal truncation mutant. *Science* 267(5196):374-377.

184. Xu J, *et al.* (1997) Prolonged photoresponses in transgenic mouse rods lacking arrestin. *Nature* 389(6650):505-509.

185. Nikonov SS, *et al.* (2008) Mouse cones require an arrestin for normal inactivation of phototransduction. *Neuron* 59:462-474.

186. Broekhuyse RM, Tolhuizen EF, Janssen AP, & Winkens HJ (1985) Light induced shift and binding of S-antigen in retinal rods. *Curr Eye Res* 4:613-618.

187. Philp NJ, Chang W, & Long K (1987) Light-stimulated protein movement in rod photoreceptor cells of the rat retina. *FEBS Lett* 225(1-2):127-132.

188. Robson JG & Frishman LJ (1995) Response linearity and kinetics of the cat retina: the bipolar cell component of the dark-adapted electroretinogram. *Visual Neuroscience* 12(5):837-850.

189. Robson JG & Frishman LJ (1996) Photoreceptor and bipolar cell contributions to the cat electroretinogram: a kinetic model for the early part of the flash response. *Journal of the Optical Society of America, A, Optics, Image Science, & Vision* 13(3):613-622.

190. Bayburt TH, *et al.* (2011) Rhodopsin monomer is sufficient for normal rhodopsin kinase (GRK1) phosphorylation and arrestin-1 binding. *J. Biol. Chem.* 286:1420-1428.

191. Calvert PD, *et al.* (2001) Membrane protein diffusion sets the speed of rod phototransduction. *Nature* 411:90-94.

192. Wen XH, *et al.* (2009) Overexpression of rhodopsin alters the structure and photoresponse of rod photoreceptors. *Biophys J* 96:939-950.

193. Doan T, Azevedo AW, Hurley JB, & Rieke F (2009) Arrestin competition influences the kinetics and variability of the single-photon responses of mammalian rod photoreceptors. *J Neurosci* 29:11867-11879.

194. Kim M, *et al.* (2011) Robust self-association is a common feature of mammalian visual arrestin-1. *Biochemistry* 50:in press.

195. Schubert C, *et al.* (1999) Visual arrestin activity may be regulated by self-association. *J. Biol. Chem.* 274:21186-21190.

196. Imamoto Y, Tamura C, Kamikubo H, & Kataoka M (2003) Concentration-dependent tetramerization of bovine visual arrestin. *Biophys J* 85:1186-1195.

197. Hanson SM, *et al.* (2007) Structure and function of the visual arrestin oligomer. *EMBO J* 26:1726-1736.

198. Hanson SM, *et al.* (2008) A model for the solution structure of the rod arrestin tetramer. *Structure* 16:924-934.

199. Gurevich VV & Benovic JL (1995) Visual arrestin binding to rhodopsin: diverse functional roles of positively charged residues within the phosphorylation-recignition region of arrestin. *J. Biol. Chem.* 270(11):6010-6016.

200. Gurevich VV, *et al.* (1995) Arrestin interaction with G protein-coupled receptors. Direct binding studies of wild type and mutant arrestins with rhodopsin, b2-adrenergic, and m2 muscarinic cholinergic receptors. *J Biol Chem* 270:720-731.

201. Vishnivetskiy SA, *et al.* (2010) The role of arrestin alpha-helix I in receptor binding. *J. Mol. Biol.* 395:42-54.

202. Vishnivetskiy SA, *et al.* (2011) Few residues within an extensive binding interface drive receptor interaction and determine the specificity of arrestin proteins. *J Biol Chem* 286:in press.

203. Hanson SM, *et al.* (2006) Differential interaction of spin-labeled arrestin with inactive and active phosphorhodopsin. *Proc Natl Acad Sci U S A* 103:4900-4905.

204. Hanson SM & Gurevich VV (2006) The differential engagement of arrestin surface charges by the various functional forms of the receptor. *J Biol Chem* 281:3458-3462.

205. Gurevich VV, Hanson SM, Gurevich EV, & Vishnivetskiy SA (2007) How rod arrestin achieved perfection: regulation of its availability and binding selectivity. *In: Methods in signal transduction series (Kisselev, O., Fliesler S.J., Eds)*:55-88. Boca Raton, FL: CRC Press.

206. Elias RV, Sezate SS, Cao W, & McGinnis JF (2004) Temporal kinetics of the light/dark translocation and compartmentation of arrestin and alpha-transducin in mose photoreceptor cells. *Mol Vis* 10(672-681).

207. Orisme W, *et al.* (2010) Light-dependent translocation of arrestin in rod photoreceptors is signaled through a phospholipase C cascade and requires ATP. *Cell Signal* 22:447-456.

208. Peet JA, *et al.* (2004) Quantification of the cytoplasmic spaces of living cells with EGFP reveals arrestin-EGFP to be in disequilibrium in dark adapted rod photoreceptors. *J Cell Sci* 117:3049-3059.

209. Slepak VZ & Hurley JB (2008) Mechanism of light-induced translocation of arrestin and transducin in photoreceptors: interaction-restricted diffusion. *IUBMB Life* 60:2-9.

210. Nair KS, *et al.* (2004) Direct binding of visual arrestin to microtubules determines the differential subcellular localization of its splice variants in rod photoreceptors. *J Biol Chem* 279:41240-41248.

211. Hanson SM, Francis DJ, Vishnivetskiy SA, Klug CS, & Gurevich VV (2006) Visual arrestin binding to microtubules involves a distinct conformational change. *J Biol Chem* 281:9765-9772.

212. Huang SP, Brown BM, & Craft CM (2010) Visual Arrestin 1 acts as a modulator for N-ethylmaleimide-sensitive factor in the photoreceptor synapse. *J Neurosci* 30:9381-9391.

213. Smith WC, *et al.* (2011) Interaction of arrestin with enolase1 in photoreceptors. *Invest Ophthalmol Vis Sci*:in press.

214. Eckmiller MS (2000) Microtubules in a rod-specific cytoskeleton associated with outer segment incisures. *Vis Neurosci* 17:711-722.

215. Chen CK, Woodruff ML, Chen FS, Chen D, & Fain GL (2010) Background light produces a recoverin-dependent modulation of activated-rhodopsin lifetime in mouse rods. *J Neurosci* 30:1213-1220.

216. Wilden U, Hall SW, & Kühn H (1986) Phosphodiesterase activation by photoexcited rhodopsin is quenched when rhodopsin is phosphorylated and binds the intrinsic 48-kDa protein of rod outer segments. *Proc Natl Acad Sci USA* 83:1174-1178.

217. Zhan X, Gimenez LE, Gurevich VV, & Spiller BW (2011) Crystal structure of arrestin-3 reveals the basis of the difference in receptor binding between two non-visual subtypes. *J Mol Biol* 406(3):467-478.

218. Sutton RB, *et al.* (2005) Crystal structure of cone arrestin at 2.3A: evolution of receptor specificity. *J Mol Biol* 354(5):1069-1080.

219. Han M, Gurevich VV, Vishnivetskiy SA, Sigler PB, & Schubert C (2001) Crystal structure of beta-arrestin at 1.9 A: possible mechanism of receptor binding and membrane Translocation. *Structure* 9(9):869-880.

220. Gurevich VV & Benovic JL (1993) Visual arrestin interaction with rhodopsin. Sequential multisite binding ensures strict selectivity toward light-activated phosphorylated rhodopsin. *J Biol Chem* 268(16):11628-11638.

221. Gurevich VV (1998) The selectivity of visual arrestin for light-activated phosphorhodopsin is controlled by multiple nonredundant mechanisms. *J Biol Chem* 273(25):15501-15506.

222. Gurevich VV & Gurevich EV (2004) The molecular acrobatics of arrestin activation. *Trends Pharmacol Sci* 25(2):105-111.

223. Kovoor A, Celver J, Abdryashitov RI, Chavkin C, & Gurevich VV (1999) Targeted construction of phosphorylation-independent b-arrestin mutants with constitutive activity in cells. *J. Biol. Chem.* 274:6831-6834.

224. Celver J, Vishnivetskiy SA, Chavkin C, & Gurevich VV (2002) Conservation of the phosphate-sensitive elements in the arrestin family of proteins. *J. Biol. Chem.* 277(11):9043-9048.

225. Gurevich VV & Gurevich EV (2010) Custom-designed proteins as novel therapeutic tools? The case of arrestins. *Expert Rev Mol Med* 12:e13.

226. Gurevich VV & Gurevich EV (2003) The new face of active receptor bound arrestin attracts new partners. *Structure* 11(9):1037-1042.

227. Van Eps N, *et al.* (2011) Interaction of a G protein with an activated receptor opens the interdomain interface in the alpha subunit. *Proc Natl Acad Sci U S A* 108(23):9420-9424.

228. Altenbach C, Kusnetzow AK, Ernst OP, Hofmann KP, & Hubbell WL (2008) High-resolution distance mapping in rhodopsin reveals the pattern of helix movement due to activation. *Proc Natl Acad Sci U S A* 105(21):7439-7444.

229. Gurevich VV & Benovic JL (2000) Arrestin: mutagenesis, expression, purification, and functional characterization. *Methods Enzymol* 315:422-437.

230. Hanson SM, *et al.* (2006) Differential interaction of spin-labeled arrestin with inactive and active phosphorhodopsin. *Proc Natl Acad Sci U S A* 103(13):4900-4905.

231. Hanson SM, *et al.* (2007) Structure and function of the visual arrestin oligomer. *Embo J* 26(6):1726-1736.

232. Vishnivetskiy SA, *et al.* (2007) Regulation of arrestin binding by rhodopsin phosphorylation level. *J Biol Chem* 282:32075-32083.

233. Jeschke G, *et al.* (2006) DeerAnalysis2006 - a comprehensive software package for analyzing pulsed ELDOR data. (Translated from English) *Applied magnetic resonance* 30(3-4):473-498 (in English).

234. Hirst SJ, Alexander N, McHaourab HS, & Meiler J (2011) RosettaEPR: an integrated tool for protein structure determination from sparse EPR data. (Translated from eng) *Journal of structural biology* 173(3):506-514 (in eng).

235. Alexander N, Bortolus M, Al-Mestarihi A, McHaourab H, & Meiler J (2008) De novo high-resolution protein structure determination from sparse spin-labeling EPR data. (Translated from eng) *Structure* 16(2):181-195 (in eng).

236. Gurevich VV & Gurevich EV (2006) The structural basis of arrestin-mediated regulation of G-protein-coupled receptors. *Pharmacol Ther* 110(3):465-502.

237. Skegro D, *et al.* (2007) N-terminal and C-terminal domains of arrestin both contribute in binding to rhodopsin. (Translated from eng) *Photochemistry and photobiology* 83(2):385-392 (in eng).

238. Vishnivetskiy SA, Hosey MM, Benovic JL, & Gurevich VV (2004) Mapping the arrestin-receptor interface. Structural elements responsible for receptor specificity of arrestin proteins. *J Biol Chem* 279(2):1262-1268.

239. Li J, Edwards PC, Burghammer M, Villa C, & Schertler GF (2004) Structure of bovine rhodopsin in a trigonal crystal form. *J Mol Biol* 343(5):1409-1438.

240. Vishnivetskiy SA, *et al.* (2010) The role of arrestin alpha-helix I in receptor binding. *J Mol Biol* 395(1):42-54.

241. Schleicher A, Kuhn H, & Hofmann KP (1989) Kinetics, binding constant, and activation energy of the 48-kDa protein-rhodopsin complex by extra-metarhodopsin II. *Biochemistry* 28(4):1770-1775.

242. Palczewski K, Pulvermuller A, Buczylko J, & Hofmann KP (1991) Phosphorylated rhodopsin and heparin induce similar conformational changes in arrestin. *J Biol Chem* 266:18649-18654.

243. Ohguro H, Palczewski K, Walsh KA, & Johnson RS (1994) Topographic study of arrestin using differential chemical modifications and hydrogen/deuterium exchange. *Protein Sci* 3(12):2428-2434.

244. Zhuang T, Vishnivetskiy SA, Gurevich VV, & Sanders CR (2010) Elucidation of inositol hexaphosphate and heparin interaction sites and conformational changes in arrestin-1 by solution nuclear magnetic resonance. *Biochemistry* 49(49):10473-10485.

245. Vishnivetskiy SA, *et al.* (2000) An additional phosphate-binding element in arrestin molecule. Implications for the mechanism of arrestin activation. *J Biol Chem* 275(52):41049-41057.

246. Hanson SM, *et al.* (2007) Arrestin mobilizes signaling proteins to the cytoskeleton and redirects their activity. *J Mol Biol*:in press.

247. Hilser VJ (2010) Biochemistry. An ensemble view of allostery. (Translated from eng) *Science* 327(5966):653-654 (in eng).

248. Vishnivetskiy SA, *et al.* (2011) Few residues within an extensive binding interface drive receptor interaction and determine the specificity of arrestin proteins. *J Biol Chem* 286:24288-24299.

249. Coffa S, Breitman M, Spiller BW, & Gurevich VV (2011) A single mutation in arrestin-2 prevents ERK1/2 activation by reducing c-Raf1 binding. *Biochemistry* 50:6951-6958.

250. Ahmed MR, *et al.* (2011) Ubiquitin ligase parkin promotes Mdm2-arrestin interaction but inhibits arrestin ubiquitination. *Biochemistry*:3749-3763.

251. Feuerstein SE, *et al.* (2009) Helix formation in arrestin accompanies recognition of photoactivated rhodopsin. *Biochemistry* 48(45):10733-10742.

252. Sommer ME, Farrens DL, McDowell JH, Weber LA, & Smith WC (2007) Dynamics of arrestin-rhodopsin interactions: loop movement is involved in arrestin activation and receptor binding. *J Biol Chem* 282(35):25560-25568.

253. Scheerer P, *et al.* (2008) Crystal structure of opsin in its G-protein-interacting conformation. (Translated from eng) *Nature* 455(7212):497-502 (in eng).

254. Rasmussen SG, *et al.* (2011) Crystal structure of the β2 adrenergic receptor-Gs protein complex. *Nature* 477:549-555.

255. Pao CS, Barker BL, & Benovic JL (2009) Role of the amino terminus of G protein-coupled receptor kinase 2 in receptor phosphorylation. *Biochemistry* 48:7325-7333.

256. Huang CC, Orban T, Jastrzebska B, Palczewski K, & Tesmer JJ (2011) Activation of G protein-coupled receptor kinase 1 involves interactions between its N-terminal region and its kinase domain. *Biochemistry* 50:1940-1949.

257. Boguth CA, Singh P, Huang CC, & Tesmer JJ (2010) Molecular basis for activation of G protein-coupled receptor kinases. *Embo J* 29:3249-3259.

258. Hanson SM, *et al.* (2007) Each rhodopsin molecule binds its own arrestin. *Proc Natl Acad Sci U S A* 104(9):3125-3128.

259. Bayburt TH, *et al.* (2011) Rhodopsin monomer is sufficient for normal rhodopsin kinase (GRK1) phosphorylation and arrestin-1 binding. *J Biol Chem* 286:1420-1428.

260. Hanson SM & Gurevich VV (2006) The differential engagement of arrestin surface charges by the various functional forms of the receptor. *J Biol Chem* 281(6):3458-3462.

261. Gao H, *et al.* (2004) Identification of beta-arrestin2 as a G protein-coupled receptor-stimulated regulator of NF-kappaB pathways. *Mol Cell* 14:303-317.

262. Witherow DS, Garrison TR, Miller WE, & Lefkowitz RJ (2004) beta-Arrestin inhibits NF-kappaB activity by means of its interaction with the NF-kappaB inhibitor IkappaBalpha. *Proc Natl Acad Sci U S A* 101:8603-8607.

263. Wang P, Wu Y, Ge X, Ma L, & Pei G (2003) Subcellular localization of beta-arrestins is determined by their intact N domain and the nuclear export signal at the C terminus. *J Biol Chem* 278:11648-11653.

264. Barak LS, Ferguson SS, Zhang J, & Caron MG (1997) A beta-arrestin/green fluorescent protein biosensor for detecting G protein-coupled receptor activation. *J Biol Chem* 272:27497-27500.

265. Gurevich VV & Gurevich EV (2006) The structural basis of arrestin-mediated regulation of G-protein-coupled receptors. *Pharmacol Ther* 110:465-502.

266. Hanson SM, Francis DJ, Vishnivetskiy SA, Klug CS, & Gurevich VV (2006) Visual arrestin binding to microtubules involves a distinct conformational change. *J Biol Chem* 281:9765-9772.

267. Hanson SM, *et al.* (2007) Arrestin mobilizes signaling proteins to the cytoskeleton and redirects their activity. *J Mol Biol*:in press.

268. Kim M, *et al.* (2011) Robust self-association is a common feature of mammalian visual arrestin-1. *Biochemistry* 50:2235-2242.